Synthetic Analogues of the Active Sites of Iron−Sulfur Proteins

P. Venkateswara Rao and R. H. Holm*

Department of Chemistry and Chemical Biology, Harvard University, Cambridge, Massachusetts 02138

Received March 17, 2003

Contents

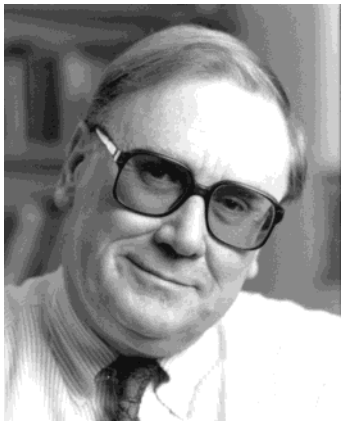

Richard H. Holm was born in Boston, MA, spent his younger years on Nantucket Island and Cape Cod, and graduated from the University of Massachusetts (B.S.) and Massachusetts Institute of Technology (Ph.D.) He has served on the faculties of the University of Wisconsin, Massachusetts Institute of Technology, and Stanford University. Since 1980, he has been at Harvard University, where he has been Chair of the Department of Chemistry and, from 1983, Higgins Professor of Chemistry. His research interests are centered in inorganic and bioinorganic chemistry, with particular reference to the synthesis and properties of molecules whose structures and reactions are pertinent to biological processes.

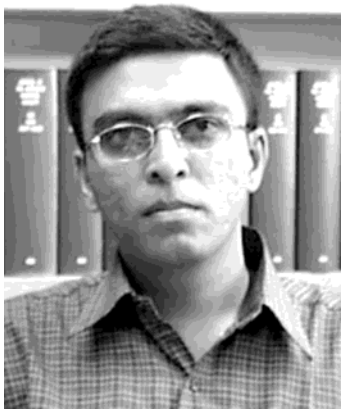

Venkateswara Rao Pallem was born in Hyderabad, India. He received his M.Sc. degree in chemistry in 1995 from Osmania University, Hyderabad, and his Ph.D. in chemistry in 2001 at the Indian Institute of Technology, Bombay, India, under the guidance of Professor Chebrolu P. Rao. He is currently working as a postdoctoral fellow with Professor Richard H. Holm. His research interests include the design and study of synthetic analogues of biologically related molecules.

1. Introduction

The synthetic analogue approach to the metal sites in iron−sulfur proteins was initiated in the early 1970s. Structures of sites **1**−**8** defined by X-ray crystallography are collected in Figure 1, and analogues **9**−**13** synthesized then and later are depicted in Figure 2. In 1970−1972, structure **1** of oxidized rubredoxin[1] and the cubane-type cluster **5** in a bacterial ferredoxin[2,3] and a "high-potential" iron protein[3] were established by protein crystallography. Further, in 1966, through analysis of EPR spectra and limited magnetic data, the antiferromagnetically coupled diferric site **2a** was deduced in oxidized spinach ferredoxin.[4−6] This model was widely accepted prior to an X-ray structure determination.[7] Consequently, the stage was set for an elucidation of these sites by the synthesis and investigation of low-molecular-weight complexes available in highly pure and crystalline form and whose properties are intrinsic in the sense that they are not modulated

10.1021/cr020615+ CCC: $48.50
Published on Web 10/30/2003

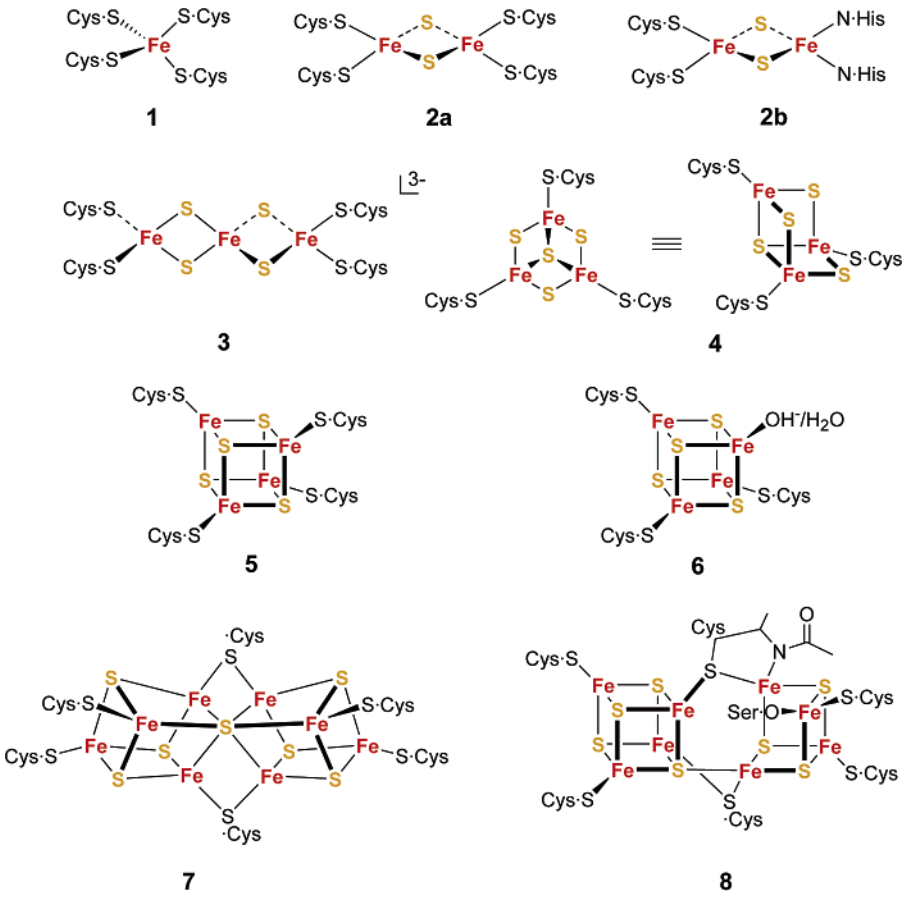

Figure 1. Schematic representations of crystallographically demonstrated protein sites containing one (**1**), two (**2**), three (**3**, **4**), four (**5**, **6**), and eight (**7**, **8**) iron atoms. Formulas **7** and **8** describe the P cluster of nitrogenase is the as-isolated (P^N) and two-electron oxidized (P^{OX}) states, respectively.

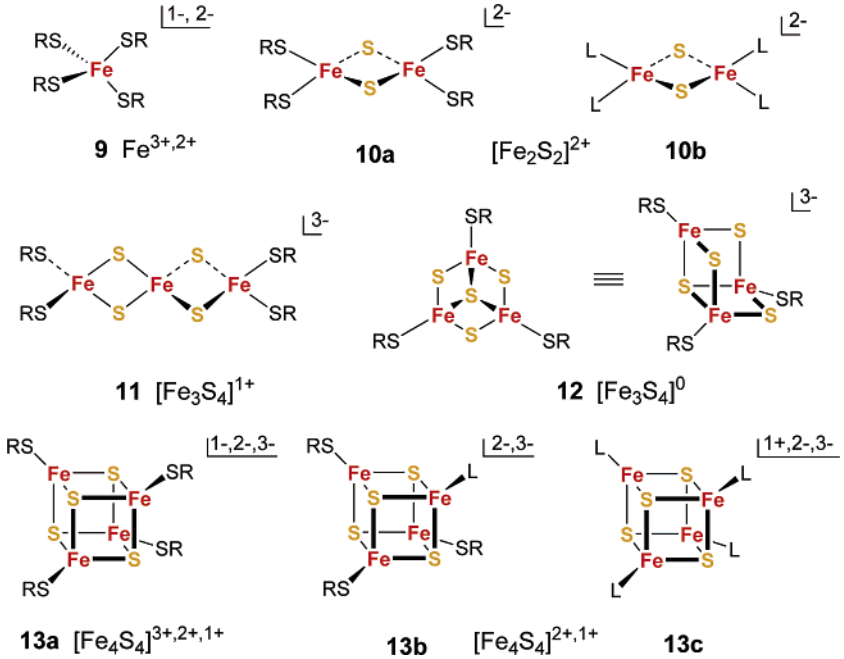

Figure 2. Synthetic analogues of protein sites containing one (**9**), two (**10a**), three (**11**, **12**), and four (**13ab**) iron atoms. Known oxidation states in isolated compounds are indicated. Clusters **10b** and **13c** with L = RO^-, halide, and other non-thiolate ligands are not analogues but are included to indicate the substantial number of known clusters of these types. In **13bc**, L is neutral or a monoanion.

by protein structure. Indeed, iron−sulfur protein sites provided a strong incentive for the initiation and development of the synthetic analogue strategy in the beginnings of what is now bioinorganic chemistry.

Within the four-year period 1972−1975, analogues of the three recognized protein sites were prepared. The first was **13a**, obtained in 1972 as $[Fe_4S_4(SCH_2Ph)_4]^{2-}$ and shown to have a cubane-type

Table 1. Evolution of Iron−Sulfur Analogue Chemistry

	developments	refs
1972−1973	$[Fe_4S_4(SR)_4]^{2-}$	8, 24
1973−1975	$[Fe_2S_2(SR)_4]^{2-}$	25, 26
1974	contact-shifted ^{1}H NMR spectra	27
1974	$[Fe_4S_4]$ multiple oxidation states	28
	thiolate ligand substitution	29, 30
	$[Fe_4S_4]$ Cys peptides	31
1975−1977	water-soluble Fe_4S_4 clusters	32−34
1975−1977	$[Fe(SR)_4]^{-,2-}$	9, 35−37
1975−1978	$[Fe_2S_2]$ and $[Fe_4S_4]$ protein core extrusion	38−40
1977−1978	$[Fe_4S_4(SR)_4]^{3-}$	41, 42
1981	pathways of $[Fe_4S_4(SR)_4]^{2-}$ formation	43
1982−1983	$[Fe_3S_4(SR)_4]^{3-}$ (linear)	22, 44
1983−1986	$[Fe_2S_2]$ Cys peptides	45−47
1985−1986	$[Fe_4S_4(SR)_4]^{-}$	48, 49
1986−1987	site-differentiated $[Fe_4S_4]$ clusters	50, 51
1988−1990	cuboidal Fe_3S_4 cluster fragment	52−54
1991	synthetic Fd	55, 56
1993−1996	$[Fe_4S_4]-S-Fe^{III}$ bridged assemblies	57−59
1994	synthetic Rd	60
1995−1996	$[Fe_3S_4(SR)_3]^{3-}$ (cuboidal)	20, 61
1995−1997	metal incorporation in Fe_3S_4 cores	20, 62
1998−1999	$[Fe_4S_4]$ Cys-peptide maquettes	63, 64
2001−2002	$[Fe_4S_4]$ bridged assemblies: peptide scaffolds	65, 66

structure.[8] Protein-bound Fe_4S_4 sites were identified in the same year. In 1973, **10a** was prepared in the form of $[Fe_2S_2(S_2\text{-}o\text{-xyl})_2]^{2-}$ with a planar rhombic core. Property comparisons then and subsequently further supported site **2a**, which was finally confirmed by crystallography of a chloroplast-type Fd in 1978.[7] In 1975, the Rd_{ox} analogue $[Fe(S_2\text{-}o\text{-xyl})_2]^{-}$ was reported.[9] The sequence of analogue preparations proceeded in the reverse order to structural complexity and does not include 3-Fe sites, which were discovered later. The existence of protein-bound trinuclear sites was first recognized in the 7-Fe protein *Azotobacter vinelandii* Fd I in 1980 by Mössbauer spectroscopy[10,11] and crystallography[12] and in inactive aconitase in 1985 by crystallography;[13] neither the sulfur content nor the structure of the site could be deduced at the time. The initial crystallographic results for *Av* Fd I were interpreted in terms of an Fe_3S_3 ring structure,[14,15] which was subsequently corrected in 1988−1989 to the cuboidal cluster **4**.[16−18] This cluster was also crystallographically established in inactive aconitase in 1989.[19] Cuboidal analogue cluster **12** was not prepared until 1995 and, as will be seen, requires a special ligand structure for stabilization.[20] Protein-bound linear cluster **3** was first detected in a partially unfolded form of aconitase in 1984[21] and was identified by a comparison of spectroscopic properties with those of synthetic cluster **11** (R = Et), which had been prepared several years earlier.[22] Since then, linear clusters have been found in several other proteins, and one cluster has been structurally analyzed by Fe K-edge EXAFS.[23]

The chronology of major developments in iron−sulfur analogue chemistry is set out in Table 1. As already noted, developments began with the synthesis and characterization of analogues of Rd and Fd sites. Other particularly noteworthy findings in the 1972−1977 period include well-resolved ^{1}H NMR spectra of paramagnetic species whose isotropic shifts are mainly contact in origin, and demonstration of thiolate ligand substitution reactions, which have led to the synthesis of a broad range of Fe_2S_2 and Fe_4S_4 analogues. Isolation of reduced Fe_4S_4 clusters in 1977−1978 provided the first analogues of Fd_{red} sites. Delineation of the pathways of formation of Fe_4S_4 clusters in 1981 provides one of the few examples in cluster chemistry generally where sequential reactions and their products leading to cluster formation have been identified. The first example of a trinuclear cluster, linear Fe_3S_4, was obtained in 1982−1983, and the first and only isolated analogue of a high-potential cluster was achieved in 1985. This was followed in 1986−1987 by the development of 3:1 site-differentiated clusters, intended as analogues for the similarly differentiated protein sites in **13b** with the property of site-specific ligand substitution. The first and only isolated cuboidal cluster was prepared and investigated in 1995−1996. It was presaged by the earlier preparations (1988−1990) of tetranuclear Fe_4S_4 and $MoFe_3S_4$ clusters in which one iron and the molybdenum site, respectively, were rendered diamagnetic by appropriate ligation, leaving the Fe_3S_4 cluster fragment magnetically isolated. In 1998−2002, cysteinyl peptides more physiologically realistic than those in the earliest experiments (1974), including some with a Fd consensus sequence, were used in the binding of Fe_4S_4 clusters. While not strictly an analogue, the chronology does acknowledge a purely synthetic Fd, indistinguishable from the native protein, obtained in 1991. The chronology, only parts of which are noted here, makes evident the substantial advancement in the subject and the increasing sophistication of analogue systems.

This account describes the leading developments in the chemistry of analogue complexes of the protein sites **1**−**6** since the beginning of the field in 1972. Narratives of the early synthetic analogue research are available,[67−69] as well as subsequent reports in 1982[70] and 1992.[71] Further sources should be consulted for more general reviews of iron−sulfur cluster chemistry.[72,73] Here we accentuate synthesis, structure, reactivity, and limited comparisons with certain protein site properties. Methods of cluster synthesis are additionally considered in a related article in this issue.[74] Bonding and electronic structure are not examined in detail. Throughout, *cluster* refers to the entire molecule $[Fe_mS_pL_l]^z$ with terminal ligands L and charge *z*, and *core* to the Fe_mS_p portion thereof. Redox potentials of analogues are referenced to the standard calomel electrode. Lastly, the collection of protein sites in Figure 1 does not include the hybrid cluster (or "prismane") proteins,[75,76] whose function is obscure and for which there are no site analogues.

In the following sections, analogues are compiled in Tables 2−5 with references to their preparations (P) and selected properties, which include absorption spectra (AS), oxidation−reduction (E) circular dichroism (CD) and magnetic circular dichroism spectra (MCD), magnetism (Mg), Mössbauer spectra (Mb), EPR and NMR spectra, X-ray absorption spectra (XAS), and X-ray crystal structures (XR). While

Table 2. $[Fe(SR)_4]^{-,2-}$ Analogues of Rubredoxin Sites

	R	properties	refs
Fe(III)	Me	P, AS, E, XR	77
	Et	P, AS, E, XR	77, 78
	Pr^i	P, AS, E	77
	o-xyl[b]	P, AS, E, EPR, Mb, XAS, XR	9, 37, 79−81
	Ph	P, AS, E, XR	77, 78, 82
	2,3,5,6-Me_4C_6H	P, AS, E, EPR, MCD, XR	77, 80, 82−84
	2,4,6-$Pr^i_3C_6H_2$	P, AS, E, XR	77, 80, 85
	Cys peptides[a]	AS	86−88
Fe(II)	Et	P, AS, NMR	22
	CH_2CH_2OH	P, E, EPR, Mb	89
	CH_2CONMe_2	P, E, XR	90
	o-xyl[b]	P, AS, E, Mb, XAS, XR	9, 37, 79, 81, 91
	Ph	P, AS, Mg, Mb, XR	35, 36, 43, 92
	2-PhC_6H_4	P, AS, MCD, XR	93, 94
	2-$NH_2C_6H_4$	P, E, NMR, XR	95
	4-XC_6H_4 (X = F, CF_3)	P, NMR	96
	2-$(RCONH)C_6H_4$ (R = Me, CF_3, Bu^t, Ph_3C)	P, E, NMR, XR	97, 98
	2,6-$(RCONH)_2C_6H_3$ (R = Me, CF_3)	P, E, NMR	98
	4-$(MeCONH)C_6H_4$	P, E, NMR	98
	Cys peptides[a]	AS, CD, MCD, NMR	99−104

[a] Generated in solution. [b] Bidentate.

inclusive of all major analogues types, the compilations are not exhaustive. The emphasis is on *isolated* compounds, which are generally obtained as dioxygen-sensitive quaternary ammonium or phosphonium salts. Nearly all complexes are prone to oxidation or oxidative decompostion in solution. Peptide complexes are included; these have prepared in solution but not isolated.

2. Rubredoxin Site Analogues

A list of analogues **9** of oxidized and reduced Rd protein site **1** is available in Table 2.

2.1. Preparation

Analogues in the Fe^{II} (Rd_{red}) and Fe^{III} (Rd_{ox}) oxidation states are readily obtained. Reduced site analogues are generally accessible through the simple reaction 1 in methanol or ethanol, followed by precipitation with an appropriate cation. Controlled

$$FeCl_2 + 4RS^- \rightarrow [Fe(SR)_4]^{2-} + 2Cl^- \qquad (1)$$

oxidation can afford the oxidized analogue. These two reactions were utilized in the synthesis of the analogues $[Fe(S_2\text{-}o\text{-}xyl)_2]^{2-,-}$.[9,37] However, species of the type $[Fe(SR)_4]^-$ are often not stable. The system $FeCl_3$/3.5NaSPh in ethanol develops immediately an intense black color which fades to yellow-brown within minutes. From this solution, the cage complex $[Fe_4(SPh)_{10}]^{2-}$ was isolated in 80% yield.[43] With excess thiolate, a transient red-violet color is developed followed by the formation of $[Fe(SPh)_4]^{2-}$. The situation is improved in the presence of a precipitating cation and/or a sterically bulky thiolate. Thus, $[Fe(SC_6H\text{-}2,3,5,6\text{-}Me_4)_4]^-$ can be isolated in the presence of Et_4N^+,[82] and intensely red $[Fe(SC_6H_2\text{-}2,4,6\text{-}Pr^i_3)_4]^-$ is described as stable for 24 h in methanol prior to isolation as the Ph_4P^+ salt.[85] Instability presumably arises from the redox reaction $Fe^{III}(SR) \rightarrow Fe^{II} + {}^1/_2RSSR$, which accounts for the bleaching of Fe^{III} solutions in the presence of thiolate. If the reaction is bimolecular,[105] decreased rates of formation of Fe^{II} are expected with large thiolates. A general solution to the problem has been found by means of ligand substitution reaction 2 with excess thiol, which affords stable Fe^{III} products with R = alkyl and aryl.[77,78] The starting phenolate complex

$$[Fe(OC_6H_3\text{-}2,6\text{-}Me_2)_4]^- + 4RSH \rightarrow [Fe(SR)_4]^- + 4\ 2,6\text{-}Me_2C_6H_3OH \qquad (2)$$

is difficult to reduce ($E_{1/2}$ = −1.30 V); phenolate ligation presumably stabilizes Fe^{III} up to the final step of ligand substitution. These reactions and variations thereof have made available an ample set of oxidized and reduced analogues for structural and electronic investigations.

2.2. Structures

From the large body of X-ray structures of both proteins and analogues, several pertinent observations are provided in Figure 3, where the preferential tetrahedral stereochemistry of four-coordinate $Fe^{III,II}$ with weak field ligands is the dominant feature. Here, oxidized and reduced structures in two proteins, *Clostridium pasteurianum* (*Cp*) $Rd_{ox,red}$[106] and *Pyrococcus furiosus* (*Pf*) Rd_{ox}[107] and Rd_{red},[108] are compared with each other and with those of oxidized and reduced analogues.[37,77,92] Although comparisons in this and other figures involve determinations with variable accuracies and different temperatures, bond lengths are sensibly consistent within the ranges $Fe^{III}-S$ = 2.25−2.31 Å and $Fe^{II}-S$ = 2.29−2.39 Å. On the basis of tetrahedral Shannon radii,[109] a bond length difference of ca. 0.1 Å is expected between oxidation states in the absence of other effects. For

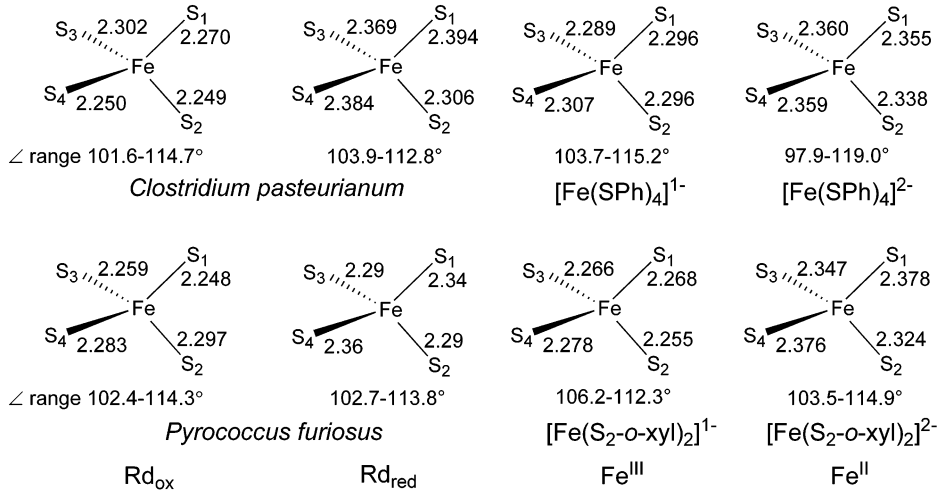

Figure 3. Comparisons of bond lengths (Å) and bond angles (deg) in the $Fe-S_4$ units of two oxidized and reduced rubredoxins and of two synthetic analogues. Protein structures were determined at resolutions of 1.5 (*Cp* Rd), 0.95 (*Pf* Rd_{ox}), and 1.8 Å (*Pf* Rd_{red}). Where given, esd's on protein bond lengths and angles are 0.03 Å (*Cp* Rd_{ox}) and 0.003 Å and 0.1° (*Pf* Rd_{ox}). Values for analogue complexes are 0.002−0.006 Å and 0.07−0.3°.

analogues, whose structures are better compared because of smaller errors, bond length differences are 0.06 and 0.09 Å for $[Fe(SPh)_4]^{-,2-}$ and $[Fe(S_2\text{-}o\text{-}xyl)_2]^{-,2-}$, respectively. The apparently large bond distance spread of ca. 0.2 Å in *Cp* Rd_{ox} in an earlier determination to 2.5 Å resolution[1] has disappeared in the more accurate structure. While bond angles are in general expected to be more dependent on protein environment, ranges between proteins and analogues are comparable, with the exception of $[Fe(SPh)_4]^{2-}$.[92] The S_2-*o*-xyl ligand was originally used[9] because the flexibility of its seven-member chelate ring does not impose significant constraints of bond angles or distances. Inspection of the full body of analogue structural data indicates that small deviations from tetrahedral symmetry arise from crystal effects. The compounds $(Et_4N)[Fe(SMe)_4]$ and $(Pr_4N)[Fe(SEt)_4]$[77] and $(Et_4N)_2[Fe(S\text{-}2\text{-}PhC_6H_4)_4]$[94] occur with S_4 crystallographic symmetry. The FeS_4 coordination units have precise D_{2d} symmetry, with one independent Fe−S bond length and two independent S−Fe−S angles. The complexes are tetragonally compressed along the S_4 axis. Values of these parameters fall close to or within the ranges for analogues in Figure 3. The FeS_4 unit in $[Fe(SEt)_4]^-$ exhibits exceedingly slight deviations from T_d symmetry, with Fe−S = 2.269(1) Å and S−Fe−S = 109.36(5)° and 109.69(9)°. This complex is the most highly symmetrized of any Rd analogue. The collective analogue structural data reveal random distortions from a perfect tetrahedral geometry and indicate that distortions of the sites **1** are not exceptional and are imposed by the protein in a manner not unlike crystal packing forces in analogue compounds. In one of the most accurate Rd_{ox} structures (1.0 Å resolution), bond distances are 2.27−2.30 Å and bond angles show an appreciable spread, 105−115°.[110] Additional considerations of the relation of analogue and protein site structures are available elsewhere.[80] As is evident from Figures 1 and 2, iron sites in all proteins and analogues manifest (distorted) tetrahedral stereochemistry.

2.3. Properties

Analogue complexes support redox reaction 3, which is generally reversible in aprotic solvents. Potentials exhibit the expected substituent dependence, as indicated by the abbreviated series 4 in acetonitrile.[22,37,77,90] Intramolecular N−H···S hydrogen bonding is reported to produce positive potential shifts relative to the $[Fe(SPh)_4]^{-/2-}$ couple.[97,98]

$$[Fe(SR)_4]^- + e^- \rightarrow [Fe(SR)_4]^{2-} \quad (3)$$

$$R = Pr^i\,(-1.11) < Et\,(-1.08) < o\text{-xyl}\,(-1.03) < 2,3,5,6\text{-}Me_4C_6H\,(-0.85) < CH_2CONMe_2\,(-0.71) < Ph\,(-0.52\ V) \quad (4)$$

In one example, the potential for the couple with R = 2-$(MeCONH)C_6H_4$ is 0.25 V more positive, and that for the couple with R = 4-$(MeCONH)C_6H_4$ is 0.04 V more negative, than the reference potential in acetonitrile.[98] Further, certain Cys peptide complexes in aprotic solvents exhibit potentials much more postive that those of alkanethiolate complexes. For example, in acetonitrile the potential of the couple $[Fe(Z\text{-Cys-Pro-Leu-Cys-OMe})_2]^{-/2-}$ is −0.54 V, compared to, e.g., −1.08 V for $[Fe(SEt)_4]^{-/2-}$.[101] The direction of the shift is that expected inasmuch as hydrogen bond formation should stabilize the more reduced form by helping dissipate added negative charge. Furthermore, the couple $[Fe(SCH_2CH_2OH)_4]^{-/2-}$ has $E_{1/2} = -0.35$ V in aqueous solution,[89] where solvation and hydrogen-bonding effects operate. When referenced to the SHE, the potential is −0.11 V, very close to the 0.10 to −0.10 V range of most native Rd proteins.

Other properties of Fe^{III} ($e^2t_2^3$, $S = {}^5/_2$) and Fe^{II} ($e^3t_2^3$, $S = 2$) complexes are consistent with the indicated spin states and approach those of protein sites in the same oxidation state. Alkylthiolate and peptide complexes display the same spectral patterns in the visible region as do Rd_{ox} and Rd_{red}.[9,37,77,101,102] Isotopomers of $[Fe(SR)_4]^-$ complexes have been quite

Table 3. $[Fe_2S_2(SR)_4]^{2-,3-}$ Analogues of Protein Sites

	R	properties	refs
$[Fe_2S_2]^{2+}$	Me	P, AS	112
	Et	P, AS, E, NMR, XAS	22, 112, 120, 121
	Bu^t	P, AS, NMR	47
	o-xyl[a]	P, AS, E, Mg, Mb, NMR, XAS, XR	25, 26, 79, 122 113, 120, 123, 124
	Ph	P, AS, E, Mg, NMR, XAS	26, 41, 113, 122 43, 120, 125
	3-, 4-$CF_3C_6H_4$	P, AS, E	126
	4-ClC_6H_4	P, AS, E, XR	26, 127
	4-FC_6H_4	P, NMR	96
	4-MeC_6H_4	P AS, E, NMR XR	26, 43, 113
	4-$NMe_3C_6H_4$[b]	P, AS, E	26
	2,4,6-$Me_3C_6H_2$	P, AS, E, NMR, XR	128
	2-$(RCONH)C_6H_4$[c]	P, E, NMR	129
	2,6-$(RCONH)_2C_6H_3$[c]	P, E, NMR, XR	129
	S_3[d]	P, XR	118, 130, 131
	Cys peptides[e]	AS, CD, EPR, NMR	45−47, 103, 132
$[Fe_2S_2]^{+}$	*o*-xyl[a]	EPR, Mb	123, 124, 133
	4-XC_6H_4 (X = H, Me, Cl)	EPR	134
	2,2′-$C_{12}H_8$[a]	EPR	134

[a] Bidentate. [b] Cluster charge 2+. [c] R = Me, Bu^t, CF_3. [d] S_5^{2-} bidentate ligand. [e] Generated in solution.

useful in vibrational assignments using normal coordinate analysis with a consistent force field for the complexes.[111] Complexes with crystallographic S_4 symmetry have proven highly amenable to polarized single-crystal absorption, MCD, and EPR spectroscopic measurements, leading to ground- and excited-state assignments for oxidized ($[Fe(SC_6H$-2,3,5,6-$Me_4)_4]^-$)[84] and reduced ($[Fe(SC_6H_4$-2-$Ph)_4]^{2-}$)[93] complexes. Using sulfur K-edge XAS, Fe−S bond covalency in three Rd_{ox} proteins have been found to be slightly less than that in $[Fe(S_2$-*o*-$xyl)_2]^-$, possibly due to N−H···S hydrogen bonding in the proteins.[81] Decreased covalency should lead to a higher effective nuclear charge on the metal and a positive potential shift. When analogue potentials are referenced to the SHE, they are always more negative than protein values. Note that the $[Fe(SCH_2CH_2OH)_4]^{-/2-}$ potential is seemingly just outside the low end of the protein range. However, comparisons are difficult because of differences in solvent media and noncovalent electrostatic interactions present in proteins but not in synthetic complexes. These studies emphasize one of the advantages of synthetic analogues. As noted already, analogues of all sites convey intrinsic properties. Deviations from the corresponding protein properties imply an influence of protein structure and environment different from solvent or crystalline perturbations and may allow identification of the protein effect. Positive potential shifts arising from hydrogen bonding is one such case, as has been tested by the synthesis of analogues without and with intramolecular hydrogen bonding. Lastly, Mössbauer spectroscopic parameters are very similar to those of the proteins. Data for protein site analogues are presented in section 6.

3. Analogues of Binuclear (Fe_2S_2) Sites

Analogues **10a** of binuclear site **2a** are collected in Table 3.

3.1. Preparation

Reactions 5−9 are the principal methods leading to analogues **10a** with the fully oxidized $[Fe_2S_2]^{2+}$ core.

$$2FeCl_3 + 4RS^- + 2HS^- + 2MeO^- \rightarrow [Fe_2S_2(SR)_4]^{2-} + 6Cl^- + 2MeOH \quad (5)$$

$$2[Fe(SR)_4]^{2-} + 2S \rightarrow [Fe_2S_2(SR)_4]^{2-} + RSSR + 2RS^- \quad (6)$$

$$2[Fe(SR)_4]^{-} + 2S \rightarrow [Fe_2S_2(SR)_4]^{2-} + 2RSSR \quad (7)$$

$$[Fe_2S_2(SR)_4]^{2-} + 4R'SH \rightleftharpoons [Fe_2S_2(SR')_4]^{2-} + 4RSH \quad (8)$$

$$[Fe_2S_2X_4]^{2-} + 4RS^- \rightarrow [Fe_2S_2(SR)_4]^{2-} + 4X^- \quad (9)$$

Reaction 5 is the route to the first such analogue, $[Fe_2S_2(S_2$-*o*-$xyl)_2]^{2-}$.[25,26] However, it is not generally useful with monodentate thiolates, leading instead to the formation of $[Fe_4S_4(SR)_4]^{2-}$ (section 5.3). Reactions 6 and 7 are examples of cluster assembly that utilize sulfur as a source of sulfide and thiolate and Fe^{II} or thiolate alone as reductants.[22,73,112] Given the generality of reaction 2, reaction 7 is one of considerable scope. Related reactions affording **10a** from $FeCl_3$, sulfur, and NaSR are available.[113] Equilibrium ligand substitution reaction 8 has proven extremely useful.[26] The reaction is essentially stoichiometric when R = alkyl and R′ = aryl, acidic thiols being the more effective reactants. However, the reaction can be fully displaced to product by a sufficient excess of reactant thiol and/or removal of product thiol from the reaction mixture. Applications include the formation of $[Fe_2S_2(SPh)_4]^{2-}$ from $[Fe_2S_2(S_2$-*o*-$xyl)_2]^{2-}$ [26] and Cys peptide complexes from $[Fe_2S_2(SBu^t)_4]^{2-}$.[47] Treat-

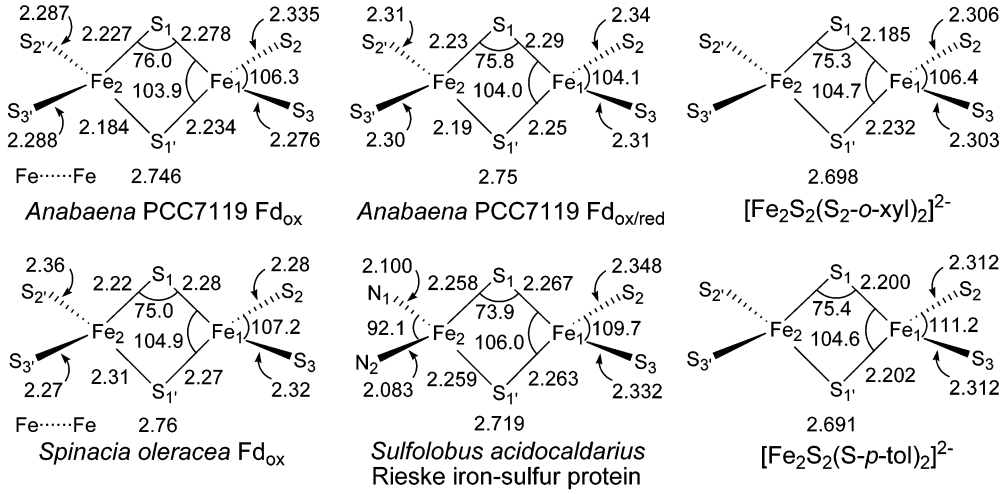

Figure 4. Comparisons of bond distances (Å) and angles (deg) in the $Fe_2(\mu_2\text{-}S)_2S_4$ portions of *Anabaena* Fd_{ox} (1.3 Å) and Fd_{red} (1.17 Å), spinach Fd_{ox} (1.7 Å, Glu92Lys mutant), and two synthetic analogues. Also included is the site in a Rieske protein (1.1 Å). Structures were determined at the indicated resolutions. Average protein bond angles are given; esd's are in the range 0.05−0.3° and 0.001−0.007 Å for most bond lengths. The crystal of *Anabaena* $Fd_{ox/red}$ is partially reduced; bond lengths are the average values of two independent molecules. Analogue complexes are centrosymmetric with esd's in the range 0.001−0.002 Å and 0.04−0.05°. All structures are of the $[Fe_2S_2]^{2+}$ oxidation state, except for the mixed sites in *Anabaena* $Fd_{ox/red}$.

ment of **10a** with 4 equiv of an acid halide affords $[Fe_2S_2X_4]^{2-}$.[114] These clusters constitute one of two sets of nonanalogue complexes **10b** (L = halide, ArO^- [115−117]) which are useful in syntheses of **10a**. They are also available by self-assembly reactions.[118] The prototype cluster is $[Fe_2S_2Cl_4]^{2-}$,[114,119] whose chloride ligands are readily displaced in reaction 9 to afford a variety of analogues including those binding Cys peptides (Table 3). From these methods, an extensive set of analogues has become available for further investigation.

3.2. Structures

The structural database for proteins with binuclear sites **2ab** (including both Fd's and Rieske proteins) is somewhat larger than that for the analogues **10a**. In Figure 4, the site structures of three proteins[135−137] and two analogues[26] are compared. All structures refer to the oxidized $[Fe_2S_2]^{2+}$ core except *Anabaena* $Fd_{ox/red}$.[136] The crystal of this protein is described as partially reduced, with about one-half of the protein molecues in the $[Fe_2S_2]^+$ state. Analogue core structures contain distorted tetrahedral Fe^{III} atoms in an Fe_2S_2 rhomb, planar (D_{2h}) and nonplanar forms of which are the fundamental building blocks in iron−sulfur cluster chemistry.[73] Rhombs in both proteins[136,138] and analogues[129] do show small nonplanar deviations from D_{2h} symmetry. There is a small tendency of the protein clusters toward longer Fe−Fe distances, also found in a green algal Fd_{ox} structure (2.733(7) Å) at 1.4 Å resolution.[139] In nearly all structures of complexes **10ab** with a variety of terminal ligands, metal−metal separations occur in the narrow interval of 2.69−2.71 Å. A similar trend in protein core Fe−S distances is less clear, particularly in view of the 2.16(1)−2.22(1) Å range in the algal protein and bovine adrenodoxin.[138] Rhomb dimensions in synthetic complexes have been discussed earlier.[140]

The structure of spinach Fd_{ox} (as the Glu92Cys mutant) is included in Figure 4 as a matter of historical interest because the correct structure of the binuclear site was deduced from the physical properties of this protein in advance of an X-ray structure. Indeed, the structure of the first site analogue, $[Fe_2S_2(S_2\text{-}o\text{-}xyl)_2]^{2-}$, preceded by 5 years the initial crystallographic identification of protein site **2a**. Overall, analogues accurately simulate all important structural features of Fd_{ox} sites. Additional accurate protein structures are required to determine whether bond distances and angles of **2a** will more closely approach convergence with analogue values. Structural comparisons cannot yet be made for Fd_{red} and analogues. While the reduced analogues $[Fe_2S_2(SR)_4]^{3-}$ have been prepared in solution (Table 3), none has been isolated. Non-disordered structures of the $[Fe_2S_2]^+$ oxidation state are expected to reflect the trapped valence $Fe^{III}Fe^{II}$ configuration determined spectroscopically for all reduced proteins and analogues.

3.3. Properties

The most clearly established function of protein sites **2a** is electron transfer utilizing the couple $[Fe_2S_2]^{2+/+}$, which usually operates at $E_0' \approx -0.42$ V vs SHE.[141] Consequently, considerable interest attends the range of the analogue electron-transfer series and the stability of its members. The reversible three-member series 10 has been demonstrated for complexes such as $[Fe_2S_2(S_2\text{-}o\text{-}xyl)_2]^{2-}$ ($E_{1/2} = -1.49$, -1.73 V) and $[Fe_2S_2(SPh)_4]^{2-}$ ($E_{1/2} = -1.13$, -1.41 V) in DMF or acetonitrile.[26,125] The complexes $[Fe_2S_2\text{-}$

$$[Fe_2S_2(SR)_4]^{4-} \leftrightarrow [Fe_2S_2(SR)_4]^{3-} \leftrightarrow [Fe_2S_2(SR)_4]^{2-} \quad (10)$$

$(SC_6H_3\text{-}2,6\text{-}(NHCOR)_2)_4]^{2-}$ exhibit quasireversible reductions in acetonitrile, whose potentials are shifted appreciably positive of the potential of the $[Fe_2S_2(SPh)_4]^{2-/3-}$ couple. This effect originates in part from intramolecular N−H···S hydrogen bonding.[129] The instability of the first reduction product arises

because the $[Fe_2S_2]^+$ core has the same oxidation state as $[Fe_4S_4]^{2+}$, which is evidently the more stable structure, as shown by the spontaneous occurrence of reaction 11. The formation of $[Fe_4S_4(SR)_4]^{2-}$ from

$$2[Fe_2S_2(SR)_4]^{3-} \rightarrow [Fe_4S_4(SR)_4]^{2-} + 4RS^- \quad (11)$$

$[Fe_2S_2(SR)_4]^{2-}$ can also occur by internal redox reaction 12, which proceeds slowly in partially aqueous or methanolic solvents. Specifically, the results

$$2[Fe_2S_2(SR)_4]^{2-} \rightarrow [Fe_4S_4(SR)_4]^{2-} + 2RS^- + RSSR \quad (12)$$

demonstrate that $[Fe_2S_2(SPh)_4]^{2-}$ in protic and $[Fe_2S_2(SPh)_4]^{3-}$ in aprotic media spontaneously convert to the cubane-type cluster $[Fe_4S_4(SPh)_4]^{2-}$.[41,43] No $[Fe_2S_2]^+$ or $[Fe_2S_2]^0$ cluster, which would be extremely easily oxidized, has been isolated in substance. The all-ferrous state has been realized in a protein but is unlikely to be physiologically significant. Reaction of spinach Fd_{ox} or *Aquifex aeolicus* with 1 equiv of a Cr^{II} macrocylic complex generates the $[Fe_2S_2]^+$ state in an inner-sphere reaction. The binding of product Cr^{III} apparently perturbs the protein such as to allow reduction to the $[Fe_2S_2]^0$ state with a second equivalent of Cr^{II} in an outer-sphere process with no Cr^{III} binding.[142,143]

As required by close structural correspondence, electronic features of the proteins are approached by analogue clusters. In oxidized analogues and Fd_{ox}, the two Fe^{III} ($S = {}^5/_2$) centers are antiferromagnetically coupled to give an $S = 0$ ground state with occupancy of higher spin states,[122] which are responsible for the occurrence of isotropically shifted ^1H NMR spectra.[22,113,122,126] As already noted, $[Fe_2S_2]^+$ clusters have not been isolated; however, they have been prepared in solution by chemical reduction of $[Fe_2S_2(SR)_4]^{2-}$ (Table 3). They closely resemble Fd_{red}, with an $S = {}^1/_2$ ground state from antiferromagnetic coupling of the $S = {}^5/_2$ and $S = 2$ centers and axial or rhombic EPR spectra centered near $g \approx 1.94$. An important property determined in early Mössbauer spectroscopic studies of Fd_{red}[144] is the existence of *trapped* $Fe^{III}Fe^{II}$ valence states. At 4.2 K, isomer shifts of Fd_{ox} are typically 0.25−0.30 mm/s. Spectra of Fd_{red} consist of two quadrupole doublets with $\delta(Fe^{III}) = 0.20-0.35$ mm/s and $\delta(Fe^{II}) \approx 0.60-0.75$ mm/s. For $[Fe_2S_2(S_2\text{-}o\text{-xyl})_2]^{2-}$, $\delta = 0.29-0.31$ mm/s in the solid and solution;[123] the reduced cluster has $\delta(Fe^{III}) = 0.33$ mm/s and $\delta(Fe^{II}) = 0.7$ mm/s in solution.[124] Here analogues provide the important experimental proof that the trapped valence state is an intrinsic property and does not arise from protein effects. However, this situation is subject to change upon certain perturbations of the $[Fe_2S_2]^+$ core. Single Cys/Ser mutations of coordinating residues produce small changes in the absorption and resonance Raman spectra of *Cp* Fd_{ox}, consistent with serinate ligation, and in the EPR spectra of Fd_{red}.[145] Unexpectedly, the mutations afford a mixture of clusters in the reduced protein, one with a normal trapped-valence $S = {}^1/_2$ ground state and the other with an $S = {}^9/_2$ ground state, as determined from MCD[146] and Mössbauer spectra.[147,148] The latter contains an $Fe^{2.5+}Fe^{2.5+}$ delocalized pair and arises from the phenonenon of double exchange (spin-dependent resonance delocalization) also found in Fe_3S_4 and Fe_4S_4 clusters.[149,150] The proportion of states is temperature-dependent. In the Cys56Ser variant at 4.2 K, the two states are present in about equal amounts. At 200 K, the delocalized state is ca. 90% populated. This behavior is interpreted in terms of increased intramolecular electron-transfer rates between the two iron atoms in the $S = {}^1/_2$ cluster, resulting in conversion to the delocalized cluster.[148] While similar behavior has been found in several synthetic binuclear iron complexes, no $[Fe_2S_2]^+$ cluster with a delocalized ground state has yet been prepared. The existence of two states must have its origin in structure, but the structural factors, possibly involving protein conformation in and around the site, have not been identified.

Analogue clusters have proven to be useful objects in the determination of Fe−S bond covalency using sulfur K-edge XAS.[121,151] Among the conclusions from this work are the following: (i) Fe−(μ_2-S) covalency is substantially higher than Fe−SR covalency; (ii) redox potentials decrease as total covalency per iron atom increases in the order $[Fe_2S_2Cl_4]^{2-/3-} < [Fe_2S_2(SPh)_4]^{2-/3-} < [Fe_2S_2(SEt)_4]^{2-/3-} < [Fe_2S_2(S_2\text{-}o\text{-xyl})_2]^{2-/3-}$; (iii) sulfide covalency is less in spinach Fd_{ox} than in the analogue $[Fe_2S_2(SEt)_4]^{2-}$, the probable cause being N−H···S hydrogen bonding in the protein. Here, three intuitive properties are directly supported by experiment.

3.4. Heteroligated Clusters

The complex $[Fe_2S_2Cl_4]^{2-}$ is a very useful starting material for the synthesis of other binuclear clusters **10b** by ligand substitution analogous to reaction 9. The cluster $[Fe_2S_2(OPh)_4]^{2-}$ and other binuclear species with areneoxide ligands were prepared in this way.[115−117] Related reactions 13 with bidentate ligands have afforded a series of chelate clusters with N_2O_2, N_2S_2, and O_2S_2 terminal ligation furnished by the deprotonated forms of molecules such as 2-(methylene-2-hydroxyphenyl)benzimidazole, 2-(2-mercaptophenyl)benzimidazole, and 2-mercaptobenzoic acid, respectively.[117,152,153] Spectroscopic and redox proper-

$$[Fe_2S_2Cl_4]^{2-} + 2(L-L)^{-,2-} \rightarrow [Fe_2S_2(L-L)_2]^{0,2-} + 4Cl^- \quad (13)$$

ties are consisent with the indicated formulation, which has been proven for one O_2S_2 complex by an X-ray structure.[117] Interest in heteroligated binuclear clusters arises from the biological occurrence of site **2b** (Figure 1). These clusters are found in Rieske proteins[154] and deviate from the normal binuclear sites in having two imidazole ligands from His residues bound to the same iron atom. This coordination mode has been established by spectroscopy and crystallography. The structure of the site in the soluble domain of an archaeal Rieske protein at 1.1-Å resolution[137] is summarized in Figure 4. The core is essentially congruent with Fd_{ox} sites. As indicated by the N−Fe−N angle of 92°, the FeN_2S_2 unit is markedly distorted from tetrahedral stereochemistry. Judg-

Table 4. Linear $[Fe_3S_4(SR)_4]^{3-}$ and Cuboidal $[Fe_3S_4(LS_3)]^{3-}$ Analogues of Protein Sites

	R	properties	refs
linear $[Fe_3S_4]^+$	Et	P, AS, E, Mb, MCD, Mg, NMR	22, 44 155−157
	o-xyl	AS	22
	Ph	P, AS, E, Mb, Mg, NMR, XR	22, 44
	2,4,6-$Me_3C_6H_2$	P, AS, NMR	158
cuboidal $[Fe_3S_4]^0$	−	P, AS, E, Mb, NMR, XR	20, 61

ing from Fe−N bond distances in the pyrrolate complex $[Fe_2S_2(C_4H_4N)_4]^{2-}$ (three at 1.87−1.96 Å, one at 2.09 Å),[117] the iron atom in the protein is coordinated to neutral imidazole groups. In this case, the redox steps of the protein are $[Fe_2S_2(N{\cdot}His)_2(S{\cdot}Cys)_2]^{0/-/2-}$, with the charges contributing to generally higher first-reduction potentials of Rieske proteins compared to Fd's. While there is some overlap of potentials, it is striking that the potentials of Rieske-type clusters are ca. 300 mV more positive than those of plant Fd's.[154] At present, there are no accurate analogues of Rieske sites. Possible routes include reaction 13 using, successively, a bis(imidazole) and a bis(thiolate) ligand. Stability to disproportionation, a matter not tested with chelating ligands on an $[Fe_2S_2]^{2+}$ core, is a necessary property. Another possibility is the use of appropriately designed Cys-His peptides.

4. Analogues of Trinuclear (Fe_3S_4) Sites

Analogues **11** and **12** of protein-bound linear cluster **3** and cuboidal cluster **4**, respectively, are listed in Table 4. Structures of a linear and a cuboidal protein cluster and their analogues are provided in Figure 5.

4.1. Linear Clusters

The initial observation of a protein-bound linear cluster occurred in 1984, with a partially unfolded form of aconitase.[21] It was definitively identified by spectroscopic comparison with $[Fe_3S_4(SEt)_4]^{3-}$, which was first prepared in 1982 by reaction 14 in a systematic study of the reactions of $[Fe(SEt)_4]^{2-}$ with variable equivalents of sulfur.[44]

$$3[Fe(SEt)_4]^{2-} + 4S \rightarrow [Fe_3S_4(SEt)_4]^{3-} + {}^5/_2EtSSEt + 3EtS^- \quad (14)$$

$$[Fe_3S_4(SEt)_4]^{3-} + 4RSH \rightarrow [Fe_3S_4(SR)_4]^{3-} + 4EtSH \quad (15)$$

Ligand substitution reaction 15 afforded three other clusters, including $[Fe_3S_4(SPh)_4]^{3-}$ whose linear structure was demonstrated crystallographically with the Et_4N^+ salt.[22,44] Reaction 14 requires careful control of stoichiometry and scale.[22] Linear clusters contain the $[Fe_3S_4]^+$ core built of two Fe_2S_2 rhombs sharing a common vertex. Bond lengths and angles are very similar to those of $[Fe_2S_2]^{2+}$ clusters (Figure 4). Mössbauer spectra (δ = 0.23−0.29 mm/s at 77 K) indicate high-spin Fe^{III} sites, which are antiferromagnetically coupled to produce an $S = {}^5/_2$ ground state that exhibits Curie paramagnetism at 5−300 K.[155] Absorption and MCD spectra readily distinguish $[Fe_3S_4(SR)_4]^{3-}$ and $[Fe_2S_2(SR)_4]^{2-}$ clusters,[22,156] whereas ^1H NMR spectra are less useful in the R = Et case because of near-overlap of contact-shifted methylene

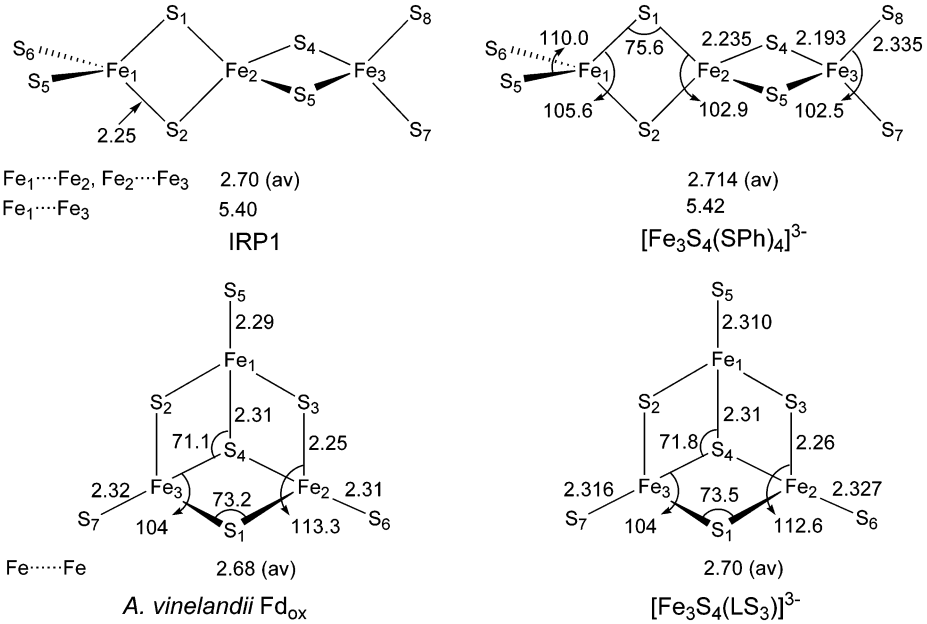

Figure 5. Geometries of the linear and cuboidal Fe_3S_4 clusters in analogues and proteins showing bond distances (Å) and angles (deg). The IRP1 bond lengths were determined by EXAFS and all others by X-ray crystallography. The crystal structure of *Av* Fd_{ox} was refined to 1.35 Å. Average values are given for distances (esd's 0.002−0.01 Å) and angles (esd's 0.1−0.3°) in the cores of protein structures. The two linear structures have the $[Fe_3S_4]^+$ oxidation state, *Av* Fd_{ox} the $[Fe_3S_4]^+$ state, and $[Fe_3S_4(LS_3)]^{3-}$ the $[Fe_3S_4]^0$ state.

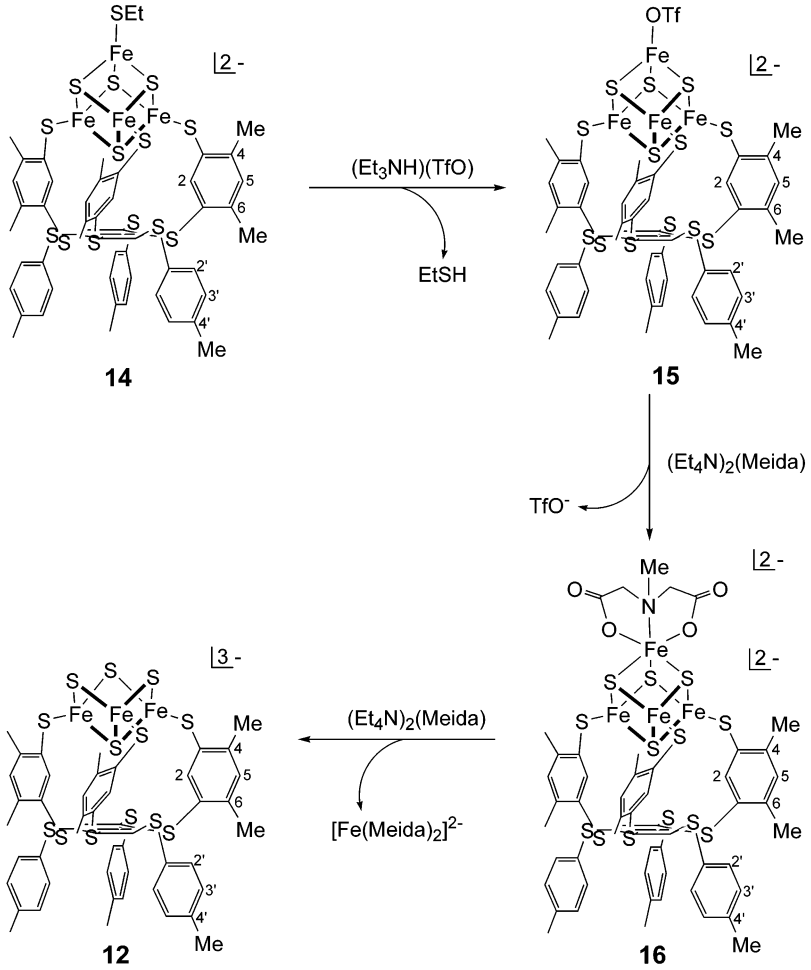

Figure 6. Synthesis of the cuboidal analogue cluster $[Fe_3S_4(LS_3)]^{3-}$ (**12**) starting from the 3:1 site-differentiated cluster $[Fe_4S_4(LS_3)(SEt)]^{2-}$ (**14**).

signals. The clusters can be reduced to the $[Fe_3S_4]^0$ level in quasi-reversible processes at rather negative potentials ($E_{1/2}$ = −1.35 V (Ph), −1.66 V (Et) in acetonitrile[22]). No reduced cluster has been isolated.

More recently, linear clusters have been claimed in a dehydratase from *Escherichia coli*,[159] in an anaerobically isolated pyruvate formate-lyase activating enzyme (10% of total iron),[160] and in an unfolded form of a bacterial 7Fe Fd.[161,162] Identification was made on the basis of absorption, MCD, or Mössbauer spectra. In contrast to these cases, a linear cluster is the only cluster present in recombinant human iron regulatory protein 1, as shown by EXAFS.[23] The average Fe−S distance and the two types of Fe−Fe distances are in excellent agreement with the synthetic cluster (Figure 5). Note that the synthesis of linear clusters preceded their recognition in proteins. It remains to be established whether linear clusters are present in proteins functioning in vivo.

A byproduct of reaction 14 is linear tetranuclear $[Fe_4S_6(SEt)_4]^{4-}$, also described as a product of the system $[Fe(SEt)_4]^{2-}/1.5S$.[163] This cluster does not correspond to any known protein site. Together with $[Fe_2S_2]^{2+}$ and $[Fe_3S_4]^{+}$ clusters, it is a solubilized fragment of the compounds M^IFeS_2 whose structure consists of linear vertex-shared FeS_4 tetrahedra with dimensions similar to those of soluble clusters.

4.2. Cuboidal Clusters

Structures of protein and analogue clusters consist of three edge-shared Fe_2S_2 rhombs which form a cuboidal cluster; i.e., a cubane cluster missing an iron atom (Figure 5). The obvious precursor to **12** is a cubane **13** by removal of an iron atom. Despite attempts in several laboratories, no stable cuboidal cluster was obtained by this or any other route with monofunctional thiolates as ligands. Indeed, an analogue of protein site **4** was not obtained until after the chemistry of mononuclear complexes **9** and clusters **10**, **11**, and **13** had been developed in considerable detail (Table 1). The eventually successful synthesis, reported in 1995−1996,[20,61] is outlined in Figure 6. The primary factor is the semirigid trifunctional cavitand ligand LS_3, designed to bind a cubane-type cluster at three points.[51,164] In the scheme, an $Fe_4S_4(SEt)$ unit is inserted by ligand substitution to give **14**, a 3:1 site-differentiated cluster. Such clusters undergo regiospecific substitution at the unique iron site. Ethanethiolate is replaced by the much more labile triflate (**15**), which in turn is displaced by *N*-methylimidodiacetate (Meida) with the formation of **16**. Reaction with additional Meida affords the desired cluster **12** as $[Fe_3S_4(LS_3)]^{3-}$, whose structure was proven by an X-ray determination. The final step is, minimally, $[Fe_4S_4]^{2+} \rightarrow [Fe_3S_4]^0 + Fe^{2+}$. Attempted removal of the core by ligand substitution

of **12** resulted in destabilization and decomposition of the cuboidal structure.[165]

Cluster **12** supports the reversible electron-transfer series 16, the first member of which contains the all-ferric oxidation state $[Fe_3S_4]^+$. The second member corresponds to a dithionite-reduced protein cluster. The most reduced member is in the $[Fe_3S_4]^-$ state,

$$[Fe_3S_4(LS_3)]^{4-} \leftrightarrow [Fe_3S_4(LS_3)]^{3-} \leftrightarrow [Fe_3S_4(LS_3)]^{2-} \quad (16)$$

which has not been established in proteins. Redox reactions of the $[Fe_3S_4]^0$ state are usually proton-linked;[166,167] the nature of reduced and protonated protein clusters below this state has not been established.

The close correspondence in average bond distances and angles between **12**[61] and *Av* Fd_{red} I,[168] both in the same oxidation state, is evident in Figure 5. Further, Fd_{red} and Fd_{ox} do not differ significantly in metric parameters (both studied at 1.4 Å resolution), consistent with a delocalized electronic structure. One synthetic cluster structure is insufficient to establish intrinsic bond parameters of the $[Fe_3S_4]^0$ core when small differences are involved. However, several observations are offered. The arrangement of the three iron atoms is close to an isosceles triangle (Fe−Fe = 2.712(2), 2.665(2), 2.731(2) Å), a feature seen in two Fd_{red} crystals, except that two distances are short and the other long (Fe−Fe = 2.73, 2.65, 2.65 Å in one crystal). This and several shorter Fe−S bonds in Fd_{red} are possible influences of the protein. Essentially the same spread of Fe−Fe separations holds in Fd_{ox}. Close relationships are also observed between synthetic $[Fe_4S_4]^{2+}/[Fe_3S_4]^0$ and protein $[Fe_4S_4]^{2+}/[Fe_3S_4]^{+,0}$ cluster structures. Removal of an iron atom from a cubane does not produce a large relaxation to a more open (or splayed) cuboidal configuration. With analogues, the mean (μ_2-S)−Fe−(μ_2-S) angle increases from 103.6° to 112.6°, and the Fe−(μ_3-S)−Fe angles contract by 2.6°. While there are other small dimensional changes, the $[Fe_3S_4]^0$ core is nearly congruent with an Fe_3S_4 fragment of $[Fe_4S_4(LS_3)Cl]^{2-}$. Two main conclusions emerge from the structural data: (i) the reorganization barrier to $[Fe_3S_4]^{+/0}$ electron transfer must be small (a structural property of **1** and all protein clusters except **7**/**8**); (ii) cuboidal fragments are well disposed to bind metal ions in the voided site with minimal structural rearrangement.

Oxidized proteins are isolated in the $[Fe_3S_4]^+$ state with an $S = {}^1/_2$ ground state, indicated by an EPR signal at $g \approx 2.02$.[11,169] One-electron reduction affords the mixed-valence $[Fe_3S_4]^0$ state. Its $S = 2$ ground state is a consequence of double exchange in a delocalized $Fe^{2.5+}/Fe^{2.5+}$ pair, giving rise to $S = {}^9/_2$, which is antiferromagnetically coupled to the $S = {}^5/_2$ spin of a valence-trapped Fe^{III} site.[170] The analogue cluster has precisely the same properties, demonstrating that this nonclassical electronic structure is an intrinsic property of an $[Fe_3S_4(SR)_3]^{3-}$ cluster.[61] While protein-bound $[Fe_3S_4]^-$ is unknown, this state can be achieved by the reaction of, e.g., Zn^{II} with an $[Fe_3S_4]^+$ protein site under reducing conditions to form $[ZnFe_3S_4]^+$, which has a spin sextet ground state. With this information, the cuboidal spin state series 17 has been established.[71,169]

$$[Fe_3S_4]^- (S = {}^5/_2) \leftrightarrow [Fe_3S_4]^0 (S = 2) \leftrightarrow [Fe_3S_4]^+ (S = {}^1/_2) \quad (17)$$

4.3. Reactivity

In addition to electron transfer, both linear and cuboidal clusters possess significant reactivity properties that afford Fe_4S_4 and heterometal MFe_3S_4 cubane-type clusters. Illustrative reactions leading to clusters **17**−**20** from linear **11** and **21**−**27** from cuboidal **12** are set out in Figure 7. Linear cluster **11** incorporates metals in redox reactions where reducing equivalents are supplied by the thiolate ligand (reactions 18 and 21) or the metal (reactions 19 and 20).[52,157,158,165,171,172]

$$[Fe_3S_4(SR)_4]^{3-} + [FeCl_4]^{2-} \rightarrow [Fe_4S_4(SR)_3Cl]^{2-} + 3Cl^- + {}^1/_2RSSR \quad (18)$$

$$[Fe_3S_4(SR)_4]^{3-} + [Ni(PPh_3)_4] \rightarrow [(Ph_3P)NiFe_3S_4(SR)_3]^{2-} + RS^- + 3PPh_3 \quad (20)$$

Although it has not been established that the Fe_3S_4 fragment remains intact in a linear to cuboidal transformation, reactions 19 and 20 may be likened conceptually to inner-sphere processes involving concerted reductive rearrangement of the trinuclear precursor and capture of the oxidized metal as M^{II}.[172] Limiting formulations of the reaction products are $[Co^{2+}(Fe_3S_4)^0]^{2+}$ ($S = {}^1/_2$) and $[Ni^{2+}(Fe_3S_4)^{1-}]^+$ ($S = {}^3/_2$), where the indicated spin state arises for antiferromagnetic coupling between tetrahedral M^{II} and the Fe_3S_4 fragment.

Minimal structural rearrangement of cuboidal cluster **12** occurs in metal-binding reactions 22−28.[20,165,173] In all reactions except 22 and 23, the $[Fe_3S_4]^0$ core oxidation level is preserved. Note that cluster **21** ($[Co^{2+}(Fe_3S_4)^-]$ ($S = 1$)) is one electron more reduced than **18** because **12** is more reduced than **11**. In comparison, **19** and **22** are isoelectronic because of the one-electron difference in oxidation state of the nickel reactants. These and other synthetic reactions demonstrate that the $[Fe_3S_4]^{0,-}$ oxidation states are sufficiently nucleophilic to bind metals. In a number of proteins with $[Fe_3S_4]^+$ cuboidal sites, metal ion incorporation occurs under reducing conditions, and the product clusters contain $[Fe_3S_4]^{0,-}$ fragments. The only exceptions so far are the highly thiophilic metals Cu^I and Tl^I, which do bind to the oxidized cluster. There are no crystal structures of proteins presumably containing heterometal cubane clusters. However, the cubane structure has been proven with many synthetic heterometallic species, including $[CoFe_3S_4]^{2+}$ and $[NiFe_3S_4]^+$ clusters.[158] Comparison of spectroscopic properties of synthetic and protein-bound clusters provides the most direct evidence that the latter are cubanes. Further discussion of the

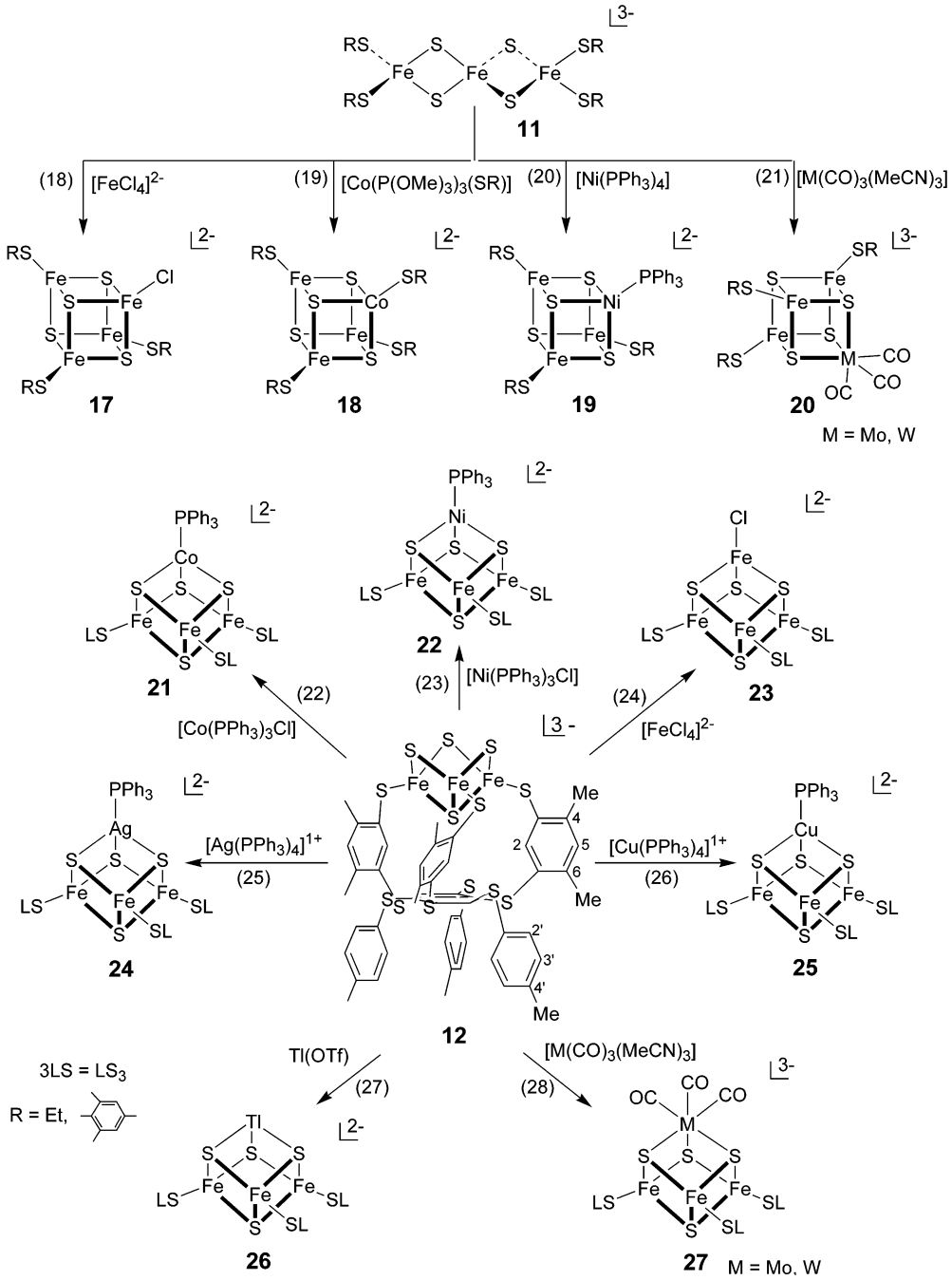

Figure 7. Reaction schemes illustrating the reactivity of linear and cuboidal Fe_3S_4 clusters as precursors to heterometal cubane-type clusters. Linear cluster **11** affords **17**−**20** in reactions that, in effect, require substantial structural rearrangement. Cuboidal cluster **12** yields **21**−**27** in reactions that involve minimal structural change.

synthesis and properties of heterometal cubane clusters is beyond the scope of this report; the subject has been summarized elsewhere.[71,169]

5. Analogues of Tetranuclear (Fe_4S_4) Sites

As is evident from the listing in Table 5, there are more cubane-type Fe_4S_4 clusters than any other analogue type in Figure 2. Over 70 homoleptic thiolate clusters **13a** have been prepared, over 30 site-differentiated clusters **13b** with variant L ligands have been isolated or generated in solution, and many nonanalogue clusters **13c** have been synthesized.[72,73] Of the last, clusters with phenolate-type[174] and, especially, halide ligands[114,118,119,175,176] are valuable starting materials for preparation of thiolate clusters. The crystal structures of some 37 clusters of this type have been determined, including instances of the same cluster with different counterions.

5.1. Electron-Transfer Series

The first identified function of protein-bound Fe_4S_4 clusters **5** is electron transfer. Two types of one-electron redox behavior were recognized: conversion between oxidized and reduced ferredoxins with midpoint potentials near −0.4 V and between oxidized and reduced "high-potential" proteins, so named because their midpoint potentials are near 0.3 V vs

Table 5. $[Fe_4S_4(SR)_4]^{-,2-,3-}$ Analogues of Protein Sites

	R	properties	refs
$[Fe_4S_4]^{3+}$	CH_2Ph[a]	ENDOR, EPR	188−190
	Ph[a]	EPR	191
	2,4,6-$Pr^i_3C_6H_2$	P, E, EPR, Mb, XR	48, 49
$[Fe_4S_4]^{2+}$	H	P, AS, E, Mb, Mg, XR	192, 193
	Me	P, AS, E, NMR	24, 27, 28
	Et	P, AS, E, NMR, XAS	22, 24, 27, 28
	Pr^i	P, AS, E, NMR	27, 28
	CH_2CH_2OH	P, AS, E, Mb, NMR, XR	34, 185, 194−198
	$CH_2CH_2NMe_3$[b]	P, E, NMR	182
	$CH_2CH_2CONH_2$	P, AS	199
	$CH_2CH_2CH_2OH$	P, AS Mb, NMR, XR	198
	$CH_2CH_2CO_2^-$	P, AS, E, XR	32, 33, 200
	$CH_2CH(OH)Me$	P, AS, Mb, NMR, XR	201
	Bu^t	P, AS, E, Mb, NMR, XR	24, 27, 183, 194 185, 202−205
	CH_2CO_2Et	P, Mb, XR	205
	$CH_2CH_2CH_2CH_2OH$	P, AS, Mb, NMR, XR	198
	CH_2CMe_3	P, XR	206
	$CH_2C_6H_{11}$	P, NMR	24, 27
	1-MeC_6H_{10}	P, AS, E, NMR	183
	1-adamantyl	P, E, XR	186, 207, 208
	CMe_2CH_2NHPh	P, E, NMR	183
	CMe_2CH_2OH	P, E, NMR	183
	CH_2Ph	P, AS, E, Mg, MCD, NMR XAS, XR	8, 24, 27, 209 79, 193, 207−210
	CH(Me)Ph	P, AS, E, NMR	183
	$CH_2C_6H_4$-4-OMe	P	211
	CH_2-2,4,6-$Pr^i_3C_6H_2$	P, E, NMR	212
	C_5H_4FeCp	P, AS, E, NMR	213
	2-C_5H_4N	P	214
	5-$NO_2C_5H_3$	P, XR	214
	Ph	P, AS, E, EPR, Mb, Mg, NMR, XAS, XR	24, 27, 28, 30 181, 194, 215, 216 191, 197, 217, 218 125, 185, 210
	C_6X_5 (X = F, Cl)	P, E	24, 28
	2-XC_6H_4 (X = OH, NH_2, OMe, SMe)	P, AS, E, Mb, Mg, XR	219
	2-$Bu^tSC_6H_4$	P, NMR	220
	4-FC_6H_4	P, NMR	96
	4-ClC_6H_4	P, AS, E	26
	2-, 3-MeC_6H_4	P, NMR	221
	4-MeC_6H_4	P, E, NMR	27, 185, 197, 221
	4-$(CHO)C_6H_4$	P	214
	3-, 4-$CF_3C_6H_4$	P, AS, NMR	126
	4-$NO_2C_6H_4$	P, NMR, XR	24, 27, 182
	3-, 4-$NH_2C_6H_4$	P, AS, E, NMR, XR	197, 222
	4-$NMe_2C_6H_4$	AS, E	28
	4-$NMe_3C_6H_4$[b]	P, AS, E	28, 182
	4-$NBu_2MeC_6H_4$[b]	P, E, NMR	182
	4-$R_3NCH_2C_6H_4$ (R = Et, Bu)[b]	P, E, NMR	182
	4-C_6H_4R (R = n-C_4H_9, n-C_6H_{17}, n-C_8H_{17}, n-$C_{12}H_{25}$)	P, E	223−225
	4-$C_6H_4Pr^i$	P	211
	4-$C_6H_4Bu^t$	P, E	211, 225
	2,4,6-$Me_3C_6H_2$	P, E, XAS, XR	184, 210, 226
	2,4,6-$Pr^i_3C_6H_2$	P, E	184, 227, 227
	2-$RCONHC_6H_4$	P, AS, E, NMR	129
	2,6-$(RCONH)_2C_6H_3$ (R = Me, Bu^t, CF_3)	P, AS, E, NMR, XR	129
	2-RCONH-6-PhC_6H_3	P, AS, E, NMR	228, 229
	4-RCONH-6-PhC_6H_3 (R = Me, Bu^t, CF_3, Ph; p-C_6H_4X, X = F, OMe)	P, AS, E, NMR	228, 229
	3-SC_6H_4, 4-SC_6H_4[c]	P, AS, Mg, E	230
	2,4,6-Me_3C_6H-3-S[c]	P, AS, E	230
	crown ether thiolates	P, E, NMR	231
	Cys(Ac)-NHMe	AS, E	28, 31, 34
	Cys peptides	CD, E, NMR	31, 232, 233 234−239
	cyclic tetrathiolates	P, AS, E	240−243 244, 245
	cyclodextrin ditholate	P, AS, E	246
	dendrimer thiolates	P, AS, E	247−249

Table 5. (Continued)

	R	properties	refs
$[Fe_4S_4]^+$	H	P, EPR, XR	250
	Me	P, EPR, Mb, Mg, NMR	251, 252
	Et	P, EPR, Mb, Mg, NMR, XR	219, 220, 249, 250
	CH_2CH_2OH	EPR	193
	Pr^i	P, EPR	252
	Bu^t	P, EPR, Mb, Mg, NMR, XR,	220, 251, 252
	C_6H_{11}	P, EPR, Mg, Mb, XR	220, 252−254
	CH_2Ph	P, EPR, Mb, Mg, NMR, XR	42, 211, 221, 255 190, 251−253, 256
	$CH_2C_6H_4$-4-OMe	P, Mb, Mg, EPR	211
	Ph	P, EPR, Mb, Mg, XR	41, 42, 211, 215 191, 220, 257
	2-$Bu^tSC_6H_4$	P, Mg, Mb, NMR, XR	220
	4-FC_6H_4	P, NMR	96
	4-BrC_6H_4	P, EPR, Mg, Mb, XR	252, 254, 258
	2-, 3-MeC_6H_4	P, NMR	221
	4-MeC_6H_4	P, EPR, Mb, Mg, NMR	211, 221, 259
	4-$Pr^iC_6H_4$	P, Mb, Mg	211
	Cys peptides	E, EPR	237, 238

[a] Irradiated crystal, cluster not isolated. [b] Cluster charge 2+. [c] Polymeric cluster.

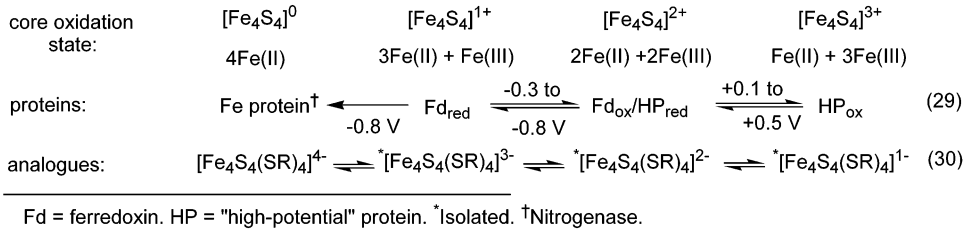

Figure 8. Electron-transfer series of Fe_4S_4 protein sites **5** and analogues **13a** showing core oxidation states and formal iron valence states. Isoelectronic species are arranged vertically.

SHE. In 1972, the relationship between Fd and HP proteins was correctly interpreted in terms of the "three-state" hypothesis,[3] which is summarized in Figure 8. Briefly, Fd_{ox} and HP_{red} were recognized to be isoelectronic with a spin-paired ($S = 0$) ground state. HP_{ox} and Fd_{red} are then one electron more oxidized and reduced, respectively, generating the protein series 29, which includes the paramagnetic states $[Fe_4S_4]^{3+,+}$ in addition to $[Fe_4S_4]^{2+}$. Protein structural and environmental influences are responsible for the relative potentials of the couples $[Fe_4S_4]^{3+/2+}$ and $[Fe_4S_4]^{2+/+}$, with the consequence that all three oxidation states are not traversed in a single reversible series in a native protein conformation. In an early demonstration of the value of the synthetic analogue approach (Table 1), the demonstration by voltammetry of the four-member electron-transfer series 30 (Figure 8) provided unambiguous confirmation of the hypothesis. The overall charges in the series immediately identify the core oxidation state and the mixed-valence composition of each member. Isoelectronic species are aligned vertically and were originally identified by comparison of spectroscopic properties. It is now possible to identify known types of protein sites by MCD or EPR spectra if paramagnetic and by Mössbauer spectroscopy (section 6) if paramagnetic or diamagnetic. The term "high-potential" is now mainly of historical context. Proteins previously designated as HP (or HiPiP) are best considered as ferredoxins that operate with a different redox couple at higher potentials. Significant variation of potentials can occur in native and mutated proteins[177−179] and even for two clusters in the same protein.[180] For the Fd_{ox}/Fd_{red} couple, the large majority of potentials in native proteins are near −0.4 V but extend as low as −0.75 V vs SHE in a mutant *Av* Fd I.[179] In 8-Fe *Av* Fd III, cluster potentials differ by 0.16 V.

Electron-transfer series 30 is the heart of Fe_4S_4 analogue chemistry and, reinforced by synthesis, establishes four core oxidation states. The series has been amply demonstrated,[28,41,181,182] although rarely with the same cluster. While the $[Fe_4S_4(SR)_4]^{2-/3-}$ step is nearly always reversible, the terminal oxidation and reduction steps are often irreversible when attempted with a given cluster. Potential modulation is readily achieved by R substituent variation, such that potentials can be tuned to improve the stability of a given oxidation state. Also important is the bulk of the R substituent, which has an apparent effect on the stability of the $[Fe_4S_4]^{3+}$ state. We proceed by summarizing leading aspects of analogue clusters **13a** in the order of descending oxidation state. Figure 9 displays schematic structures of selected analogues and protein sites in the oxidation states $[Fe_4S_4]^{3+,2+,+}$.

5.2. $[Fe_4S_4]^{3+}$ Clusters

The $[Fe_4S_4]^{3+}$ oxidation state is isoelectronic with HP_{ox}. It was first detected electrochemically by oxidation of $[Fe_4S_4(SBu^t)_4]^{2-}$ [28] and subsequently with several other clusters.[183−185] Thereafter, $[Fe_4S_4(Stibt)_4]^-$ (**28**), the first and only cluster actually isolated, was obtained by reaction 31 in dichloromethane and

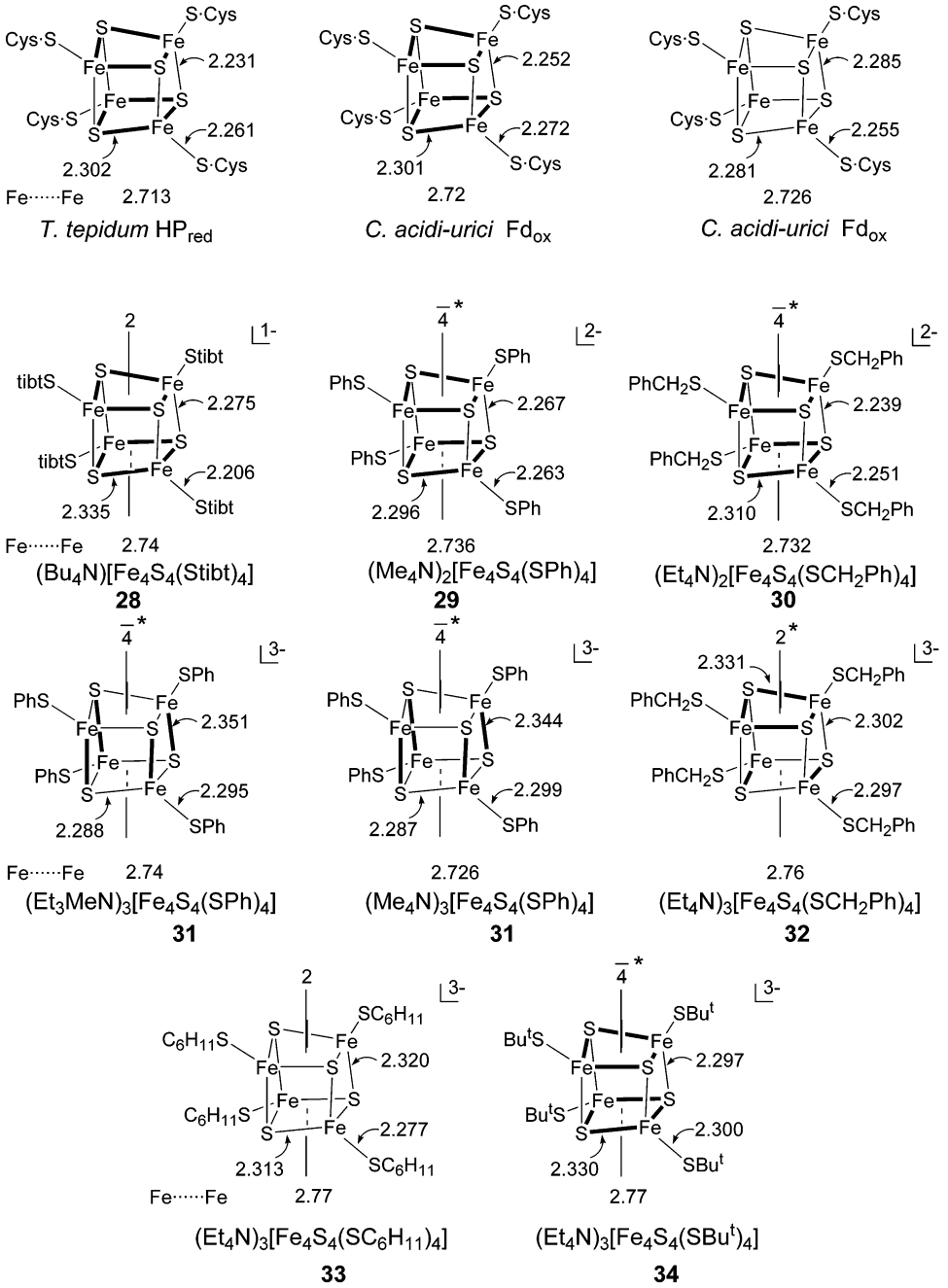

Figure 9. Schematic depictions of the structures of cubane-type clusters in proteins and analogues showing mean Fe—S and Fe···Fe distances and terminal Fe—SR distances (Å). With proteins, the core oxidation states are $[Fe_4S_4]^{3+}$ in HP_{ox} and $[Fe_4S_4]^{2+}$ in Fd_{ox}; esd's of bond distances are 0.002−0.004 Å. With analogues, the core oxidation states are $[Fe_4S_4]^{3+}$ (**28**), $[Fe_4S_4]^{2+}$ (**29**, **30**), and $[Fe_4S_4]^{+}$ (**31**−**34**). Esd's of bond distances are 0.002−0.008 Å. In clusters where mean Fe−S core distances sort into "long" and "short" sets, the long bonds are bolded. For $(Et_3MeN)_3$ $[Fe_4S_4(SPh)_4]$, mean values over two inequivalent clusters are given. Crystallographically imposed and idealized (*) symmetry axes are shown.

obtained as the Bu_4N^+ salt.[48] The starting cluster

$$[Fe_4S_4(Stibt)_4]^{2-} + [Cp_2Fe]^+ \rightarrow [Fe_4S_4(Stibt)_4]^- (\mathbf{28}) + Cp_2Fe \quad (31)$$

showed reversible steps at $E_{1/2} = -1.20$ V (reduction) and −0.12 V (oxidation) in dichloromethane. As other examples, the 1-adamantylthiolate cluster $[Fe_4S_4(SAd)_4]^{2-}$ exhibits well-defined reactions at $E_{1/2} = -1.32$ V and −0.12 V, and $[Fe_4S_4(SPh)_4]^{2-}$ shows a pseudo-reversible oxidation at −0.32 V, all in dichloromethane, but an irreversible process near 0 V in acetonitrile and DMF.[186] Quasi-reversible oxidation of $[Fe_4S_4(SAd)_4]^{2-}$ has been observed in aqueous micellar media, where both oxidation and reduction are reported to be accompanied by protonation.[186] The bulk of the evidence, however, shows that dry non-basic solvents and large hydrophobic ligands significantly improve the stability of this state, presumably by protecting the electrophilic core from attack by solvent and other nucleophiles.[185,187]

The EPR and Mössbauer spectroscopic properties of **28** prove a close relationship in electronic structure with HP_{ox}.[49] The iron atoms are inequivalent in pairs, delocalized $Fe^{2.5+}Fe^{2.5+}$ ($S = {}^9/_2$) and localized Fe^{3+}-

Fe^{3+}, as shown by oppositely signed electron−nuclear hyperfine splitting constants obtained by fits of the magnetic Mössbauer spectra to an $S = {}^1/_2$ spin Hamiltonian. The mean isomer shift at 4.2 K (0.37 mm/s) is essentially the same as that for *Chromatium* HP_{ox} (0.35 mm/s) and is 0.11 mm/s smaller than that for $[Fe_4S_4(Stibt)_4]^{2-}$, a difference that is typical for adjoining Fe_4S_4 oxidation levels. The oxidized state has also been produced by γ-irradiation of crystals of $(Et_4N)_2[Fe_4S_4(SCH_2Ph)_4]$ and studied by EPR and ENDOR spectroscopies.[189,190] Here, evidence has been adduced for $S = {}^9/_2$ or ${}^7/_2$ for the delocalized pair and $S = 4$ or 3 for the coupled Fe^{III} sites, leading to an $S = {}^1/_2$ ground state. Cluster **28** appears to be an accurate representation of the HP_{ox} state. Unfortunately, there are no crystallographic structures of this state. Two high-resolution structures of HP_{red} proteins have been reported,[260,261] one of which[261] is included in Figure 9. The structures of analogue and protein-bound clusters are examined in section 5.6.

5.3. $[Fe_4S_4]^{2+}$ Clusters

The $[Fe_4S_4]^{2+}$ oxidation state is isoelectronic with Fd_{ox} and HP_{red}. The reactivity and structural chemistry of these clusters have been extensively evolved. The original synthesis was by self-assembly reaction 32.[8,24] Subsequently, a number of other methods were devised, including the experimentally convenient assembly reactions 33 and 34,[194,196] and ligand substitution reactions 35 (X = halide) and 36 (n = 1−4).[30,126] These reactions consist of stepwise nearly statistical equilibria which may be easily monitored by ^{1}H NMR. However, mixed ligand clusters, especially with unidentate ligands in polar solvents, are not separable owing to the facile redistribution reactions 37, leading to statistical mixtures.

$$4FeCl_3 + 6RS^- + 4HS^- + 4OMe^- \rightarrow [Fe_4S_4(SR)_4]^{2-} + RSSR + 12Cl^- + 4MeOH \quad (32)$$

$$4FeCl_2 + 10RS^- + 4S \rightarrow [Fe_4S_4(SR)_4]^{2-} + 3RSSR + 8Cl^- \quad (33)$$

$$4FeCl_3 + 14RS^- + 4S \rightarrow [Fe_4S_4(SR)_4]^{2-} + 5RSSR + 12Cl^- \quad (34)$$

$$[Fe_4S_4X_4]^{2-} + nRS^- \rightleftharpoons [Fe_4S_4X_{4-n}(SR)_n]^{2-} + nX^- \quad (35)$$

$$[Fe_4S_4(SR)_4]^{2-} + nR'SH \rightleftharpoons [Fe_4S_4(SR)_{4-n}(SR')_n]^{2-} + nRSH \quad (36)$$

$$(4-n)[Fe_4S_4(SR)_4]^{2-} + n[Fe_4S_4(SR')_4]^{2-} \rightleftharpoons 4[Fe_4S_4(SR)_{4-n}(SR')_n]^{2-} \quad (37)$$

Reaction 36 is analogous to reaction 8 of binuclear analogues and is particularly useful in preparing clusters whose ligands are more acidic than the intial cluster with R = alkyl. When the stoichiometry of reaction 38a is employed in methanol solution, the cage complex $[Fe_4(SR)_{10}]^{2-}$ ("ferromantane" (**35**), with an adamantane-like structure[262]) is formed and subsequently reacts quantitatively with sulfur in reaction 38b to form the desired product.

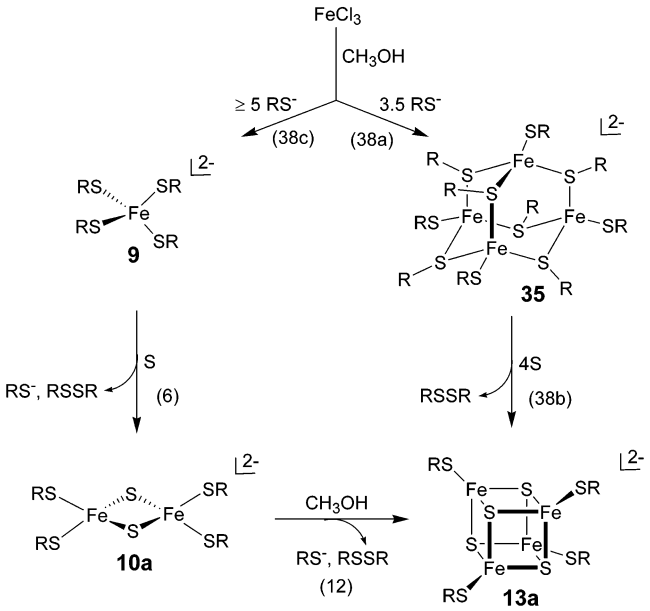

Figure 10. Depiction of the coupled reactions leading to assembly of $[Fe_4S_4(SR)_4]^{2-}$ clusters **13a** in systems with initial mol ratios RS^-:Fe^{III}:S = 3.5:1:1 and ≥5:1:1.

$$4FeCl_3 + 14RS^- \rightarrow [Fe_4(SR)_{10}]^{2-} + 2RSSR + 12Cl^- \quad (38a)$$

$$[Fe_4(SR)_{10}]^{2-} + 4S \rightarrow [Fe_4S_4(SR)_4]^{2-} + 3RSSR \quad (38b)$$

$$FeCl_3 + 5RS^- \rightarrow [Fe(SR)_4]^{2-} + {}^1/_2RSSR + 3Cl^- \quad (38c)$$

When the stoichiometry is increased to RS^-:Fe^{III}:S ≥ 5:1:1, the reaction takes a different course described by the sequential steps 38c + 6 + 12. Note the identical reaction sums 38a + 38b = 4(38c) + 2(6) + 12 = 34. Shown in Figure 10 are the two reaction pathways that lead to the same product cluster.[43] Although many elementary steps are not defined, the systems in Figure 10 are among the very few in which sequential formation of intermediates has been demonstrated in cluster synthesis.

In other reaction systems containing $Fe^{II,III}$, sulfur or sulfide, and thiolate or other terminal ligands, clusters **13a** or **13c** are often unintended side products, emphasizing that these species are thermodynamic sinks in iron−sulfur cluster synthesis.

By means of reactions 32−36, a large set of clusters has been produced (Table 5), including those with the simplest ligand (R = H), extremely bulky hydrophobic ligands (R = Ad, tibt), hydrophilic ligands whose clusters are water-soluble (R = CH_2CH_2OH, $CH_2CH_2CO_2^-$), macrocyclic, dendrimeric, and crown ether ligands, and Cys peptide ligands. This situation has led to extensive information on the properties of the $[Fe_4S_4]^{2+}$ oxidation state as dependent on ligands.

The clusters **13a** have a diamagnetic ground state and low-lying paramagnetic excited state(s) popu-

lated at 4.2 K and above and leading to $\mu_{eff} \approx 2.3\mu_B$ per cluster at room temperature.[42,215] This situation affords extremely well-resolved NMR spectra whose isotropic shifts are mainly or exclusively contact in origin.[27,221] Absorption spectra of alkylthiolate clusters are very similar to those of Fd_{ox} and HP_{red}, with bands at ca. 420 and 300 nm. Redox potentials of the couple $[Fe_4S_4(SR)_4]^{2-/3-}$ in series 30 exhibit linear free energy relationships with the substituent constants σ^* (R = alkyl) and σ_p (R = *p*-C_6H_4X).[28] In an aprotic solvent such as DMF, a typical range with common substituents is $E_{1/2} = -1.04$ V (R = Ph) to -1.42 V (R = Bu^t). The range can be extended to less negative values by suitable variation of the phenyl substituents, including quaternized ammonium groups that lead to positively charged clusters $[Fe_4S_4(SC_6H_4\text{-}p\text{-}NR_3)_4]^{2+}$.[182] The structures of two clusters, $[Fe_4S_4(SPh)_4]^{2-}$ (**29**)[30] and $[Fe_4S_4(SCH_2Ph)_4]^{2-}$ (**30**),[24] drawn from the large database of $[Fe_4S_4]^{2+}$ structures, are included in Figure 9, together with the two clusters of *C. acidi-urici* Fd_{ox} determined at atomic resolution.[263]

5.4. $[Fe_4S_4]^+$ Clusters

These species are isoelectronic with Fd_{red} and are conventionally prepared by reduction of $[Fe_4S_4(SR)_4]^{2-}$ with reducing agents having a potential of -1.5 V, as in reaction 39 with sodium acenaphthylenide radical anion.[41,42,257] Reactions are usually conducted

$$[Fe_4S_4(SR)_4]^{2-} + NaC_{12}H_8 \rightarrow [Fe_4S_4(SR)_4]^{3-} + C_{12}H_8 + Na^+ \quad (39)$$

in acetonitrile, where the rate of reduction exceeds the rate of reaction of the reductant with solvent. Reduced clusters can also be obtained with the assembly system $FeCl_2$/2NaSR/4NaSH in DMF,[251] obviating the requirement of a preisolated cluster. In this system, excess thiolate neutralizes the protons released by hydrosulfide. The oxidant required to achieve the mean oxidation $Fe^{2.25+}$ state in the product cluster has not been identified. The reduced clusters are very sensitive to dioxygen and are oxidized or decomposed by protic species.[264,265] An aqueous medium markedly stabilizes the $[Fe_4S_4]^+$ state compared to aprotic solvents. The potential of the couple $[Fe_4S_4(SCH_2CH_2OH)_4]^{2-/3-}$ is 0.42 V more positive in aqueous buffer than in Me_2SO.[34] Also, the highly negatively charged cluster $[Fe_4S_4(SCH_2CH_2CO_2)_4]^{6-}$ is reducible in two one-electron steps at -0.52 or -0.59 V and -0.98 V vs SHE in aqueous solution.[32,200]

Reduced clusters exhibit the nearly featureless absorption spectra of Fd_{red}. Most clusters have $S = {}^1/_2$ ground states, indicated by axial or rhombic EPR signals observable below ca. 20 K and typified by the axial spectrum of $[Fe_4S_4(SCH_2Ph)_4]^{3-}$ ($g_{\parallel} = 2.04$, $g_{\perp} = 1.93$).[42] Protein spectra are generally rhombic, with $g_{av} \approx 1.94-1.97$, and are observed in the same temperature regime. There are also examples of pure $S = {}^3/_2$ ground states[257] and clusters that occur as physical mixtures of $S = {}^1/_2$ and ${}^3/_2$ states,[220,252] properties also observed with certain proteins. The spin quartet state is directly detectable by EPR signals in the $g \approx 4-5$ region.[211,252] Excited spin states are occupied at higher temperatures, such that at 300 K, $\mu_{eff} = 4.0-5.1\mu_B$ per cluster.[42,211] Clusters display well-resolved ^{1}H NMR spectra with larger isotropic shifts than $[Fe_4S_4(SR)_4]^{2-}$, consistent with greater paramagnetism and dominant contact interactions.[221] Electron self-exchange reactions are rapid ($k \approx 10^6$ M^{-1} s^{-1} in acetonitrile at 300 K, indicative of a small inner-sphere reorganization barrier. The structures of four clusters **31**–**34** in five compounds are collected in Figure 9. As is evident, exact core shapes are decidedly variable.

5.5. $[Fe_4S_4]^0$ Clusters

The $[Fe_4S_4]^0$ state, a terminal member of series 30, was first detected electrochemically in aprotic solvents as a member of the couple $[Fe_4S_4(SR)_4]^{3-/4-}$ with $E_{1/2} < -1.7$ V.[28,41] The cluster $[Fe_4S_4(SPh)_4]^{2-}$ in acetonitrile shows two chemically reversible reductions at $E_{1/2} = -1.00$ V and -1.72 V. While $[Fe_4S_4(SPh)_4]^{3-}$ in various salts has been isolated and fully characterized, neither $[Fe_4S_4(SPh)_4]^{4-}$ (**36**) nor any other $[Fe_4S_4(SR)_4]^{4-}$ species has ever been isolated in substance, despite substantial effort toward that goal in this laboratory. All-ferrous cubane-type clusters are known, but not with physiological ligands. Among these is $[Fe_4S_4(CO)_{12}]$,[266] whose six-coordinate iron sites and long Fe···Fe separations (3.47 Å) accentuate its difference with analogue clusters. Certain developments with the phosphine-ligated clusters in the reaction scheme of Figure 11[267,268] are briefly considered, as they may provide a pathway to all-ferrous cubanes. The readily prepared clusters $[Fe_4S_4(PR_3)_4]^+$ (**37**, R = Bu^t, Cy, Pr^i) are reducible to putative neutral clusters **38**, which have not been isolated. Under specific conditions, the reduction product can be converted to the edge-bridged double cubane $[Fe_8S_8(PR_3)_6]$ (**39**) or the tetracubane $[Fe_{16}S_{16}(PR_3)_8]$ (**40**). It remains to be seen if the initial reduction product can be converted to **36** by ligand substitution or if, by bridge cleavage and substitution, **39** can do the same. Given the stability of **39**, it remains to be learned if a thiolate-ligated cluster will exist as a single cubane or form spontaneously a double cubane by means of edge-bridging.

An imperative for the synthesis and characterization of the $[Fe_4S_4]^0$ oxidation state follows from the demonstration of its occurrence in the fully reduced iron protein of *A. vinelandii* nitrogenase.[269–271] The protein supports the redox couples $[Fe_4S_4]^{2+/+}$ (-0.31 V) and $[Fe_4S_4]^{+/0}$ (-0.79 V) at the indicated midpoint potentials vs SHE.[272] This is the first example of a protein-bound Fe_4S_4 cluster that has been stabilized in three oxidation states in the absence of chaotropic reagents that perturb protein structure.[273] The all-ferrous state can be formed with the strong reductants Ti^{III}–citrate and Cr^{II}–EDTA. The isomer shift of 0.68 mm/s establishes the oxidation state; the iron atoms are inequivalent in a 3:1 ratio when implicated in an $S = 4$ ground state.[271] The presence of completely cysteinate-ligated cluster **5** in the fully reduced protein has been confirmed by crystallography (2.25 Å resolution).[274] The second reduction potential

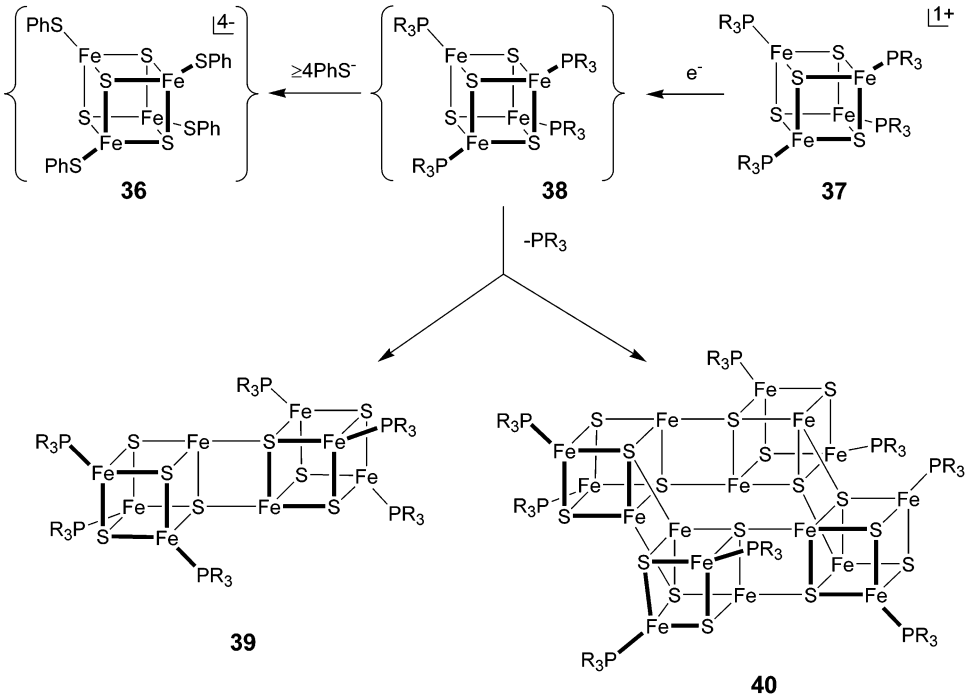

Figure 11. Reaction scheme showing the formation of all-ferrous edge-bridged dicubane **39** and tetracubane **40** by reduction of the single cubane **37**. Clusters **36** and **38** have not been isolated.

may be compared with −0.98 V noted above for $[Fe_4S_4(SCH_2CH_2CO_2)_4]^{7-/8-}$, the only available value for an analogue cluster in aqueous medium, and signifies a remarkably facile reduction compared to any analogue in an aprotic solvent. The cluster sustains at least seven hydrogen bonds and, being at the interface of the α_2 subunit structure of the iron protein, is accessible to solvent.[274] These factors presumably contribute to the enhanced reducibility of the cluster. Clearly, an analogue single-cubane cluster $[Fe_4S_4(SR)_4]^{4-}$ would be advantageous in defining intrinsic geometric and electronic structural issues and, if sufficiently stable in water, medium effects on the potential of the $[Fe_4S_4]^{+/0}$ couple.

5.6. Principal Structural Features

The term "cubane-type" includes all Fe_4S_4 cores made up of six edge-shared nonplanar Fe_2S_2 rhombs, regardless of distortions from idealized T_d symmetry. Analogue structures **28**−**34** in three oxidation states are included in Figure 9, together with clusters in two proteins that have been determined at atomic resolution.[261,263] Several other protein structures of comparable accuracy are available.[260,275] All protein structures refer to the $[Fe_4S_4]^{2+}$ oxidation state. The full set of analogue structures can be obtained from Table 5. No analogue cluster has perfect T_d symmetry; with Fe_4S_4 clusters that limiting symmetry has been found only in one salt of $[Fe_4S_4Cl_4]^{2-}$.[276] Among the structural deviations from cubic core symmetry, a compressed tetragonal distortion with four "short" bonds and eight "long" Fe−S bonds, approximately parallel and perpendicular, respectively, to an idealized 4-axis is frequently encountered. Under this D_{2d} distortion mode, core distances and angles divide as Fe−S and S···S (4 + 8), Fe−Fe (2 + 4), and Fe−Fe−Fe, S−Fe−S, Fe−S−Fe (4 + 8). The distortion is often identified subjectively by the pattern of core Fe−S bond distances and is prevalent for clusters in the $[Fe_4S_4]^{2+}$ oxidation state. A more rigorous analysis to identify D_{2d} vs T_d symmetry has been presented,[24] as has a geometrical analysis of the D_{2d} structure in terms of shape parameters, which allows calculation of core volume.[70] The structures in Figure 9, which are idealized by use of average values of core Fe−Fe and Fe−S and terminal Fe−SR bond distances, nonetheless usefully convey the dominant distortion type and cluster dimensions. Occasionally, as in $(Bu_4N)_2[Fe_4S_4(SBu^t)_4]$[203] and $(Et_4N)_2[Fe_4S_4(SBu^t)_4]$,[183] a D_{2d} distortion is crystallographically imposed. In other cases, such as **29**, **30**, $(Me_3NCH_2Ph)_2[Fe_4S_4(SBu^t)_4]$,[183] and $(Ph_4As)_2[Fe_4S_4(SAd)_4]$,[186] a tetragonal distortion is readily recognized but is not imposed. The occurrence of various modes of distortion from idealized T_d core symmetry indicates that packing effects dependent on counterion and/or R substituent influence structural details. Among such cases are the monoclinic and orthorhombic modifications of $(Bu_4N)_2[Fe_4S_4(SPh)_4]$, in which the cluster does not exhibit the D_{2d} distortion of the Me_4N^+ salt.[191,217,218]

Certain structural trends can be recognized. As the oxidation level decreases, Fe−SR bond lengths increase owing to the increased ferrous character of the core (Figure 9). The Shannon radius of tetrahedral Fe^{II} is 0.14 Å larger than that for tetrahedral Fe^{III}.[109] Thus, in **28** the bond length is 2.21 Å,[48] the mean of **29** and **30** is 2.26 Å,[24,30] and the mean of **31**−**34** is 2.29 Å.[42,251,252,255,257] Cluster **28** is the only structure of the $[Fe_4S_4]^{3+}$ state. On this basis the $[Fe_4S_4(SR)_4]^{-}$ regime is demarcated at 2.21 Å. With a large data set, the $[Fe_4S_4(SR)_4]^{2-}$ regime covers 2.25−2.28 Å and that of $[Fe_4S_4(SR)_4]^{3-}$ at distances longer than 2.28 Å. These data refer to mean values. The longest

terminal bond is 2.32 Å in $(Et_4N)_3[Fe_4S_4(SH)_4]\cdot Et_4NCl$.[250] A similar trend in Fe−Fe and core Fe−S distances is sometimes discernible if all such values are averaged for a given structure. Other parameters of interest are the volumes of the Fe_4 and S_4 distorted tetrahedra and the Fe_4S_4 core volume.[70,183,255] Reduction of $[Fe_4S_4(SR)_4]^{2-}$ to the trianion results in a small increase in the core volume. Changes are in the range of about 2−3% and depend on the cation and crystalline environment. For $[Fe_4S_4(SCH_2Ph)_4]^{2-,3-}$, the volume increases from 9.61 to 9.86 Å^3, or 2.6%. For $[Fe_4S_4(SPh)_4]^{2-,3-}$, the change is 1.9%. These values were calculated for idealized D_{2d} distortions. On the basis of this trend, further reduction to the $[Fe_4S_4]^0$ state would be expected to lead to a volume increase. The only available example is the all-ferrous cluster of *Av* nitrogenase.[274] The Fe_4 volume (2.17 Å^3) is 8.8% smaller and the S_4 volume (6.17 Å^3) is 11% larger than for the clusters in *C. acidi-urici* Fd_{ox};[263] the core volume (9.23 Å^3) is 6.4% smaller than in $[Fe_4S_4(SCH_2Ph)_4]^{3-}$. At least in terms of the latter parameter, the core volume trend does not continue. The cause of this behavior is unclear; all-ferrous cluster volumes were calculated by a different procedure than other values. Core bond length and volume increases are consistent with the addition of an electron to an antibonding orbital with substantial Fe−S character.

The historical advantage of precise analogue structures is now being attenuated by the advent of protein structures at atomic resolution. Structures are now available for HP_{red}[260,261] and Fd_{ox}[263,275] proteins at 0.80−1.20 Å resolution, permitting detailed metric comparison with analogue clusters. Close agreement in core bond lengths, angles, and volumes is found among the isolectronic protein-bound clusters themselves and with $[Fe_4S_4]^{2+}$ analogues. Idealized D_{2d} distortions occur in some cases, as in one of the two clusters of *C. acidi-urici* Fd_{ox} (Figure 9). X-ray structures of HP_{ox} and Fd_{red} proteins have not been reported.

Lastly, reduced clusters **31**−**34** display three different idealized distorted modes with $\bar{4}$- and 2-fold axes. Actually, even more distortions have been observed with other clusters, and considerable effort has been extended to determine if there is any correlation between the type of distortion and the ground electronic state $S = {}^1/_2$ or ${}^3/_2$.[190,220,254,257] While no convincing correlation has emerged, it has become very clear that the $[Fe_4S_4]^+$ core exhibits a plasticity evident by multiple distortion modes and electronic ground states that are very sensitive to environment. This is evident by variant core distortions in the crystalline state and the existence of two spin ground states and of physical mixtures of spin states of the same cluster compound. In one striking example, crystalline $(Et_4N)_3[Fe_4S_4(SPh)_4]\cdot DMF$ has an $S = {}^1/_2$ ground state, whereas in the unsolvated compound the ground state is $S = {}^3/_2$.[256] At present, analogue clusters provide the only structural data on the $[Fe_4S_4]^+$ oxidation state and imply that reduced protein clusters will adopt different distortions, dependent upon protein structure and environment. Overall, analogue structures of all types, while subject to perturbations in their own crystalline environments, will continue to afford the only means to assess structural variability in the absence of protein structure and environment.

5.7. Specialized Clusters

In this section, we depart from the theme of strictly homoleptic clusters **5** and examine developments in related areas. These include clusters ligated by cysteinyl peptides, site-differentiated clusters whose synthesis was first motivated by cluster **6** in active aconitase, and the formation of analogues of protein-bound bridged assemblies in which a site-differentiated Fe_4S_4 cluster is covalently linked to another metal component.

5.7.1. Peptide Clusters

Ligation of cysteinyl peptides represents the next logical step in the evolution of analogue clusters past the level of relatively simple thiolate-bound species such as **13a**. Work with Fe_4S_4 clusters is the most advanced. Peptide clusters have been prepared by two methods. Reaction 40 with a preformed cluster is an extension of ligand substitution reaction 36 in which, usually, four Cys residues are bound and often $n = 1$ and $x = 4$. The charge on the cluster does not

$$[Fe_4S_4(SR)_4]^{2-} + n(Cys)_x \text{ peptide} \rightarrow [Fe_4S_4\{(Cys)_x\text{peptide}\}_n]^{2-} + 4RSH \quad (40)$$

include contributions from residues other than Cys. In the early development of the analogue field, this reaction with R = Bu^t was used with Ac-Cys-NHMe and Gly-Cys oligopeptides to produce the first Cys-bound clusters.[31] The procedure was subsequently extended to other peptides of this type[232] and to small cysteinyl peptides.[233−235] Larger peptides have been shown to bind the cluster, as in the reaction of water-soluble $[Fe_4S_4(SCH_2CH_2OH)_4]^{2-}$ with 63-residue peptides containing the ferredoxin consensus sequence 41 and one or two additional Cys residues.[65] Further, this cluster has been incorporated into a specially engineered form of thioredoxin designed to bind an Fe_4S_4 cluster.[277]

Cys-Ile-Ala-**Cys**-Gly-Ala-**Cys** (41)

The second method for forming peptide clusters is based on cluster reconstitution using $FeCl_3$, Na_2S, a reductant such as $HOCH_2CH_2SH$, and the peptide in aqueous buffer. The procedure, which is obviously related to cluster assembly reaction 32, traces back to the classic work by Rabinowitz,[278] who reformed ferredoxins from apoproteins in this way. The reconstitution procedure has been used to introduce a cluster into the 16-residue peptide 42 (containing sequence 41) and related peptides,[237,238] and into a simplified 31-residue version of the apoprotein of *Desulfovibrio gigas* Fd II.[279] A cluster−peptide com-

H_2N-Lys-Leu-**Cys**-Glu-Gly-Gly-**Cys**-Ile-
Ala-**Cys**-Gly-Ala-**Cys**-Gly-Gly-Trp-$CONH_2$ (42)

plex has beenformed with a 67-residue peptide having two ca. 27-residue helical segments joined by a loop containing the tetracysteinyl portion of 42.[236] Reconstitution of the totally synthetic 55-residue apoprotein of *Cp* Fd has afforded the holoprotein with two clusters whose properties very closely match those of the native protein.[55]

Peptide-ligated clusters have generated several useful applications. Among the first was the indication that N−H···S hydrogen bonding to cluster sulfur atoms effected small positive potential shifts of the $[Fe_4S_4]^{2+/+}$ transition.[103,233−235] The *Cp* Fd apoprotein has been strategically mutated to determine the effects on stability and redox potentials.[237,280,281] As noted, certain clusters contain the ferredoxin consensus sequence 41. Sequence 42 carries the residue spacing Cys-$(X)_3$-Cys-$(X)_2$-Cys-$(X)_2$-Cys often found in Fd's and has been shown to support efficiently cluster reconstitution.[237] This cluster exhibits a proton-coupled $[Fe_4S_4]^{2+/+}$ redox reaction with a midpoint potential of −350 mV vs NHE,[239] within the range of native Fd's. The integrated EPR spectrum was assigned 100% of the expected spin per peptide as the criterion of complete cluster formation. The cluster has been employed in an interesting way to assess the effects of peptide structure on cluster formation under constant reconstitution conditions.[237,238] When reduced with dithionite to the $[Fe_4S_4]^+$ state, the cluster shows a protein-like $g = 1.94$-type EPR spectrum. Variation of ligating and nonligating residues and different truncations of sequence 42, followed by cluster reconstitution, reduction, and comparative EPR spin integration, showed that virtually any modification of the sequence resulted in a diminished ability of the peptide to support cluster reconstitution, sometimes eliminating it entirely. Significant conclusions include the following. (i) Cys ligation is stabilizing over that by any other residue. (ii) Three Cys residues allow cluster formation, with an exogenous ligand occupying the remaining position on the fourth iron site; sequence 41 is optimal in this respect. (iii) The spacing Cys-$(X)_2$-Cys-$(X)_2$-Cys is critical for Cys ligation. (iv) The identities of nonligating (second shell) residues are as consequential as the binding residues in stabilizing $[Fe_4S_4]^{2+,+}$ clusters. These results provide a guideline for securing a cluster bound to relatively small peptides where protein folding is not a factor.

Designed peptides can be used to provide structures in synthetic assemblies that would be extremely difficult to achieve otherwise. The insightfully designed helix−loop−helix motif of the foregoing 67-residue peptide maquette is constructed such that two His residues in each helical run bind heme groups as bridges between helices.[236] This assembly, with one cluster and two hemes, places these redox sites in close juxtaposition in the same molecule, as might be the case in certain oxidoreductases. The same motif was built into a 63-residue peptide designed as a scaffold for the stabilization of metal ions bridged to an Fe_4S_4 cluster by a Cys residue.[65] In the loop, the consensus sequence was preceded by another binding residue in the run Cys-Glu-Cys-Ile-Ala-Cys-Gly-Ala-Cys. The helices contain His or His and Cys binding residues placed in positions near the cluster binding loop. In one case, the cluster is bound to the Cys residues of the consensus sequence and also to the first Cys, which functions as a bridge to Ni(II), giving the planar coordination unit Ni(μ_2-S·Cys)(N·His)$_3$. This formulation is consistent with spectroscopic data and nickel K-edge EXAFS.[66] This work provides an encouraging prognosis for de novo designed peptides as scaffolds for the stabilization of analogues of complex bridged assemblies found in metalloproteins.[282]

5.7.2. Site-Differentiated Clusters

The first recognized occurrence of any type of protein-bound site-differentiated cluster (not including all clusters **5** whose Cys residues are, in principle, inequivalent) was with the enzyme aconitase, which converts citrate to isocitrate in the tricarboxylic acid cycle.[283,284] The resting form of the active enzyme contains the 3:1 site-differentated cluster **6,** whose unique iron atom, as shown by crystallography of the mitochondrial enzyme,[285] is the site of subtrate binding and catalysis. Aconitase has had a major impact on iron−sulfur biochemistry and chemistry. It was the first iron−sulfur *enzyme* recognized, extending the biological function of clusters beyond electron transfer to catalysis. The inactive form of aconitase contains cuboidal cluster **4**, derived from **6** by a reversible iron insertion reaction with very little change in structure.[286] The cluster interconversion reaction is an essential paradigm for other protein-bound clusters which in the cubane form lack a fourth Cys residue for binding to an iron site. It is the iron atom at the differentiated site that is labile.

Examples of synthetic site-differentiated clusters **13b** have already been encountered as the 3:1 species **14**−**17** (Figures 6 and 7). The site-differentiated 2:2 clusters $[Fe_4S_4(SPh)_2Cl_2]^{2-}$ and $[Fe_4S_4(SPh)_2(OC_6H_4$-p-$Me)_2]^{2-}$ have been isolated as crystalline salts.[216,287] Further, neutral clusters such as $[Fe_4S_4I_2L_2]$ (L = Ph_3P, thioureides),[288−291] $[Fe_4S_4(SPh)_2(PBu^t_3)_2]$,[292] and $[Fe_4S_4(PR_3)_3L]$ (L = halide, PhS^-)[268,292] have been prepared and structurally characterized. However, the utility of such clusters is quite limited unless their reactivity in solution can be examined. Certain neutral clusters are stable to disproportion to ionic species in low dielectric solvents such as THF, dichloromethane, and toluene. This is not the case with charged clusters in more polar media such as acetonitrile, DMF, and Me_2SO, in which their quaternary ammonium salts are generally soluble. Disproportion and equilibration of clusters with monofunctional ligands in reactions like 37 is the general rule in these solvents. In analogue chemistry, charged clusters are prevalent; designed ligands must be utilized to avoid cluster disproportionation.

Five trithiols whose deprotonated forms sustain 3:1 site-differentiated clusters are given in Figure 12. The trianion (LS_3) of compound **41** is the first example of a ligand of this type.[50,51] Alternate groups around the central benzene ring are forced above and below the ring by steric factors. The three thiol "arms" are on the same side, buttressed in that

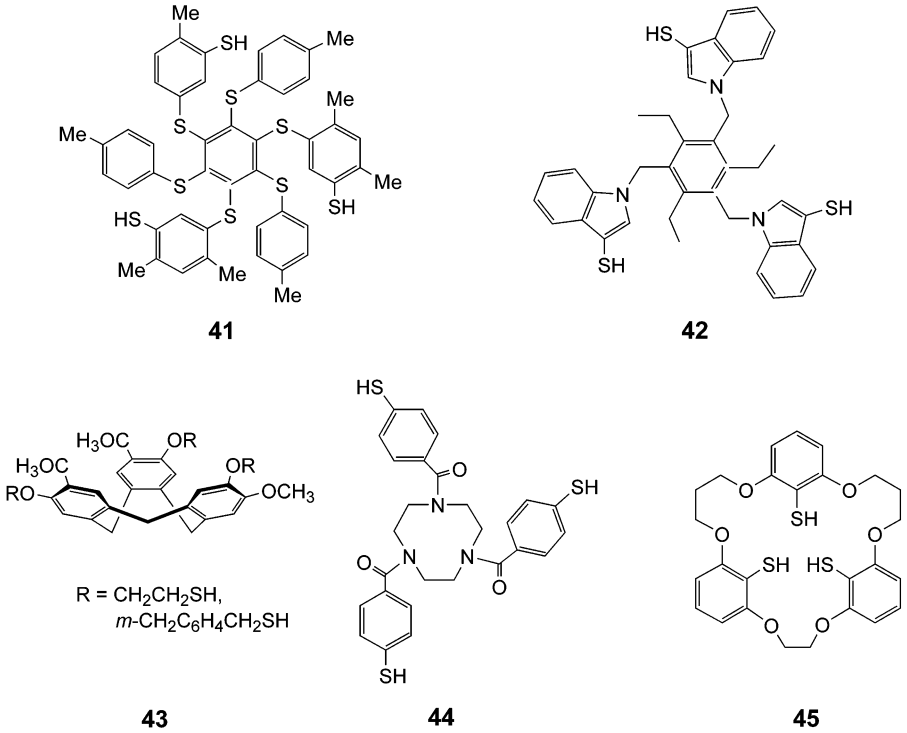

Figure 12. Trithiols **41**−**45** whose deprotonated forms stabilize 3:1 site-differentiated Fe_4S_4 clusters. The trianions of **41**−**44** bind clusters in a trigonally symmetric arrangement where clusters bound to the trianion of **45** have mirror symmetry.

position by the three *p*-tolylthio "legs". That conformation results in a semirigid cavitand ligand whose thiolate sulfur atoms are preorganized to capture a cluster in a cavity whose walls are the arms and whose floor is the central ring. This description follows from a conformational and molecular dynamics analysis.[164] Trithiol **42**, with three ethyl and three indolethiolate groups, is constructed on the same principle.[293] Conformations of the bowl-shaped cyclotriveratrylene building block of **43**[294,295] and the triazacyclononane ring of **44**[296] place thiol substituents on the same side of the molecule. Clusters derived from the trianions of **41**−**44** are expected to have three-fold symmetry. Crystallographic proof is available for $[Fe_4S_4(LS_3)L']^z$ clusters (vide infra) and a cluster from **42** with benzenethiolate at the unique iron site.[293] Trithiol **45** is conformationally flexible and forms clusters with mirror symmetry.[297] X-ray structures of clusters derived from **43**−**45** have not been reported; cluster symmetries in solution follow from ^{1}H NMR spectra. Site-specific substitution reactions have been described for clusters from **43**,[298] **44**,[296,299] and **45**.[297] The chemistry of LS_3 clusters is highly developed; leading aspects are next considered.

Reaction 36 (R = Et, 3R′SH = $L(SH)_3$) is used to prepare $[Fe_4S_4(LS_3)(SEt)]^{2-}$ (**14**), which in turn may be converted to $[Fe_4S_4(LS_3)Cl]^{2-}$ (**46**), of proven structure, by reaction with pivaloyl chloride.[51] These two clusters provide entry to a wide variety of new clusters arising from regiospecific substitution[54,58,300−304] or, in the synthesis of cuboidal **12** (Figure 6), removal of the unique iron atom. Cluster **14** is substituted with certain protic reactants (thiols, phenols, and others), whereas the labile chloride of cluster **46** is subject to replacement with a wide variety of ligands. Selected site-specific reactions of **46** are set out in Figure 13. Reactions can be monitored in situ by ^{1}H NMR because of the exquisite sensitivity of the isotropic shifts of substituents at the 4-, 5-, and 6-positions of the coordinating arms of LS_3 (Figure 6) to the identity of the ligand at the unique site. Simple substitution reactions with monoanions afford clusters **47**−**50**. Phenolate cluster **48**[302,304] is an analogue of the $Fe_4S_4(S{\cdot}Cys)_3(O{\cdot}Ser)$ cluster in the Cys77Ser mutant of *Chromatium* HP_{red},[305] and hydroxide cluster **50**[302] is an analogue of the active aconitase site **6**. Imidazole cluster **51**[304] relates to the $Fe_4S_4(S{\cdot}Cys)_3(N{\cdot}His)$ cluster in the Cys199His mutant of the *E. coli* DNA repair enzyme MutY,[306] and to the cluster distal to the active site in the electron-transfer chain of *Dg* Ni−Fe hydrogenase.[307] Clusters **52**−**54** demonstrate five-coordination at the unique site and its effect on redox potentials and Mössbauer parameters.[301,302] Similarly, clusters **55**−**57** provide six-coordinate sites, as shown by the X-ray structure of the Fe_4Se_4 analogue of **56**.[304] The tris(isocyanide) clusters **55** were significant in elucidating the electronic properties of cuboidal clusters. Because the unique site contains six-coordinate low-spin Fe^{II}, the $[Fe_3S_4]^0$ portion of the core is magnetically isolated. Magnetic and Mössbauer spectroscopic properties demonstrated the $S = 2$ ground state and electronic features very similar to inactive aconitase and *Dg* Fd II[54] and, later, to synthetic cluster **12**. Chloride cluster **46** is also a percursor to bridged double cubanes **58**,[302] **59**,[58,300] and **60**.[300]

The foregoing is a part of the large body of substitution reactions of 3:1 site-differentiated clusters that has led to a comprehensive family of such clusters, permitting elucidation of the consequences

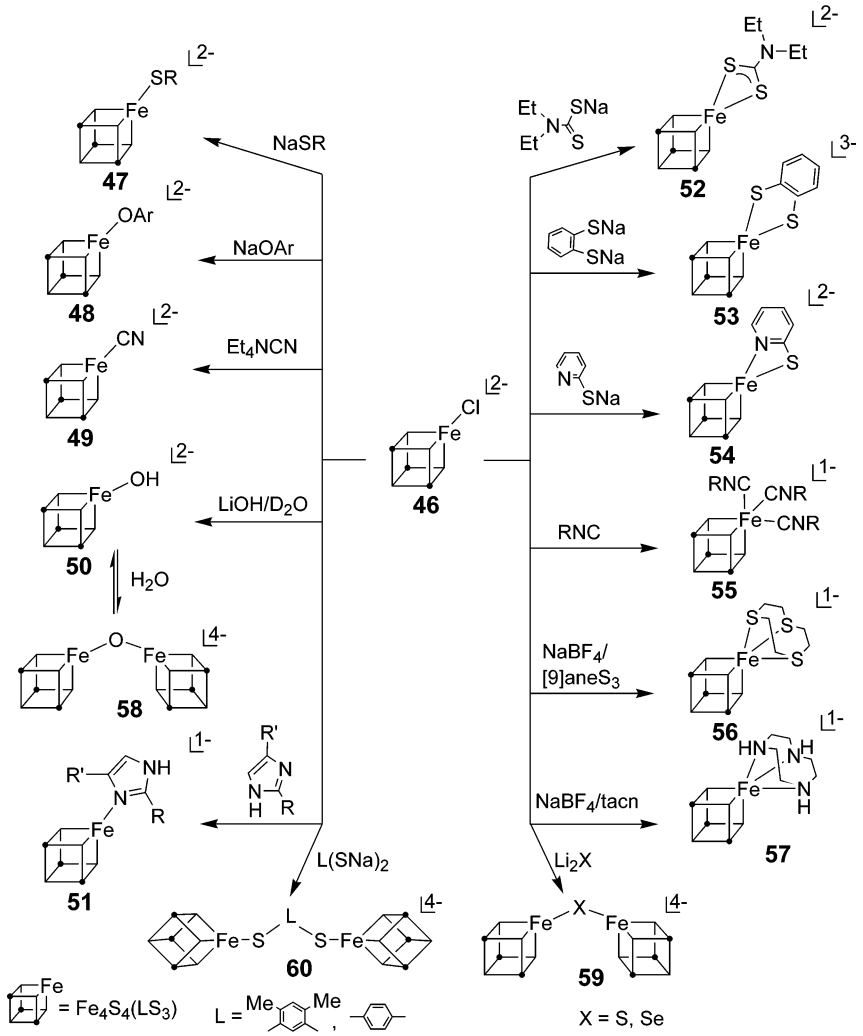

Figure 13. Selected site-specific reactions of $[Fe_4S_4(LS_3)Cl]^{2-}$ (**46**) to afford a variety of product clusters, including single cubanes with four-, five-, and six-coordinate unique sites and bridged double cubanes.

of ligand type, charge, and coordination number on properties such as NMR isotropic shifts, redox potentials, and charge distribution as inferred from ^{57}Fe isomer shifts. For example, many $[Fe_4S_4(LS_3)L']^z$ clusters undergo reversible electrochemical reduction to the $[Fe_4S_4]^+$ level, and several to the $[Fe_4S_4]^0$ level, at potentials that are modulated by the change of a single ligand.[182,302,304] A similar influence is observed for the $[Fe_4S_4]^{2+/+}$ couple of clusters derived from trithiol **43**.[295] The difference in reduction potentials of **12** and **46** is 0.12 V for the $[Fe_4S_4]^{2+/+}$ couple, with the thiolate cluster having the more negative potential. Alteration of cluster charge has a pronounced effect on potentials. The difference between **14** and monanion **51** is 0.32 V for the same couple, with the latter more easily reduced. Potential differences refer to acetonitrile solutions. For trianion **53** in Me_2SO, the $[Fe_4S_4]^{2+/+}$ potential ($E_{1/2} = -1.38$ V) is shifted by -0.41 V vs $[Fe_4S_4(LS_3)(SPh)]^{2-}$ as a reference, and the $[Fe_4S_4]^{3+/2+}$ couple appears at $E_{1/2} = -0.62$ V. The latter couple of the reference cluster is irreversible in Me_2SO and acetonitrile but is observed at 0.02 V in dichloromethane.[301] Potential shifts of the same sign are expected to apply to related protein-bound clusters. Other data and conclusions from electrochemical and spectroscopic measurements are too extensive to summarize here; the original literature should be consulted.

A limited set of 2:2 site-differentiated clusters has been synthesized, some of which are noted above. Other examples are the products of reactions 43 and 44 (R = Et, Ph).[308]

$$[Fe_4S_4Cl_4]^{2-} + 6Bu^tNC \rightarrow [Fe_4S_4Cl_2(Bu^tNC)_6] + 2Cl^- \quad (43)$$

$$[Fe_4S_4Cl_2(Bu^tNC)_6] + 2NaSR \rightarrow [Fe_4S_4(SR)_2(Bu^tNC)_6] + 2NaCl \quad (44)$$

The clusters contain on opposite Fe_2S_2 faces two low-spin Fe^{II} sites separated by 3.46 Å and overall closely approach idealized C_2 symmetry. The tetrahedral Fe^{III} sites are part of an Fe_2S_2 rhomb (Fe−Fe 2.73 Å) whose dimensions are quite similar to a face of an Fe_4S_4 cluster. While not site analogues, the hexakis(isonitrile) clusters have provided a unique way to determine magnetic parameters of current interest.[309] These neutral clusters contain an antiferromagnetically coupled $Fe^{III}Fe^{III}$ pair in a geometry very similar to that of the corresponding pair in $[Fe_3S_4]^{+,0}$ and $[Fe_4S_4]^{3+}$ cores.

Values of $J = 240-280$ cm^{-1} ($H = J\mathbf{S}_1\cdot\mathbf{S}_2$) were obtained from magnetic measurements. These are the first directly determined J-values for $[Fe_2(\mu_3\text{-}S)_2]^{2+}$ fragments, and the best available initial values in interpreting magnetic properties of protein clusters.

5.7.3. Bridged Assemblies

Iron−sulfur clusters are implicated in active sites considerably more complicated than structures **2**−**6**. The next level of complexity about the cubane-type cluster is the electron-transfer P cluster of nitrogenase,[310] shown in Figure 1 in its crystallographically defined P^N (**7**) and P^{OX} (**8**) states.[311,312] There are no strict synthetic analogues of these clusters, but the overall topology of the P^N state has been achieved in clusters with $M_2Fe_6S_9$ cores (M = V, Mo).[313,314] The P clusters are members of a group of protein-bound clusters designated as bridged assemblies, which in general consist of two discrete fragments that are coupled by one or more covalent bridges. Assemblies containing Fe_4S_4 clusters also include those in *E. coli* sulfite reductase ($[Fe_4S_4]$-(μ_2-S·Cys)-siroheme)[315,316] and *Clostridium thermoaceticum* carbon monoxide dehydrogenase/acetyl-CoA synthase ($[Fe_4S_4]$-(μ_2-S·Cys)-Cu(L)-{(μ_2-S·Cys)$_2$Gly}Ni].[317] In site analogue chemistry as a whole, the greatest challenges now lie in the synthesis and characterization of accurate representations of bridged analogues. Previously, we have called attention to bridged assemblies and considered means by which 3:1 site-differentiated clusters could be used in the synthesis of analogues.[282,318]

The first Fe_4S_4 bridged assemblies were obtained in the period 1989−1991. They include dithiolate-bridged **60** (Figure 13) and sulfide-bridged **61** (3RS = LS_3), the latter by coupling reaction 45.[300] This cluster is depicted in Figure 14, together with other bridged species. These clusters were isolated but did not yield diffraction-quality crystals. This work was quickly followed by reaction 46, which provided the first X-ray structure proof of a bridged double cubane.[319]

$$2[Fe_4S_4(LS_3)Cl]^{2-} + Li_2S \rightarrow \{[Fe_4S_4(LS_3)]_2(\mu_2\text{-}S)\}^{4-} + 2LiCl \quad (45)$$

$$2[Fe_4S_4Cl_4]^{2-} + Li_2S \rightarrow \{[Fe_4S_4Cl_3]_2(\mu_2\text{-}S)\}^{4-} + 2LiCl \quad (46)$$

In a mixed cation salt, the individual clusters were found in a cisoid arrangement with an imposed C_2 axis containing the μ_2-S atom. The Fe−S−Fe bridge angle is 102.2°, and the iron atoms are separated by 3.43 Å. Sometime later, the bridged structure of $\{[Fe_4Se_4(LS_3)]_2Se\}^{4-}$ with Fe−Se−Fe = 112.7° and 115.5° in two inequivalent anions, was similarly established,[320] providing also a structure proof of **61**. In the next development, oxo-bridged **58** was shown to exist in equilibrium 47 with hydroxo cluster **50** (Figure 13). The clusters were not isolated but were identified electrochemically, **50** showing a reduction at $E_{1/2} = -1.05$ V and **58** showing two coupled reductions at $E_{1/2} = -1.24$ and -1.47 V in Me_2SO containing ca. 1 mM water.[302] Coupled redox steps are characteristic of double cubanes with sufficiently short bridges. For example, **61** (0.24 V), its selenide analogue (0.25 V), $\{[Fe_4S_4Cl_3]_2(\mu_2\text{-}S)\}^{4-}$ (0.31 V), and **58** with R = 1,2-$C_2H_4S_2^{2-}$ (0.07 V), together with a number of heterometal bridged double cubanes, show this effect;[300,320] potential separations are indicated. Its presence is one means of identifying bridged clusters.

$$\{[Fe_4S_4(LS_3)]_2O\}^{4-} + H_2O \rightleftarrows 2[Fe_4S_4(LS_3)(OH)]^{2-} \quad (47)$$

Cluster **61** has also been observed in labile equilibrium 48, from which it may be isolated.[57,58] The hydrosulfide single cubane is accessible from the reaction of $[Fe_4S_4(LS_3)(SEt)]^{2-}$ with H_2S or by the reaction of **14** with HS^-.

$$2[Fe_4S_4(LS_3)(SH)]^{2-} \rightleftarrows \{[Fe_4S_4(LS_3)]_2(\mu_2\text{-}S)\}^{4-} + H_2S \quad (48)$$

$$[Fe_4S_4(SEt)_4]^{2-} + 4H_2S \rightleftarrows [Fe_4S_4(SH)_4]^{2-} + 4EtSH \quad (49)$$

By continued reaction of $[Fe_4S_4(LS_3)(SH)]^{2-}$ with H_2S, or more simply by reaction **49**, the most elementary homoleptic cluster **13a** has been prepared. The cluster had been obtained much earlier by a nonrational route and its structure determined.[192] It is prone to self-condensation in solution, but unlike reaction **48**, multiple products are possible. In acetonitrile, the cluster exists in dynamic equilibrium with self-condensation products formed by elimination of H_2S and formation of sulfide-bridged clusters.[193] One of the latter appears to be prevalent, leading to a simplified description of the system in terms of reaction 50. The product cluster is a sulfide-bridged assembly whose proposed structure involves a central cubane forming two sulfide bridges to other cubanes in an acyclic arrangement. The cluster has not been isolated.

$$3[Fe_4S_4(SH)_4]^{2-} \rightleftarrows \{[Fe_4S_4(SH)_3]_2[Fe_4S_4(SH)_2](\mu_2\text{-}S)_2\}^{6-} + 2H_2S \quad (50)$$

With the formation of bridged cubane assemblies demonstrated, attention was directed to other types of assemblies. The cluster $[Fe_4S_4(LS_3)(S\text{-}4\text{-}py)]$ and its 3-pyridyl variant are readily prepared from $[Fe_4S_4(LS_3)(SMe)]^{2-}$ and the pyridylthiol. The pyridyl portion provides a binding site for a metal, as in the assembly **62**, for which the formation constants are 790 M^{-1} (R = Me) and 920 M^{-1} (R = CF_3) for binding to the high-spin Fe^{II} complexes.[303] Other choices of binding groups and complexes could eliminate the complicating feature of a labile equilibrium. This work, in which the bridge is nonphysiological, demonstrates that assemblies with extended bridges can be prepared. This type of cluster assembly has been little pursued past the initial report, possibly because no extended organic bridges have yet been found with protein-bound Fe_4S_4 clusters.

Assemblies **63** and **64** (Figure 14) provide approaches to the active site of sulfite reductase, which

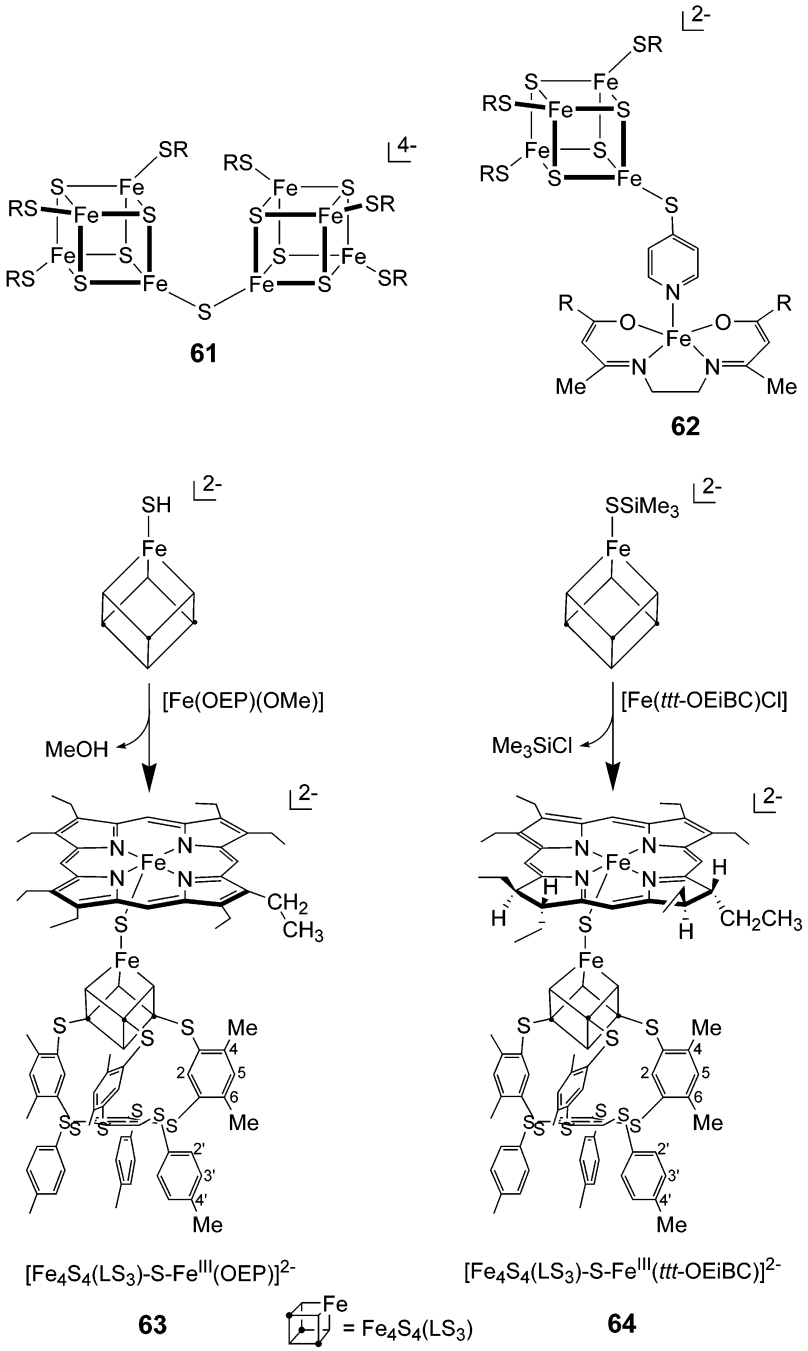

Figure 14. Various bridged assemblies based on the site-differentiated cluster $Fe_4S_4(LS_3)$, including the sulfide-bridged cubane (**61**) and hemes (**63**, **64**), and an extended organic bridge binding to a planar Fe^{II} complex (**62**).

catalyzes the reaction $SO_3^{2-} + 7H^+ + 6e^- \rightarrow HS^- + 3H_2O$. All attempts in this laboratory and elsewhere[321] to bind a heme group to a cluster by a thiolate bridge have not rendered the desired result. A subclass of these reductases is thought to have a sulfide rather than a cysteinate bridge. Heme cluster sulfide-bridged assemblies have been prepared as outlined in Figure 14 using 3:1 differentiated clusters. The method leading to $[Fe_4S_4(LS_3)-(\mu_2\text{-}S)-Fe^{III}(OEP)]^{2-}$ (**63**) is one of four coupling reactions that form this product.[57,58] The assembly $[Fe_4S_4(LS_3)-(\mu_2\text{-}S)-Fe^{III}(salen)]^{2-}$ was prepared in a related reaction involving $\{[Fe(salen)]_2O\}$, $[Fe_4S_4(LS_3)(SH)]^{2-}$, and Et_3NH^+.[58] Sulfite reductase contains siroheme, an iron complex of sirohydrochlorin which, with adjacent pyrroline rings reduced, is at the isobacteriochlorin oxidation level. The assembly $[Fe_4S_4(LS_3)-(\mu_2\text{-}S)-Fe^{III}(OEiBC)]^{2-}$ (**64**) is a closer approach to the enzyme site because it contains the diastereomeric isobacteriochlorin fragment Fe^{III}(*ttt*-OEiBC).[59] The preparative route relies on the ca. 35 kcal/mol energy difference between Si−Cl and Si−S bonds. The principal electronic feature of the bridged assemblies is the greatly enhanced isotropic shifts of the cluster ligand arising from spin delocalization across the high-spin $Fe^{III}-S-Fe_{cluster}$ bridge, which, together with the methods of synthesis, supports the bridged structures of **63** and **64** in the absence of crystallographic proof. While these structures, with their unsupported bridges, are insufficiently robust to serve in functional analogue reaction systems, they are among the most complex analogue-bridged as-

semblies yet prepared, Further, they illustrate solutions (albeit specific ones) to the likely general problem of unsymmetrical coupling in preparing analogues of bridged biological assemblies. Lastly, we reemphasize the potential of designed peptides, illustrated with the aformentioned $(Cys{\cdot}S)_3Fe_4S_4-(\mu_2\text{-}S{\cdot}Cys)-Ni$ unit,[65] a means of stabilizing bridged assemblies.

6. Mössbauer Parameters and Oxidation States

Nearly all modern spectroscopic and magnetic techniques have been applied to the protein-bound iron−sulfur centers and their synthetic analogues for the elucidation of geometrical and electronic structure. Iron−sulfur clusters, especially cuboidal Fe_3S_4 and cubane-type Fe_4S_4, have served as spectroscopic laboratories over the past two decades, in which such concepts as electron delocalization and magnetic exchange coupling and double exchange have been revisited in an entirely new context. EPR spectroscopy has occupied an historical place in iron−sulfur biochemistry since 1960, when the classical $g = 1.94$-type EPR signal was detected in beef heart mitochondria and in succinate and DPNH dehydrogenase preparations.[322,323] Subsequently, very similar signals were found in purified proteins containing $[Fe_2S_2]^+$ and $[Fe_4S_4]^+$ centers. In favorable circumstances, EPR can differentiate sites **2ab**, **4**, and **5**. In more recent times, variable-temperature MCD spectra have proven incisive in identifying protein sites with paramagnetic ground states. Mössbauer spectroscopy has been of compelling significance to iron−sulfur biochemistry in site identification, determination of oxidation states, and elucidation of magnetic coupling and electronic ground states. These and other physical techniques indispensable to modern bioinorganic chemisty have been elaborated in current and highly useful sources.[324,325]

While spectroscopic properties have not been examined in detail in this account, it is the case that results for sites and their synthetic analogues are in good agreement. Therefore, in general protein structure and environment induce perturbations on electronic properties rather than discontinuous changes. Among the techniques that have been most effectual in correlating site and analogue properties is Mössbauer spectroscopy.[326,327] Isomer shifts directly reflect s-electron density at the ^{57}Fe nucleus, which is influenced by variation of the valence shell s density and by shielding effects of p and d electron distributions. The database of protein site and analogue Mössbauer parameters is now extensive. Ranges of isomer shifts δ and quadrupole splittings ΔE_Q, dependent on oxidation and spin state and ligand type, for compounds of biological interest have been tabulated.[327] Here we present a summary of isomer shifts for analogue species of known structure and oxidation state.

Presented in Figure 15 are distribution plots of ^{57}Fe isomer shifts for different (mean) oxidation states at 4.2 and 77 K, two common temperatures of measurement. The data refer to tetrahedral $FeS_n(SR)_{4-n}$ sites ($n = 0, 2, 3$) in synthetic species. Results from the much smaller database of FeS_3L shifts ($L = ArO^-$, halide, R_3P) are not included, nor are protein data. They define the order $\delta = Cl^- > RS^- > R_3P$ at parity of oxidation state. The $Fe^{2+,3+}$ results derive mainly from $[Fe(SR)_4]^{2-,-}$ species, and the remaining data from $[Fe_4S_4(SR)_4]^{-,2-,3-}$ clusters. In compiling the results, weighted average shifts were used for delocalized species that were fit with more than one quadrupole doublet. For $Fe^{2.75+}$, the only datum is from **28** (Figure 9). As is evident, the majority of the data refer to $[Fe_4S_4(SR)_4]^{2-,3-}$ clusters, for which there are appreciable variations. For the $Fe^{2.5+}$ case, the nature of the counterion and lattice effects can cause small modulations in isomer shift at fixed temperature.[198,202,204,205] Isomer shifts at the two temperatures were fit to the linear relationships 51 ($R = 0.996$) and 52 ($R = 0.951$), where s is the oxidation state.

$$\delta = 1.51 - 0.41s \qquad (4.2\ \text{K}) \qquad (51)$$

$$\delta = 1.43 - 0.40s \qquad (77\ \text{K}) \qquad (52)$$

Similar fits have been presented in the past based on less data; the most recent of these is $\delta = 1.36 - 0.36s$.[328] These relationships should be helpful in assigning oxidation states of new compounds. This approach has been employed to assign oxidation states in MFe_3S_4 heterometal clusters, including several in Figure 7. With the appropriate database, the oxidation state of the site FeS_4 (or more generally FeS_3L) is assigned, and the oxidation state of atom M is obtained by difference knowing the core charge.[158,328−330] The resultant description of charge distribution is formalistic but useful, provided atom M does not largely perturb the isomers shifts intrinsic to the FeS_3L site.

Summarized in Table 6 are ranges of isomer shifts for tetrahedral FeS_4 and other sites with coordination numbers five and six. Examples of the sites $FeS_3L_{2,3}$ are not widespread in proteins; substrate-bound aconitase is perhaps the most familiar example.[284] A relatively small set of such sites occur in analogue complexes.[53,219,301,304,308,331,332] All are obtained by ligand substitution of a $[Fe_4S_4]^{2+}$ cluster, often $[Fe_4S_4(LS_3)Cl]^{2-}$ (**46**, Figure 13).[301] For all but isocyanide-ligated sites and one phosphine-ligated species, isomer shifts tend to be higher than for tetrahedral $Fe^{2.5+}$, consistent with an effectively more reduced site. Local spins at the higher coordinate sites have not been established, except in the case of $FeS_3(CNR)_3$, which contain low-spin Fe^{II}, as in cluster **54** (Figure 13). The $[Fe_4S_4]^{2+}$ core has undergone electron redistribution such that one Fe^{3+} ($\delta = 0.34$ mm/s) and a delocalized pair $Fe^{2.5+}$ ($\delta = 0.46-0.47$ mm/s) are developed.[53] The electronic structure reduces to that of the $[Fe_3S_4]^0$ core, already described. This is the most extreme case known of a five- or six-coordinate site influencing electron distribution within a cluster core. The isomer shifts in Table 6 may be useful in detecting $FeS_3L_{2,3}$ sites in synthetic and protein-bound clusters. In using these data, it should be realized that FeS_4N, FeS_3N_2, and FeS_3N_3 sites are described as such on the assumption of bidentate or tridentate binding of ligands rather than from X-ray structure proof. This seems a particulary safe as-

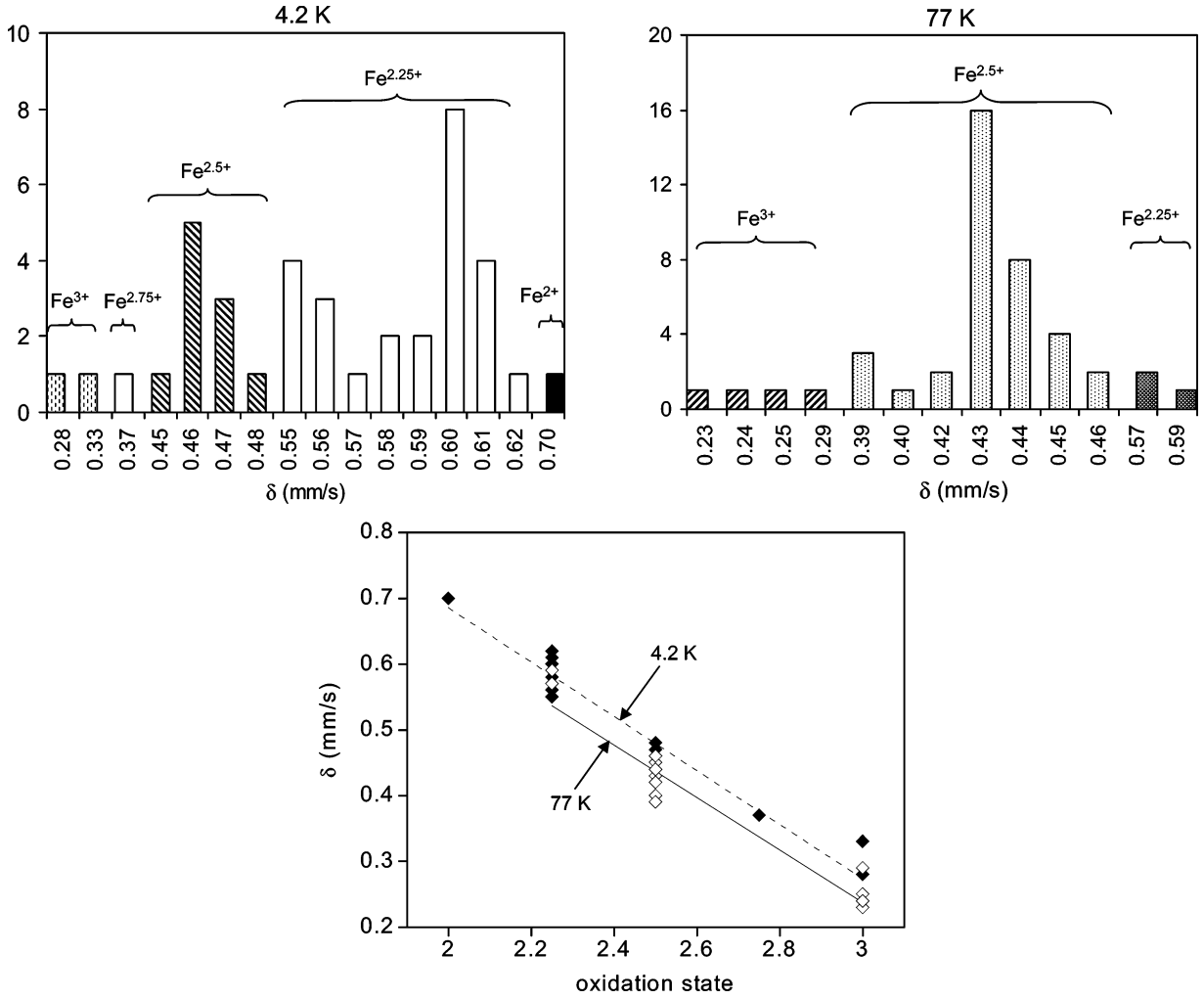

Figure 15. (Upper) Distribution plots of ^{57}Fe isomer shifts for the indicated (mean) oxidation states at 4.2 and 77 K. (Lower) Plots of isomers shifts vs (mean) oxidation state at two temperatures. Data at 4.2 K (- - -) and 77 K (—) were fitted by linear regression analysis.

Table 6. Mössbauer Data for FeS_3L_n Sites (L = N, O, S; n = 1−3)

site	T (K)	δ (mm/s)[a]	ΔE_Q (mm/s)	refs
FeS_4		*b*	*c*	
$Fe^{2.0}$	4.2	0.70		
$Fe^{2.25+}$	4.2	0.55−0.62		
	77	0.57−0.59		
$Fe^{2.5+}$	4.2	0.45−0.48		
	77	0.39−0.46		
$Fe^{2.75+}$	4.2	0.37		
$Fe^{3.0+}$	4.2	0.28−0.33		
	77	0.23−0.29		
FeS_5[d]	4.2	0.64−0.67	1.84−1.97	219, 301
	77	0.64	1.84	331
FeS_4O	4.2	0.63−0.64	1.47−1.84	219, 301
FeS_4N	4.2	0.64	1.70	301
FeS_3N_2	4.2	0.95	2.38	301
FeS_3P_2	125	0.31	0.71	332
FeS_3N_3	4.2	0.80−0.95	1.55−2.38	301
$FeS_3(CNR)_3$[e]	4.2	0.20	0.50	53
	77	0.16−0.19	0.43−0.49	308

[a] Relative to Fe metal at room temperature. [b] Diverse values, not tabulated. [c] Cf. Tables 2−5. [d] All five- and six-coordinate sites are in $[Fe_4S_4]^{2+}$ clusters. [e] Low-spin Fe^{II}.

sumption for $[Fe_4S_4(LS_3)(2\text{-S-py})]^{2-}$, with a strongly chelating ligand, and for $[Fe_4S_4(LS_3)(tacn)]^{-}$ and $[Fe_4S_4(LS_3)(HBpz_3)]^{2-}$, given the six-coordinate site in $[Fe_4Se_4(LS_3)(9\text{-ane}S_3)]^{-}$ (related to **56**, Figure 13). In the case of aconitase, addition of substrate caused the Mössbauer parameters of the resting cluster **6** (δ = 0.44 mm/s, ΔE_Q = 0.83, 1.30 mm/s) to change. In samples equilibrated with citrate, there appear two new quadrupole doublets with $\delta/\Delta E_Q$ = 0.85/1.23 mm/s and 0.90/1.80 mm/s (80%) and sites with unchanged parameters (17%).[333,334] These doublets have been interpreted in terms of five- or six-coordinate sites with pronounced Fe^{II} character, an assignment supported by X-ray crystallography and ENDOR spectroscopy.[284,285,335] Note that the parameters are comparable with those of the five- and six-coordinate sites $FeS_3N_{2,3}$ (Table 6).

7. Structural Conversions

A highly significant feature of iron−sulfur analogue species is facile *conversion* between structures, as first elucidated in 1977−1981,[41,43] and subsequently observed in proteins. Some of the earliest examples occur with aconitase and include the transformations $[Fe_3S_4]^{+} \rightarrow [Fe_4S_4]^{2+}$ under reducing conditions[336] and cuboidal $[Fe_3S_4]^{+}$ to linear $[Fe_3S_4]^{+}$ upon partial unfolding.[21] Conversion reactions, some of which have been previously cited in the context of synthesis, are schematically illustrated in Figure 16 and are collected in Table 7. Reactions are written

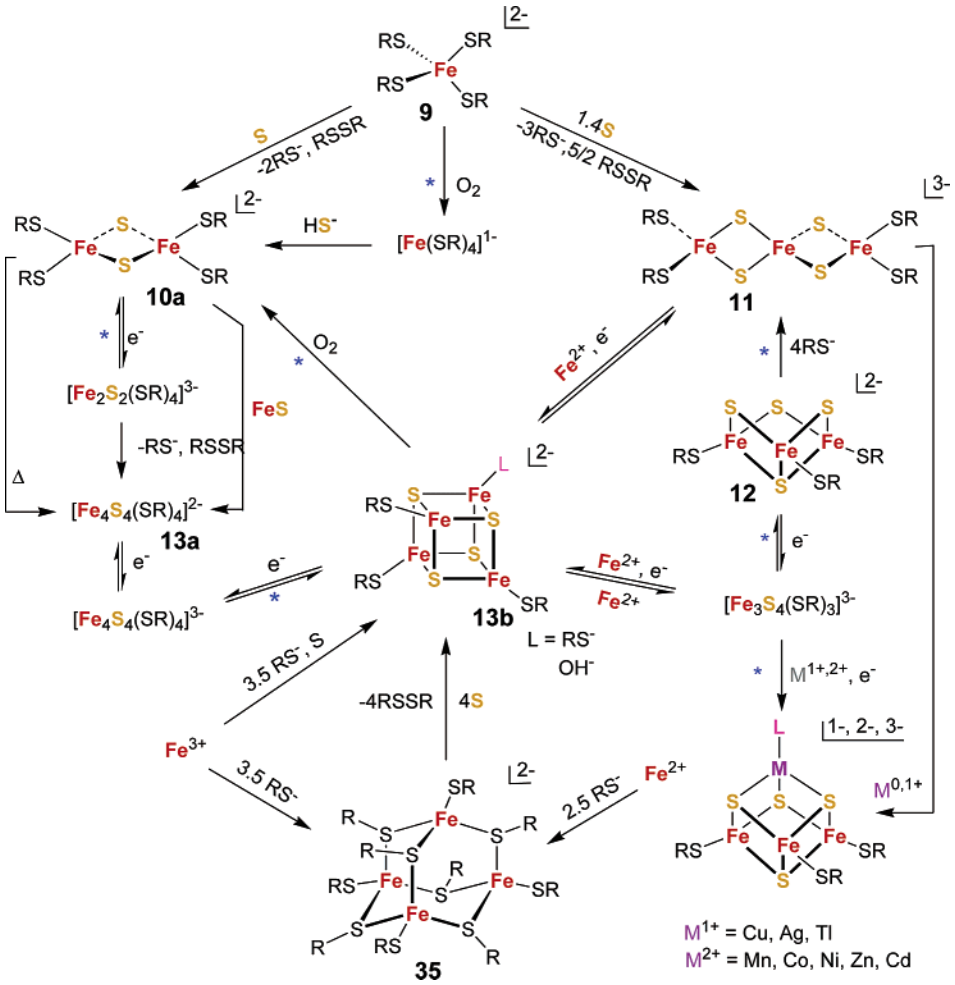

Figure 16. Structural conversions among iron−sulfur complexes and clusters. Those marked with an asterisk have been observed in proteins.

Table 7. Conversion Reactions of Complexes and Clusters

no.	reaction	refs
	$Fe^{2+} \rightleftharpoons Fe^{3+}$	
53	$[Fe(SR)_4]^{2-} + {}^1/_2O_2 \rightarrow [Fe(SR)_4]^- + {}^1/_2O_2^-$	9, 37
54	$4[Fe(SR)_4]^- \rightarrow [Fe_4(SR)_{10}]^{2-} + 2RSSR + 2RS^-$	43
55	$[Fe(SR)_4]^- + RS^- \rightarrow [Fe(SR)_4]^{2-} + {}^1/_2\ RSSR$	43
	$Fe^{2+,3+} \rightarrow [Fe_2S_2]^{2+}$	
6	$2\ [Fe(SR)_4]^{2-} + 2S \rightarrow [Fe_2S_2(SR)_4]^{2-} + RSSR + 2RS^-$	22
7	$2\ [Fe(SR)_4]^- + 2S \rightarrow [Fe_2S_2(SR)_4]^{2-} + 2RSSR$	112
	$[Fe_2S_2]^{+,2+} \rightarrow [Fe_4S_4]^{2+}$	
11	$2[Fe_2S_2(SR)_4]^{3-} \rightarrow [Fe_4S_4(SR)_4]^{2-} + 4RS^-$	41
12	$2[Fe_2S_2(SR)_4]^{2-} \rightarrow [Fe_4S_4(SR)_4]^{2-} + RSSR + 2RS^-$	22, 41, 43
	$Fe^{2+}_4 \rightarrow [Fe_4S_4]^{2+}$	
38b	$[Fe_4(SR)_{10}]^{2-} + 4S \rightarrow [Fe_4S_4(SR)_4]^{2-} + 3RSSR$	43
	$[Fe_3S_4]^{+,0} \rightarrow [Fe_4S_4]^{2+}$	
56	$[Fe_3S_4(SR)_4]^{3-} + Fe^{2+} + RS^- \rightarrow [Fe_4S_4(SR)_4]^{2-} + {}^1/_2RSSR$	22
57	$[Fe_3S_4(SR)_3]^{3-} + Fe^{2+} + RS^- \rightarrow [Fe_4S_4(SR)_4]^{2-}$	61, 62
	$[Fe_4S_4]^{2+} \rightarrow [Fe_3S_4]^0$	
58	$[Fe_4S_4(SR)_3L]^{2-} + (L')^z \rightarrow [Fe_3S_4(SR)_3]^{3-} + Fe(L')^{z+2} + L$	20, 61
	$[Fe_3S_4]^{+,0} \rightarrow [MFe_3S_4]^{2+,+,0}$	
21[a]	$[Fe_3S_4(SR)_4]^{3-} + [M(CO)_3(MeCN)_3] \rightarrow [(OC)_3MFe_3S_4(SR)_3]^{3-} + {}^1/_2RSSR + 3MeCN$	52, 157
60[b,c]	$[Fe_3S_4(SR)_4]^{3-} + [ML_n]^{+,0} \rightarrow [LMFe_3S_4(SR)_3]^{2-,-} + RS^- + (n\text{-}1)L$	158, 172, 173
28[a]	$[Fe_3S_4(SR)_3]^{3-} + [M(CO)_3(MeCN)_3] \rightarrow [(OC)_3MFe_3S_4(SR)_3]^{3-} + 3MeCN$	173
61[b–d]	$[Fe_3S_4(SR)_3]^{3-} + [ML_n]^+ \rightarrow [LMFe_3S_4(SR)_3]^{2-} + (n-1)L$	20, 173

[a] M = Mo, W. [b] M = Co, Ni. [c] Reaction written with L as a neutral ligand. [d] M = Cu, Ag, Tl.

with idealized stoichiometries and in general form without implication that a given reaction occurs for all R substituents. Selected examples with proteins are cited below. Extensive consideration of protein site conversions is beyond the purview of this account; these have been summarized elsewhere.[149]

Reactions 53 and 55 are, strictly speaking, not conversion reactions because both reactant and product **9** are tetrahedral. They are included because of their relation to certain protein reactions. Reaction 53 is an oxidative transformation observed with $[Fe(SR)_4]^{2-}$. However, it is sometimes difficult to control and not always a desirable synthetic reaction. Reaction 54 generates the cage complex $[Fe_4(SR)_{10}]^{2-}$, which has no recognized protein-bound counterpart but is useful in synthesis. Reaction 55 occurs, sometimes slowly, when a Rd_{ox} analogue is allowed to stand in the presence of excess thiolate. Reactions 53 and 55 are versions of the redox couple $Rd_{ox} + e^- \rightleftarrows Rd_{red}$. Aerial oxidation of Rd_{red} is a familiar reaction, as is the reduction of Rd_{ox} with an agent such as dithionite.

Reactions 6 and 7 are mononuclear-to-binuclear conversions in synthetic routes to cluster **10a** from Fe^{II} and Fe^{III}, respectively. Reactions 11 and 12 are binuclear-to-tetranuclear conversions. Reaction 11 is favored because the cores of reactant and product have the same oxidation level and it occurs spontaneously. As observed previously, no $[Fe_2S_2]^+$ cluster has ever been isolated. Reaction 12 is more likely to occur in protic media, owing to stabilization of liberated thiolate. In general, this reaction does not intervene in dry aprotic solvents. Note that the species $[Fe_2S_2(SBu^t)_4]^{2-}$, containing a strongly reducing thiolate, has been isolated (Table 3). Reactions 6, 12, 38b, and 54 are implicated in reaction pathways leading to the cluster dianion **13a** (Figure 10).

In proteins, the tetranuclear-to-binuclear conversion $[Fe_4S_4]^{2+} \rightarrow [Fe_2S_2]^{2+}$ effected by dioxygen alone is widespread and has been well documented for a number of proteins from *E. coli*, including biotin synthase,[337−339] lipoate synthase,[338] anaerobic ribonucleotide reductase,[340,341] pyruvate formate−lyase activating enzyme,[342,343] and the FNR transcription factor in vitro[344] and in whole cells.[345] With some proteins, the reaction is reversible under reducing conditions and corresponds to a $[Fe_2S_2]^+ \rightarrow [Fe_4S_4]^{2+}$ transformation. In all cases, complete or nearly complete cysteinate terminal ligation is indicated by ^{57}Fe isomer shifts and resonance Raman spectroscopy. These examples are derived from adenosylmethionine-dependent enzymes, for which a summary account of the role of iron−sulfur clusters is available.[346] In analogue clusters, the aerobic transformation $[Fe_4S_4(SR)_4]^{2-} \rightarrow [Fe_2S_2(SR)_4]^{2-}$ is not well documented, and its stoichiometry is obscure.

Reactions 56 and 57 are trinuclear-to-tetranuclear conversions with different initial clusters. In reaction 56, linear cluster **11** is converted to a cubane-type product. It is closely related to reaction 18, in which bound thiolate functions as the reductant. In minimal form, the transformation is $[Fe_3S_4]^+ + Fe^{2+} + e^- \rightarrow [Fe_4S_4]^{2+}$ and accounts for the reconstitution of the tetranuclear site in aconitase. In reaction 57, cuboidal cluster **12** is converted to the same product by incorporating Fe^{2+} at the vacant core site in a process analogous to reaction 24 (Figure 7). In most proteins, this process starts with the oxidized site, in which case the minimal reaction is $[Fe_3S_4]^+ + Fe^{2+} + e^- \rightarrow [Fe_4S_4]^{2+}$ upon addition of a reductant. Reaction 58 is effectively the reverse of 57 and requires the addition of some ligand L′ to complex the Fe^{II}. The only example in analogue chemistry is the two-step reaction **15** → **16** → **12** (Figure 6); in the last step L = L′, and both ligands bind Fe^{II}. In proteins, the conversion from a cubane to a cuboidal cluster usually occurs when the latter carries a non-protein ligand at one site, as in site **6** of active aconitase. Oxidation of the cluster facilitates the minimal reaction $[Fe_4S_4]^{3+} \rightarrow [Fe_3S_4]^+ + Fe^{2+}$, by which Fe^{2+} is lost, owing to decreased sulfide nucleophilicity in the oxidized core and the absence of a restraining protein ligand.

Reactions 21, 28, 60, and 61 result in the formation of heterometal cubane clusters which are exemplified in Figure 7. In reaction 21, the core of linear cluster **11** is reduced by coordinated thiolate, and the M^0 fragment is bound in $[MFe_3S_4]^0$. Reaction 60 proceeds by one- or two-electron reduction of the linear $[Fe_3S_4]^+$ core by an M^+ or M^0 species, respectively, followed by capture of M^{2+} in $[MFe_3S_4]^{2+}$ or $[MFe_3S_4]^+$. Reactions 19 and 20 are specific examples of heterometal cluster formation by electron transfer. Reactions 28 and 61 involve cuboidal cluster **12** and its $[Fe_3S_4]^0$ core. Reactions 21 and 28 differ in that the latter is not a redox process; the initial core binds the M^0 fragment. In reaction 61, thiophilic monocations such as Cu^I bind without electron transfer, while Co^I and Ni^I reduce the core and bind as $[MFe_3S_4]^+$. Overall, protein-bound cuboidal clusters bind a variety of monovalent and divalent ions to afford products to which a cubane-type structure is assigned.[71,169] While no MFe_3S_4 cluster of biosynthetic origin has yet been found, it would be not entirely surprising if such clusters do appear naturally, given their ease of formation and usually stable structures. This matter has been considered by others.[347]

8. Perspective

The development of synthetic analogues of the active sites of iron−sulfur proteins has played a significant role in the evolution of bioinorganic chemistry since the early 1970s. It has been shown how inorganic chemistry and biochemistry can be brought together in a synergistic manner. The inorganic approach has clarified and extended our knowledge of protein sites through original synthesis and physicochemical and reactivity examination, while the existence and problems posed by the biological sites have inspired new chemistry which never would have been conceived in the absence of these products of biosynthesis. No two metal and non-metal elements in combination have ever generated as large a number of structure types as those encompassed by iron−sulfur clusters,[73] the majority of which are not known to occur naturally. Nearly all properties can be attributed to the *weak-field* nature of the complexes and clusters: tetrahedral site stereochemistry and attendant high-spin $d^{5,6}$ electron configurations in two readily accessible oxidation states ($Fe^{II,III}$), magnetic ground states modulated by exchange coupling, low inner-sphere barriers to electron exhange, kinetic lability to substitution of terminal ligands, and facile structural conversions of a scope

not encountered elsewhere. These features derive from the weak-field properties of thiolate and sulfide, and the propensity of the latter to maintain the effective S^{2-} oxidation state (Fe−S bond covalency notwithstanding), even in the presence of one or more Fe^{III} interactions. A further advantage is the nucleophilicity of coordinated thiolate, facilitating various types of substitution reactions. These fascinating properties collectively outweigh certain practical experimental difficulties, the most pronounced of which are sensitivities to dioxygen, water and other protic acids, and bases.

Iron−sulfur analogue chemistry is now a mature subject in large part. While certain details remain, it is likely that the leading features of protein sites **1**−**6** and their synthetic analogues **9**−**13** have been delineated experimentally and theoretically. Investigators who utilize the synthetic analogue approach in iron−sulfur biochemistry now turn their attention to far more complicated objectives which include, inter alia, the FeMo cofactor and P cluster (**7**, **8**) of nitrogenase,[311,312,348] and the clusters in iron hydrogenases,[349,350] nickel−iron hydrogenases,[307,351] and carbon monoxide dehydrogenase.[352,353] These objectives expand to heterometal iron−sulfur clusters and will require new reaction methodology to meet the desired goals. Returning to iron clusters, we note the emergence of a large class of iron arylimido clusters of nuclearities 2−4 and structures quite similar to **2**−**5**.[73,354−356] These, too, are weak-field clusters, but certain differences are already evident: stabilization of higher oxidation levels, the stable existence of an Fe═NR terminal imide on an $Fe_4(NBu^t)_4$ cubane-type cluster (no Fe═S group is known in any molecule), and a much higher sensitivity to protic impurities. Property comparisons between iron−sulfide and iron−imide clusters should prove illuminating. Finally, one is given to conjecture whether iron−nitrogen chemistry will ultimately provide a route to clusters with interstitial atoms. This is a particularly difficult problem in that no methodology exists for the deliberate construction of interstitial molecular clusters in solution. The synthesis of the FeMo-cofactor cluster with its newly recognized interstitial atom, possibly nitride[348] (i.e., $MoFe_7NS_9$), poses a challenge to the analogue chemist no less imposing than that of any other complex natural product.

9. Acknowledgments

Research in the authors' laboratory in the field of iron−sulfur chemistry has been supported by NIH Grant GM 28856. We thank Dr. S. C. Lee for useful discussions.

10. Abbreviations

AS	absorption spectra
Ad	1-adamantyl
9-aneS_3	1,4,7-trithiacyclononane
Av	*Azotobacter vinelandii*
Cp	*Clostridium pasteurianum*
E	electrochemistry, redox potential
Fd	ferredoxin
$HBpz_3$	tris(pyrazolyl)hydroborate(1−)
HP	high-potential iron−sulfur protein
L	ligand (generalized)
LS_3	1,3,5-tris((4,6-dimethyl-3-mercaptophenyl)thio)-2,4,6-tris(*p*-tolylthio)benzene(3−)
Meida	*N*-methylimidodiacetate(2−)
Mb	Mössbauer spectroscopy/spectra
Mg	magnetism
MCD	magnetic circular dichroism spectroscopy/spectra
OEiBC	octaethylisobacteriochlorinate(2−)
OEP	octaethylporphyrinate(2−)
P	preparation
Pf	*Pyrococcus furiosus*
Rd	rubredoxin
salen	*N*,*N*′-salicylideneaminoethylenediamine(2−)
S_2-*o*-xyl	*o*-xylyl-α,α′-dithiolate(2−)
S-2/3/4-py	pyridine-2/3/4-thiolate(1−)
tacn	1,4,7-triazacyclononane
tibt	2,4,6-triisopropylphenyl
XAS	X-ray absorption spectroscopy/spectra
XR	X-ray structure

11. References

(1) Herriott, J. R.; Sieker, L. C.; Jensen, L. H. *J. Mol. Biol.* **1970**, *50*, 391.
(2) Sieker, L. C.; Adman, E.; Jensen, L. H. *Nature* **1972**, *235*, 40.
(3) Carter, C. W.; Kraut, J.; Freer, S. T.; Alden, R. A.; Sieker, L. C.; Adman, E.; Jensen, L. H. *Proc. Natl. Acad. Sci. U.S.A.* **1972**, *69*, 3526.
(4) Brintzinger, H.; Palmer, G.; Sands, R. H. *Proc. Natl. Acad. Sci. U.S.A.* **1966**, *55*, 397.
(5) Gibson, J. F.; Hall, D. O.; Thornley, J. H. M.; Whatley, F. R. *Proc. Natl. Acad. Sci. U.S.A.* **1966**, *56*, 987.
(6) Thornley, J. H. M.; Gibson, J. F.; Whatley, F. R.; Hall, D. O. *Biochem. Biophys. Res. Commun.* **1966**, *24*, 877.
(7) Tsukihara, T.; Fukuyama, K.; Tahara, H.; Katsube, Y.; Matsuura, Y.; Tanaka, N.; Kakudo, M.; Wada, K.; Matsubara, H. *J. Biochem. (Tokyo)* **1978**, *84*, 1645.
(8) Herskovitz, T.; Averill, B. A.; Holm, R. H.; Ibers, J. A.; Phillips, W. D.; Weiher, J. F. *Proc. Natl. Acad. Sci. U.S.A.* **1972**, *69*, 2437.
(9) Lane, R. W.; Ibers, J. A.; Frankel, R. B.; Holm, R. H. *Proc. Natl. Acad. Sci. U.S.A.* **1975**, *72*, 2868.
(10) Emptage, M.; Kent, T. A.; Huynh, B. H.; Rawlings, J.; Orme-Johnson, W. H.; Münck, E. *J. Biol. Chem.* **1980**, *255*, 1793.
(11) Beinert, H.; Thomson, A. J. *Arch. Biochem. Biophys.* **1983**, 333.
(12) Stout, C. D.; Ghosh, D.; Pattabhi, V.; Robbins, A. H. *J. Biol. Chem.* **1980**, *255*, 1797.
(13) Robbins, A. H.; Stout, C. D. *J. Biol. Chem.* **1985**, *260*, 2328.
(14) Ghosh, D.; Furey, W.; O'Donnell, S.; Stout, C. D. *J. Biol. Chem.* **1981**, *256*, 4185.
(15) Ghosh, D.; O'Donnell, S.; Furey, W.; Robbins, A. H.; Stout, C. D. *J. Mol. Biol. 1982*, *158*, 73.
(16) Stout, C. D. *J. Biol. Chem.* **1988**, *263*, 9256.
(17) Stout, G. H.; Turley, S.; Sieker, L. C.; Jensen, L. H. *Proc. Natl. Acad. Sci. U.S.A.* **1988**, *85*, 1020.
(18) Stout, C. D. *J. Mol. Biol.* **1989**, *205*, 545.
(19) Robbins, A. H.; Stout, C. D. *Proteins: Struct., Funct. Genet.* **1989**, *5*, 289.
(20) Zhou, J.; Holm, R. H. *J. Am. Chem. Soc.* **1995**, *117*, 11353.
(21) Kennedy, M. C.; Kent, T. A.; Emptage, M.; Merkle, H.; Beinert, H.; Münck, E. *J. Biol. Chem.* **1984**, *259*, 14463.
(22) Hagen, K. S.; Watson, A. D.; Holm, R. H. *J. Am. Chem. Soc.* **1983**, *105*, 3905.
(23) Gailer, J.; George, G. N.; Pickering, I. J.; Prince, R. C.; Kohlhepp, P.; Zhang, D.; Walker, F. A.; Winzerling, J. J. *J. Am. Chem. Soc.* **2001**, *123*, 10121.
(24) Averill, B. A.; Herskovitz, T.; Holm, R. H.; Ibers, J. A. *J. Am. Chem. Soc.* **1973**, *95*, 3523.
(25) Mayerle, J. J.; Frankel, R. B.; Holm, R. H.; Ibers, J. A.; Phillips, W. D.; Weiher, J. F. *Proc. Natl. Acad. Sci. U.S.A.* **1973**, *70*, 2429.
(26) Mayerle, J. J.; Denmark, S. E.; DePamphilis, B. V.; Ibers, J. A.; Holm, R. H. *J. Am. Chem. Soc.* **1975**, *97*, 1032.
(27) Holm, R. H.; Phillips, W. D.; Averill, B. A.; Mayerle, J. J.; Herskovitz, T. *J. Am. Chem. Soc.* **1974**, *96*, 2109.
(28) DePamphilis, B. V.; Averill, B. A.; Herskovitz, T.; Que, L., Jr.; Holm, R. H. *J. Am. Chem. Soc.* **1974**, *96*, 4159.
(29) Bobrik, M. A.; Que, L., Jr.; Holm, R. H. *J. Am. Chem. Soc.* **1974**, *96*, 285.
(30) Que, L., Jr.; Bobrik, M. A.; Ibers, J. A.; Holm, R. H. *J. Am. Chem. Soc.* **1974**, *96*, 4168.
(31) Que, L., Jr.; Anglin, J. R.; Bobrik, M. A.; Davison, A.; Holm, R. H. *J. Am. Chem. Soc.* **1974**, *96*, 6042.

(32) Job, R. C.; Bruice, T. C. *Proc. Natl. Acad. Sci. U.S.A.* **1975**, *72*, 2478.
(33) Carrell, H. L.; Glusker, J. P.; Job, R.; Bruice, T. C. *J. Am. Chem. Soc.* **1977**, *99*, 3683.
(34) Hill, C. L.; Renaud, J.; Holm, R. H.; Mortenson, L. E. *J. Am. Chem. Soc.* **1977**, *99*, 2549.
(35) Holah, D. G.; Coucouvanis, D. *J. Am. Chem. Soc.* **1975**, *97*, 6917.
(36) Coucouvanis, D.; Swenson, D.; Baenziger, N. C.; Holah, D. G.; Kostikas, A.; Simopoulos, A.; Petrouleas, V. *J. Am. Chem. Soc.* **1976**, *98*, 5721.
(37) Lane, R. W.; Ibers, J. A.; Frankel, R. B.; Papaefthymiou, G. C.; Holm, R. H. *J. Am. Chem. Soc.* **1977**, *99*, 84.
(38) Que, L., Jr.; Holm, R. H.; Mortenson, L. E. *J. Am. Chem. Soc.* **1975**, *97*, 463.
(39) Gillum, W. O.; Mortenson, L. E.; Chen, J.-S.; Holm, R. H. *J. Am. Chem. Soc.* **1977**, *99*, 584.
(40) Averill, B. A.; Bale, J. R.; Orme-Johnson, W. H. *J. Am. Chem. Soc.* **1978**, *100*, 3034.
(41) Cambray, J.; Lane, R. W.; Wedd, A. G.; Johnson, R. W.; Holm, R. H. *Inorg. Chem.* **1977**, *16*, 2565.
(42) Laskowski, E. J.; Frankel, R. B.; Gillum, W. O.; Papaefthymiou, G. C.; Renaud, J.; Ibers, J. A.; Holm, R. H. *J. Am. Chem. Soc.* **1978**, *100*, 5322.
(43) Hagen, K. S.; Reynolds, J. G.; Holm, R. H. *J. Am. Chem. Soc.* **1981**, *103*, 4054.
(44) Hagen, K. S.; Holm, R. H. *J. Am. Chem. Soc.* **1982**, *104*, 5496.
(45) Balasubramanian, A.; Coucouvanis, D. *Inorg. Chim. Acta* **1983**, *78*, L35.
(46) Ueyama, N.; Ueno, S.; Nakata, M.; Nakamura, A. *Bull. Chem. Soc. Jpn.* **1984**, *57*, 984.
(47) Ueno, S.; Ueyama, N.; Nakamura, A.; Tukihara, T. *Inorg. Chem.* **1986**, *25*, 1000.
(48) O'Sullivan, T.; Millar, M. M. *J. Am. Chem. Soc.* **1985**, *107*, 4096.
(49) Papaefthymiou, V.; Millar, M. M.; Münck, E. *Inorg. Chem.* **1986**, *25*, 3010.
(50) Stack, T. D. P.; Holm, R. H. *J. Am. Chem. Soc.* **1987**, *109*, 2546.
(51) Stack, T. D. P.; Holm, R. H. *J. Am. Chem. Soc.* **1988**, *110*, 2484.
(52) Coucouvanis, D.; Al-Ahmad, S.; Salifoglou, A.; Dunham, W. R.; Sands, R. H. *Angew. Chem., Int. Ed. Engl.* **1988**, *27*, 1353.
(53) Weigel, J. A.; Holm, R. H.; Surerus, K. K.; Münck, E. *J. Am. Chem. Soc.* **1989**, *111*, 9246.
(54) Weigel, J. A.; Srivastava, K. K. P.; Day, E. P.; Münck, E.; Holm, R. H. *J. Am. Chem. Soc.* **1990**, *112*, 8015.
(55) Smith, E. T.; Feinberg, B. A.; Richards, J. H.; Tomich, J. M. *J. Am. Chem. Soc.* **1991**, *113*, 688.
(56) Smith, E. T.; Tomich, J. M.; Iwamoto, T.; Richards, J. H.; Mao, Y.; Feinberg, B. A. *Biochemistry* **1991**, *30*, 11669.
(57) Cai, L.; Weigel, J. A.; Holm, R. H. *J. Am. Chem. Soc.* **1993**, *115*, 9289.
(58) Cai, L.; Holm, R. H. *J. Am. Chem. Soc.* **1994**, *116*, 7177.
(59) Zhou, C.; Cai, L.; Holm, R. H. *Inorg. Chem.* **1996**, *35*, 2767.
(60) Christensen, H. E. M.; Hammerstadt-Pedersen, J. M.; Holm, A.; Iversen, G.; Jensen, M. H.; Ulstrup, J. *Eur. J. Biochem.* **1994**, *224*, 97.
(61) Zhou, J.; Hu, Z.; Münck, E.; Holm, R. H. *J. Am. Chem. Soc.* **1996**, *118*, 1966.
(62) Zhou, J.; Raebiger, J. W.; Crawford, C. A.; Holm, R. H. *J. Am. Chem. Soc.* **1997**, *119*, 6242.
(63) Mulholland, S. E.; Gibney, B. R.; Rabanal, F.; Dutton, P. L. *J. Am. Chem. Soc.* **1998**, *120*, 10296.
(64) Mulholland, S. E.; Gibney, B. R.; Rabanal, F.; Dutton, P. L. *Biochemistry* **1999**, *38*, 10442.
(65) Laplaza, C. E.; Holm, R. H. *J. Am. Chem. Soc.* **2001**, *123*, 10255.
(66) Musgrave, K. B.; Laplaza, C. E.; Holm, R. H.; Hedman, B.; Hodgson, K. O. *J. Am. Chem. Soc.* **2002**, *124*, 3083.
(67) Holm, R. H. *Endeavour* **1975**, *34*, 38.
(68) Holm, R. H. *Acc. Chem. Res.* **1977**, *10*, 427.
(69) Holm, R. H.; Ibers, J. A. In *Iron−Sulfur Proteins*; Lovenberg, W., Ed.; Academic Press: New York, 1997; Vol. III, Chapter 7.
(70) Berg, J. M.; Holm, R. H. In *Iron−Sulfur Proteins*; Spiro, T. G., Ed.; Wiley-Interscience: New York, 1982; Chapter 1.
(71) Holm, R. H. *Adv. Inorg. Chem.* **1992**, *38*, 1.
(72) Ogino, H.; Inomata, S.; Tobita, H. *Chem. Rev.* **1998**, *98*, 2093.
(73) Holm, R. H. In *Comprehensive Coordination Chemistry*; Que, L., Jr., Tolman, W. A., Eds.; Elsevier: New York, 2003; Vol. 8, in press.
(74) Lee, S. C.; Holm, R. H. *Chem. Rev.* **2004**, *104*, 1135 (in this issue).
(75) Arendsen, A. F.; Hadden, J.; Card, G.; McAlpine, A. S.; Bailey, S.; Zaitsev, V.; Duke, E. H. M.; Lindley, P. F.; Kröckel, M.; Trautwein, A. X.; Feiters, M. C.; Charnock, J. M.; Garner, C. D.; Marritt, S. J.; Thomson, A. J.; Kooter, I. M.; Johnson, M. K.; van den Berg, W. A. M.; van Dongen, W. M. A. M.; Hagen, W. R. *J. Biol. Inorg. Biochem.* **1998**, *3*, 81.
(76) Macedo, S.; Mitchell, E. P.; Romão, C. V.; Cooper, S. J.; Coelho, R.; Liu, M. Y.; Xavier, A. V.; LeGall, J.; Bailey, S.; Garner, C. D.; Hagen, W. R.; Teixeira, M.; Carrondo, M. A.; Lindley, P. *J. Biol. Inorg. Chem.* **2002**, *7*, 514.
(77) Maelia, L. E.; Millar, M.; Koch, S. A. *Inorg. Chem.* **1992**, *31*, 4594.
(78) Koch, S. A.; Maelia, L. E.; Millar, M. *J. Am. Chem. Soc.* **1983**, *105*, 5944.
(79) Teo, B. K.; Shulman, R. G.; Brown, G. S.; Meixner, A. E. *J. Am. Chem. Soc.* **1979**, *101*, 5624.
(80) Millar, M.; Lee, J. F.; O'Sullivan, T.; Koch, S. A.; Fikar, R. *Inorg. Chim. Acta* **1996**, *243*, 333.
(81) Rose, K.; Shadle, S. E.; Eidsness, M. K.; Kurtz, D. M., Jr.; Scott, R. A.; Hedman, B.; Hodgson, K. O.; Solomon, E. I. *J. Am. Chem. Soc.* **1998**, *120*, 10743.
(82) Millar, M.; Lee, J. F.; Koch, S. A.; Fikar, R. *Inorg. Chem.* **1982**, *21*, 4106.
(83) Deaton, J. C.; Gebhard, M. S.; Koch, S. A.; Millar, M.; Solomon, E. I. *J. Am. Chem. Soc.* **1988**, *110*, 6241.
(84) Gebhard, M. S.; Deaton, J. C.; Koch, S. A.; Millar, M.; Solomon, E. I. *J. Am. Chem. Soc.* **1990**, *112*, 2217.
(85) Millar, M.; Koch, S. A.; Fikar, R. *Inorg. Chim. Acta* **1984**, *88*, L15.
(86) Christou, G.; Ridge, B.; Rydon, H. N. *J. Chem. Soc., Chem. Commun.* **1977**, 908.
(87) Ueyama, N.; Nakata, M.; Nakamura, A. *Bull. Chem. Soc. Jpn.* **1981**, *54*, 1727.
(88) Nakata, M.; Ueyama, N.; Terakawa, T.; Nakamura, A. *Bull. Chem. Soc. Jpn.* **1983**, *56*, 3647.
(89) Werth, M. T.; Kurtz, D. M., Jr.; Howes, B. D.; Huynh, B. H. *Inorg. Chem.* **1989**, *28*, 1357.
(90) Bose, K.; Huang, J.; Haggerty, B. S.; Rheingold, A. L.; Salm, R. J.; Walters, M. A. *Inorg. Chem.* **1997**, *36*, 4596.
(91) Chung, W. P.; Dewan, J.; Tuckerman, M.; Walters, M. A. *Inorg. Chim. Acta* **1999**, *291*, 388.
(92) Coucouvanis, D.; Swenson, D.; Baenziger, N. C.; Murphy, C.; Holah, D. G.; Sfarnas, N.; Simopoulos, A.; Kostikas, A. *J. Am. Chem. Soc.* **1981**, *103*, 3350.
(93) Gebhard, M. S.; Koch, S. A.; Millar, M.; Devlin, F. J.; Stephens, P. J.; Solomon, E. I. *J. Am. Chem. Soc.* **1991**, *113*, 1640.
(94) Silver, A.; Koch, S. A.; Millar, M. *Inorg. Chim. Acta* **1993**, *205*, 9.
(95) Huang, J.; Dewan, J.; Walters, M. A. *Inorg. Chim. Acta* **1995**, *228*, 199.
(96) Mascharak, P. K.; Smith, M. C.; Armstrong, W. H.; Burgess, B. K.; Holm, R. H. *Proc. Natl. Acad. Sci. U.S.A.* **1982**, *79*, 7056.
(97) Ueyama, N.; Okamura, T.; Nakamura, A. *J. Chem. Soc., Chem. Commun.* **1992**, 1019.
(98) Okamura, T.; Takamizawa, S.; Ueyama, N.; Nakamura, A. *Inorg. Chem.* **1998**, *37*, 18.
(99) Anglin, J. R.; Davison, A. *Inorg. Chem.* **1975**, *14*, 234.
(100) Nakata, M.; Ueyama, N.; Fuji. M.-A.; Nakamura, A.; Wada, K.; Matsubara, H. *Biochim. Biophys. Acta* **1984**, *788*, 306.
(101) Sun, W.-Y.; Ueyama, N.; Nakamura, A. *Inorg. Chem.* **1991**, *30*, 4026.
(102) Ueyama, N.; Nakata, M.; Fuji, M.; Terakawa, T.; Nakamura, A. *Inorg. Chem.* **1985**, *24*, 2190.
(103) Nakamura, A.; Ueyama, N. *Adv. Inorg. Chem.* **1989**, *33*, 39.
(104) Nivorozhkin, A. L.; Segal, B. M.; Musgrave, K. B.; Kates, S. A.; Hedman, B.; Holm, R. H. *Inorg. Chem.* **2000**, *39*, 2306.
(105) Ellis, K. J.; Lappin, A. G.; McAuley, A. *J. Chem. Soc., Dalton Trans.* **1975**, 1930.
(106) Min, T.; Ergenekan, C. E.; Eidsness, M. K.; Ichiye, T.; Kang, C. *Protein Sci.* **2001**, *10*, 613.
(107) Bau, R.; Rees, D. C.; Kurtz, D. M., Jr.; Scott, R. A.; Huang, H.; Adams, M. W. W.; Eidsness, M. K. *J. Biol. Inorg. Chem.* **1998**, *3*, 484.
(108) Day, M. W.; Park, J.-B.; Zhou, Z. H.; Adams, M. W. W.; Rees, D. C. *Protein Sci.* **1992**, *1*, 1494.
(109) Shannon, R. D. *Acta Crystallogr.* **1976**, *A32*, 751.
(110) Dauter, Z.; Sieker, L. C.; Wilson, K. S. *Acta Crystallogr.* **1992**, *B48*, 42.
(111) Czernuszewicz, R. S.; Kilpatrick, L. K.; Koch, S. A.; Spiro, T. G. *J. Am. Chem. Soc.* **1994**, *116*, 7134.
(112) Han, S.; Czernuszewicz, R. S.; Spiro, T. G. *Inorg. Chem.* **1986**, *25*, 2276.
(113) Reynolds, J. G.; Holm, R. H. *Inorg. Chem.* **1980**, *19*, 3257.
(114) Wong, G. B.; Bobrik, M. A.; Holm, R. H. *Inorg. Chem.* **1978**, *17*, 578.
(115) Cleland, W. E.; Averill, B. A. *Inorg. Chem.* **1984**, *23*, 4192.
(116) Beardwood, P.; Gibson, J. F. *J. Chem. Soc., Chem. Commun.* **1985**, 102.
(117) Salifoglou, A.; Simopoulos, A.; Kostikas, A.; Dunham, R. W.; Kanatzidis, M. G.; Coucouvanis, D. *Inorg. Chem.* **1988**, *27*, 3394.
(118) Müller, A.; Schladerbeck, N.; Krickemeyer, E.; Bögge, H.; Bill, E.; Trautwein, A. X. *Z. Anorg. Allg. Chem.* **1989**, *570*, 7.
(119) Bobrik, M. A.; Hodgson, K. O.; Holm, R. H. *Inorg. Chem.* **1977**, *16*, 1851.
(120) Rose, K.; Shadle, S. E.; Glaser, T.; de Vries, S.; Cherepanov, A.; Canters, G. W.; Hedman, B.; Hodgson, K. O.; Solomon, E. I. *J. Am. Chem. Soc.* **1999**, *121*, 2353.
(121) AnxolabéhPre-Mallart, E.; Glaser, T.; Frank, P.; Aliverti, A.; Hodgson, K. O.; Solomon, E. I. *J. Am. Chem. Soc.* **2001**, *123*, 5444.

(122) Gillum, W. O.; Frankel, R. B.; Foner, S.; Holm, R. H. *Inorg. Chem.* **1976**, *15*, 1095.
(123) Mascharak, P. K.; Papaefthymiou, G. C.; Frankel, R. B.; Holm, R. H. *J. Am. Chem. Soc.* **1981**, *103*, 6110.
(124) Beardwood, P.; Gibson, J. F.; Johnson, C. E.; Rush, J. D. *J. Chem. Soc., Dalton Trans.* **1982**, 2015.
(125) Fabre, P. L.; de Montauzon, D.; Poilblanc, R. *Bull. Soc. Chim. Fr.* **1991**, *128*, 123.
(126) Wong, G. B.; Kurtz, D. M., Jr.; Holm, R. H.; Mortenson, L. E.; Upchurch, R. G. *J. Am. Chem. Soc.* **1979**, *101*, 3078.
(127) Cai, J.; Cheng, C. *Jiegou Huaxue* **1988**, *7*, 43.
(128) Ueyama, N.; Ueno, S.; Sugawara, T.; Tatsumi, K.; Nakamura, A.; Yasuoka, N. *J. Chem. Soc., Dalton Trans.* **1991**, 2723.
(129) Ueyama, N.; Yamada, Y.; Okamura, T.; Kimura, S.; Nakamura, A. *Inorg. Chem.* **1996**, *35*, 6473.
(130) Coucouvanis, D.; Swenson, D.; Stremple, P.; Baenziger, N. C. *J. Am. Chem. Soc.* **1979**, *101*, 3392.
(131) Kanatzidis, M. G.; Coucouvanis, D. *Inorg. Chem.* **1984**, *23*, 403.
(132) Ueyama, N.; Ueno, S.; Nakamura, A.; Wada, K.; Matsubara, H.; Kumagai, S.-I.; Sakakibara, S.; Tsukihara, T. *Biopolymers* **1992**, *32*, 1535.
(133) Beardwood, P.; Gibson, J. F.; Bertrand, P.; Gayda, J.-P. *Biochim. Biophys. Acta* **1983**, *742*, 426.
(134) Beardwood, P.; Gibson, J. F. *J. Chem. Soc., Dalton Trans.* **1983**, 737.
(135) Binda, C.; Coda, A.; Aliverti, A.; Zanetti, G.; Mattevi, A. *Acta Crystallogr.* **1998**, *D54*, 1353.
(136) Morales, R.; Chron, M.-H.; Hudry-Clergeon, G.; Pétillot, Y.; Norager, S.; Medina, M.; Frey, M. *Biochemistry* **1999**, *38*, 15764.
(137) Bönisch, H.; Schmidt, C. L.; Schäfer, G.; Ladenstein, R. *J. Mol. Biol.* **2002**, *319*, 791.
(138) Müller, A.; Müller, J. J.; Muller, Y. A.; Uhlmann, H.; Bernhardt, R.; Heinemann, U. *Structure* **1998**, *6*, 269.
(139) Bes, M. T.; Parisini, E.; Inda, L. A.; Saraiva, L. M.; Peleato, M. L.; Sheldrick, G. M. *Structure* **1999**, *7*, 1201.
(140) Maelia, L. E.; Koch, S. *Inorg. Chem.* **1986**, *25*, 1896.
(141) Matsubara, H.; Saeki, K. *Adv. Inorg. Chem.* **1992**, *38*, 223.
(142) Im, S.-C.; Kohzuma, T.; McFarlane, W.; Gaillard, J.; Sykes, A. G. *Inorg. Chem.* **1997**, *36*, 1388.
(143) Yoo, S. J.; Meyer, J.; Münck, E. *J. Am. Chem. Soc.* **1999**, *121*, 10450.
(144) Sands, R. H.; Dunham, W. R. *Q. Rev. Biophys.* **1975**, *7*, 443.
(145) Meyer, J.; Fujinaga, J.; Gaillard, J.; Lutz, M. *Biochemistry* **1994**, *33*, 13642.
(146) Crouse, B. R.; Meyer, J.; Johnson, M. K. *J. Am. Chem. Soc.* **1995**, *117*, 9612.
(147) Achim, C.; Golinelli, M.-P.; Bominaar, E.; Meyer, J.; Münck, E. *J. Am. Chem. Soc.* **1996**, *118*, 8168.
(148) Achim, C.; Bominaar, E.; Meyer, J.; Peterson, J.; Münck, E. *J. Am. Chem. Soc.* **1999**, *121*, 3704.
(149) Beinert, H.; Holm, R. H.; Münck, E. *Science* **1997**, *277*, 653.
(150) Noodleman, L.; Lovell, T.; Liu, T.; Himo, F.; Torres, R. A. *Curr. Opin. Chem. Biol.* **2002**, *6*, 259.
(151) Rose, K.; Shadle, S. E.; Glaser, T.; de Vries, S.; Cherepanov, A.; Canters, G. W.; Hedman, B.; Hodgson, K. O.; Solomon, E. I. *J. Am. Chem. Soc.* **1999**, *121*, 2353.
(152) Beardwood, P.; Gibson, J. F. *J. Chem. Soc., Chem. Commun.* **1985**, 1345.
(153) Beardwood, P.; Gibson, J. F. *J. Chem. Soc., Chem. Commun.* **1986**, 490.
(154) Link, T. A. *Adv. Inorg. Chem.* **1999**, *47*, 83.
(155) Girerd, J.-J.; Papaefthymiou, G. C.; Watson, A. D.; Gamp, E.; Hagen, K. S.; Edelstein, N.; Frankel, R. B.; Holm, R. H. *J. Am. Chem. Soc.* **1984**, *106*, 5941.
(156) Richards, A. J. M.; Thomson, A. J.; Holm, R. H.; Hagen, K. S. *Spectrochim. Acta* **1990**, *46A*, 987.
(157) Coucouvanis, D.; Al-Ahmad, S. A.; Salifoglou, A.; Papaefthymiou, V.; Kostikas, A.; Simopoulos, A. *J. Am. Chem. Soc.* **1992**, *114*, 2472.
(158) Zhou, J.; Scott, M. J.; Hu, Z.; Peng, G.; Münck, E.; Holm, R. H. *J. Am. Chem. Soc.* **1992**, *114*, 10843.
(159) Flint, D. H.; Emptage, M. H.; Finnegan, M. G.; Fu, W.; Johnson, M. K. *J. Biol. Chem.* **1993**, *268*, 14732.
(160) Krebs, C.; Henshaw, T. F.; Cheek, J.; Huynh, B. H.; Broderick, J. B. *J. Am. Chem. Soc.* **2000**, *122*, 12497.
(161) Wittung-Stafshede, P.; Gomes, C. M.; Teixeira, M. *J. Inorg. Biochem.* **2000**, *78*, 35.
(162) Jones, K.; Gomes, C. M.; Huber, H.; Teixeira, M.; Wittung-Stafshede, P. *J. Biol. Inorg. Chem.* **2002**, *7*, 357.
(163) Al-Ahmad, S. A.; Kampf, J. W.; Dunham, W. R.; Coucouvanis, D. *Inorg. Chem.* **1991**, *30*, 1163.
(164) Stack, T. D. P.; Weigel, J. A.; Holm, R. H. *Inorg. Chem.* **1990**, *29*, 3745.
(165) Raebiger, J. W.; Crawford, C. A.; Holm, R. H. *Inorg. Chem.* **1997**, *36*, 994.
(166) Fawcett, S. E. J.; Davis, D.; Breton, J. L.; Thomson, A. J.; Armstrong, F. A. *Biochem. J.* **1998**, *335*, 357.
(167) Chen, K.; Hirst, J.; Camba, R.; Bonagura, C. A.; Stout, C. D.; Burgess, B. K.; Armstrong, F. A. *Nature* **2000**, *45*, 814.
(168) Schipke, C. G.; Goodin, D. B.; McFee, D. E.; Stout, C. D. *Biochemistry* **1999**, *38*, 8228.
(169) Johnson, M. K.; Duderstadt, R. E.; Duin, E. C. *Adv. Inorg. Chem.* **1999**, *47*, 1.
(170) Papaefthymiou, V.; Girerd, J.-J.; Moura, I.; Moura, J. J. G.; Münck, E. *J. Am. Chem. Soc.* **1987**, *109*, 4703.
(171) Ciurli, S.; Yu, S.-B.; Holm, R. H.; Srivastava, K. K. P.; Münck, E. *J. Am. Chem. Soc.* **1990**, *112*, 8169.
(172) Ciurli, S.; Ross, P. K.; Scott, M. J.; Yu, S.-B.; Holm, R. H. *J. Am. Chem. Soc.* **1992**, *114*, 5415.
(173) Zhou, J.; Raebiger, J. W.; Crawford, C. A.; Holm, R. H. *J. Am. Chem. Soc.* **1997**, *119*, 6242.
(174) Cleland, W. E.; Holtman, D. A.; Sabat, M.; Ibers, J. A.; DeFotis, G. C.; Averill, B. A. *J. Am. Chem. Soc.* **1983**, *105*, 6021.
(175) Rutchik, S.; Kim, S.; Walters, M. A. *Inorg. Chem.* **1988**, *27*, 1513.
(176) Pohl, S.; Saak, W. *Z. Naturforsch.* **1988**, *43b*, 457.
(177) Stephens, P. J.; Jollie, D. R.; Warshel, A. *Chem. Rev.* **1996**, *96*, 2491.
(178) Battistuzzi, G.; D'Onofrio, M.; Borsari, M.; Sola, M.; Macedo, A. L.; Moura, J. J. G.; Rodriques, P. *J. Biol. Inorg. Chem.* **2000**, *5*, 748.
(179) Iismaa, S. E.; Vázquez, A. E.; Jensen, G. M.; Stephens, P. J.; Butt, J. N.; Armstrong, F. A.; Burgess, B. K. *J. Biol. Chem.* **1991**, *266*, 21563.
(180) Gao-Sheridan, H. S.; Pershad, H. R.; Armstrong, F. A.; Burgess, B. K. *J. Biol. Chem.* **1998**, *273*, 5514.
(181) Pickett, C. J. *J. Chem. Soc., Chem. Commun.* **1985**, 323.
(182) Zhou, C.; Raebiger, J. W.; Segal, B. M.; Holm, R. H. *Inorg. Chim. Acta* **2000**, *300*−*302*, 892.
(183) Mascharak, P. K.; Hagen, K. S.; Spence, J. T.; Holm, R. H. *Inorg. Chim. Acta* **1983**, *80*, 157.
(184) Ueyama, N.; Sugawara, T.; Fuji, M.; Nakamura, A. *Chem. Lett.* **1984**, 1287.
(185) Blonk, H. L.; Kievit, O.; Roth, E. K. H.; Jordanov, J.; van der Linden, J. G. M.; Steggerda, J. J. *Inorg. Chem.* **1991**, *30*, 3231.
(186) Kambayashi, H.; Nagao, H.; Tanaka, K.; Nakamoto, M.; Peng, S.-M. *Inorg. Chim. Acta* **1993**, *209*, 143.
(187) Ohno, R.; Ueyama, N.; Nakamura, A. *Chem. Lett.* **1989**, 399.
(188) Rius, G.; Lamotte, B. *J. Am. Chem. Soc.* **1989**, *111*, 2464.
(189) Mouesca, J.-M.; Rius, G.; Lamotte, B. *J. Am. Chem. Soc.* **1993**, *115*, 4714.
(190) Gloux, J.; Gloux, P.; Lamotte, B.; Mouesca, J.-M.; Rius, G. *J. Am. Chem. Soc.* **1994**, *116*, 1953.
(191) Gloux, J.; Gloux, P.; Hendriks, H.; Rius, G. *J. Am. Chem. Soc.* **1987**, *109*, 3220.
(192) Müller, A.; Schladerbeck, N.; Bögge, H. *J. Chem. Soc., Chem. Commun.* **1987**, 35.
(193) Hoveyda, H. R.; Holm, R. H. *Inorg. Chem.* **1997**, *36*, 4571.
(194) Christou, G.; Garner, C. D. *J. Chem. Soc., Dalton Trans.* **1979**, 1093.
(195) Christou, G.; Garner, C. D.; Drew, M. G. B.; Cammack, R. *J. Chem. Soc., Dalton Trans.* **1981**, 1550.
(196) Bonomi, F.; Werth, M. T.; Kurtz, D. M., Jr. *Inorg. Chem.* **1985**, *24*, 4331.
(197) Ollerenshaw, T. J.; Bristow, S.; Anand, B. N.; Garner, C. D. *J. Chem. Soc., Dalton Trans.* **1986**, 2013.
(198) Barclay, J. E.; Davies, S. C.; Evans, D. J.; Hughes, D. L.; Longhurst, S. *Inorg. Chim. Acta* **1999**, *291*, 101.
(199) Moulis, J.-M.; Meyer, J. *Biochemistry* **1982**, *21*, 4762.
(200) Henderson, R. A.; Sykes, A. G. *Inorg. Chem.* **1980**, *19*, 3103.
(201) Davies, S. C.; Evans, D. J.; Henderson, R. A.; Hughes, D. L.; Longhurst, S. *J. Chem. Soc., Dalton Trans.* **2002**, 3470.
(202) Evans, D. J.; Hills, A.; Hughes, D. L.; Leigh, G. J.; Houlton, A.; Silver, J. *J. Chem. Soc., Dalton Trans.* **1990**, 2735.
(203) Hu, N.-H.; Liu, Y.-S.; Xu, J.-Q.; Yan, Y.-Z.; Wei, Q. *Chin. J. Struct. Chem.* **1991**, *10*, 117.
(204) Barclay, J. E.; Evans, D. J.; Leigh, G. J.; Newton, M. S.; Silver, J. *Gazz. Chim. Ital.* **1994**, *124*, 367.
(205) Silver, J.; Fern, G. R.; Miller, J. R.; McCammon, C. A.; Evans, D. J.; Leigh, G. J. *Inorg. Chem.* **1999**, *38*, 4256.
(206) Hauptmann, R.; Schneider, J.; Köckerling, M.; Henkel, G. *Acta Crystallogr.* **1999**, *C55*, 190.
(207) Nakamoto, M.; Tanaka, K.; Tanaka, T. *J. Chem. Soc., Chem. Commun.* **1988**, 1422.
(208) Nakamoto, M.; Fukaishi, K.; Tagata, T.; Kambayashi, H. *Bull. Chem. Soc. Jpn.* **1999**, *72*, 407.
(209) Stephens, P. J.; Thomson, A. J.; Keiderling, T. A.; Rawlings, J.; Rao, K. K.; Hall, D. O. *Proc. Natl. Acad. Sci. U.S.A.* **1978**, *75*, 5273.
(210) Glaser, T.; Rose, K.; Shadle, S. E.; Hedman, B.; Hodgson, K. O.; Solomon, E. I. *J. Am. Chem. Soc.* **2001**, *123*, 442.
(211) Laskowski, E. J.; Reynolds, J. G.; Frankel, R. B.; Foner, S.; Papaefthymiou, G. C.; Holm, R. H. *J. Am. Chem. Soc.* **1979**, *101*, 6562.
(212) Lenormand, A.; Iveson, P.; Jordanov, J. *Inorg. Chim. Acta* **1996**, *251*, 119.
(213) Tanaka, K.; Nakamoto, M.; Tashiro, Y.; Tanaka, T. *Bull. Chem. Soc. Jpn.* **1985**, *58*, 316.

(214) Mochida, T.; Ueda, M.; Moriyama, H. *Mol. Cryst. Liq. Cryst.* **2000**, *342*, 91.
(215) Papaefthymiou, G. C.; Laskowski, E. J.; Frota-Pessôa, S.; Frankel, R. B.; Holm, R. H. *Inorg. Chem.* **1982**, *21*, 1724.
(216) Kanatzidis, M. G.; Baenziger, N. C.; Coucouvanis, D.; Simopoulos, A.; Kostikas, A. *J. Am. Chem. Soc.* **1984**, *106*, 4500.
(217) Lin, G.; Zhang, H.; Hu, S.-Z.; Mak, T. C. W. *Acta Crystallogr.* **1987**, *C43*, 352.
(218) Excoffon, P.; Laugier, J.; Lamotte, B. *Inorg. Chem.* **1991**, *30*, 3075.
(219) Johnson, R. E.; Papaefthymiou, G. C.; Frankel, R. B.; Holm, R. H. *J. Am. Chem. Soc.* **1983**, *105*, 7280.
(220) Carney, M. J.; Papaefthymiou, G. C.; Frankel, R. B.; Holm, R. H. *Inorg. Chem.* **1989**, *28*, 1497.
(221) Reynolds, J. G.; Laskowski, E. J.; Holm, R. H. *J. Am. Chem. Soc.* **1978**, *100*, 5315.
(222) Ollerenshaw, T. J.; Garner, C. D.; Odell, B.; Clegg, W. *J. Chem. Soc., Dalton Trans.* **1985**, 2161.
(223) Tanaka, K.; Tanaka, T.; Kawafune, I. *Inorg. Chem.* **1982**, *23*, 518.
(224) Tanaka, K.; Moriya, M.; Tanaka, T. *Inorg. Chem.* **1986**, *25*, 835.
(225) Nakamoto, M.; Tanaka, K.; Tanaka, T. *Bull. Chem. Soc. Jpn.* **1988**, *61*, 4099.
(226) Ueyama, N.; Sugawara, T.; Fuji, M.; Nakamura, A.; Yasuoka, N. *Chem. Lett.* **1985**, 175.
(227) Roth, E. K. H.; Jordanov, J. *Inorg. Chem.* **1992**, *31*, 240.
(228) Ueno, T.; Ueyama, N.; Nakamura, A. *J. Chem. Soc., Dalton Trans.* **1996**, 3859.
(229) Ueno, T.; Inohara, M.; Ueyama, N.; Nakamura, A. *Bull. Chem. Soc. Jpn.* **1997**, *70*, 1077.
(230) Ueyama, N.; Sugawara, T.; Nakamura, A.; Yamaguchi, K.; Fueno, T. *Chem. Lett.* **1988**, 223.
(231) Gebbink, R. J. M. K.; Klink, S. I.; Feiters, M.; Nolte, R. J. M. *Eur. J. Inorg. Chem.* **2000**, 253.
(232) Burt, R. J.; Ridge, B.; Rydon, H. N. *J. Chem. Soc., Dalton Trans.* **1980**, 1228.
(233) Ueyama, N.; Terakawa, T.; Nakata, M.; Nakamura, A. *J. Am. Chem. Soc.* **1983**, *105*, 7098.
(234) Ueyama, N.; Kajiwara, A.; Terakawa, T.; Ueno, S.; Nakamura, A. *Inorg. Chem.* **1985**, *24*, 4700.
(235) Ohno, R.; Ueyama, N.; Nakamura, A. *Inorg. Chem.* **1991**, *30*, 4887.
(236) Gibney, B. R.; Mulholland, S. E.; Rabanal, F.; Dutton, P. L. *Proc. Natl. Acad. Sci. U.S.A.* **1996**, *93*, 15041.
(237) Mulholland, S. E.; Gibney, B. R.; Rabanal, F.; Dutton, P. L. *J. Am. Chem. Soc.* **1998**, *120*, 10296.
(238) Mulholland, S. E.; Gibney, B. R.; Rabanal, F.; Dutton, P. L. *Biochemistry* **1999**, *38*, 10442.
(239) Kennedy, M. L.; Gibney, B. R. *J. Am. Chem. Soc.* **2002**, *124*, 6826.
(240) Okuno, Y.; Uoto, K.; Yonemitsu, O.; Tomohiro, T. *J. Chem. Soc., Chem. Commun.* **1987**, 1018.
(241) Okuno, Y.; Uoto, K.; Sasaki, Y.; Yonemitsu, O.; Tomohiro, T. *J. Chem. Soc., Chem. Commun.* **1987**, 874.
(242) Okuno, H.; Uoto, K.; Tomohiro, T.; Youinou, M.-T. *J. Chem. Soc., Dalton Trans.* **1990**, 3375.
(243) Tomohiro, T.; Uoto, K.; Okuno, H. *J. Chem. Soc., Dalton Trans.* **1990**, 2459.
(244) Uoto, K.; Tomohiro, T.; Okuno, H. *Inorg. Chim. Acta* **1990**, *170*, 123.
(245) Tomohiro, T.; Okuno, H. *Inorg. Chim. Acta* **1993**, *204*, 147.
(246) Kuroda, Y.; Sasaki, Y.; Shiroiwa, Y.; Tabushi, I. *J. Am. Chem. Soc.* **1988**, *110*, 4049.
(247) Gorman, C. B.; Parkhurst, B. L.; Su, W. Y.; Chen, K.-Y. *J. Am. Chem. Soc.* **1997**, *119*, 1141.
(248) Gorman, C. B.; Hager, M. W.; Parkhurst, B. L.; Smith, J. C. *Macromolecules* **1998**, *31*, 815.
(249) Gorman, C. B.; Smith, J. C.; Hager, M. W.; Parkhurst, B. L.; Sierzputowska-Gracz, H.; Haney, C. A. *J. Am. Chem. Soc.* **1999**, *121*, 9958.
(250) Segal, B. M.; Hoveyda, H. R.; Holm, R. H. *Inorg. Chem.* **1998**, *37*, 3440.
(251) Hagen, K. S.; Watson, A. D.; Holm, R. H. *Inorg. Chem.* **1984**, *23*, 2984.
(252) Carney, M. J.; Papaefthymiou, G. C.; Spartalian, K.; Frankel, R. B.; Holm, R. H. *J. Am. Chem. Soc.* **1988**, *110*, 6084.
(253) Watt, G. D.; McDonald, J. W. *Biochemistry* **1985**, *24*, 7226.
(254) Carney, M. J.; Holm, R. H.; Papaefthymiou, G. C.; Frankel, R. B. *J. Am. Chem. Soc.* **1986**, *108*, 3519.
(255) Berg, J. M.; Hodgson, K. O.; Holm, R. H. *J. Am. Chem. Soc.* **1979**, *101*, 4586.
(256) Gloux, J.; Gloux, P.; Laugier, J. *J. Am. Chem. Soc.* **1996**, *118*, 11644.
(257) Carney, M. J.; Papaefthymiou, G. C.; Whitener, M. A.; Spartalian, K.; Frankel, R. B.; Holm, R. H. *Inorg. Chem.* **1988**, *27*, 346.
(258) Stephan, D. W.; Papaefthymiou, G. C.; Frankel, R. B.; Holm, R. H. *Inorg. Chem.* **1983**, *22*, 1550.
(259) Collison, D.; Mabbs, F. E. *J. Chem. Soc., Dalton Trans.* **1982**, 1565.
(260) Parisini, E.; Capozzi, F.; Lubini, P.; Lamzin, V.; Luchinat, C.; Sheldrick, G. M. *Acta Crystallogr.* **1999**, *D55*, 1773.
(261) Liu, L.; Nogi, T.; Kobayashi, M.; Nozawa, T.; Miki, K. *Acta Crystallogr.* **2002**, *D58*, 1085.
(262) Hagen, K. S.; Stephan, D. W.; Holm, R. H. *Inorg. Chem.* **1982**, *21*, 3928.
(263) Dauter, Z.; Wilson, K. S.; Sieker, L. C.; Meyer, J.; Moulis, J.-M. *Biochemistry* **1997**, *36*, 16065.
(264) Yamamura, T.; Christou, G.; Holm, R. H. *Inorg. Chem.* **1983**, *22*, 939.
(265) Grönberg, K. L. C.; Henderson, R. A.; Oglieve, K. E. *J. Chem. Soc., Dalton Trans.* **1998**, 3093.
(266) Nelson, L. L.; Lo, F. Y. K.; Rae, A. D.; Dahl, L. F. *J. Organomet.Chem.* **1982**, *225*, 309.
(267) Goh, C.; Segal, B. M.; Huang, J.; Long, J. R.; Holm, R. H. *J. Am. Chem. Soc.* **1996**, *118*, 11844.
(268) Zhou, H.-C.; Holm, R. H. *Inorg. Chem.* **2003**, *42*, 11.
(269) Musgrave, K. B.; Angove, H. C.; Burgess, B. K.; Hedman, B.; Hodgson, K. O. *J. Am. Chem. Soc.* **1998**, *120*, 5325.
(270) Yoo, S. J.; Angove, H. C.; Burgess, B. K.; Münck, E.; Peterson, J. *J. Am. Chem. Soc.* **1998**, *120*, 9704.
(271) Yoo, S. J.; Angove, H. C.; Burgess, B. K.; Hendrich, M. P.; Münck, E. *J. Am. Chem. Soc.* **1999**, *121*, 2534.
(272) Guo, M.; Sulc, F.; Ribbe, M. W.; Farmer, P. J.; Burgess, B. K. *J. Am. Chem. Soc.* **2002**, *124*, 12100.
(273) Cammack, R. *Biochem. Biophys. Res. Commun.* **1973**, *54*, 548.
(274) Strop, P.; Takahara, P. M.; Chiu, H.-J.; Angove, H. C.; Burgess, B. K.; Rees, D. C. *Biochemistry* **2001**, *40*, 651.
(275) Fukuyama, K.; Okada, T.; Kakuta, Y.; Takahashi, Y. *J. Mol. Biol.* **2002**, *315*, 1155.
(276) Willems, J. B.; Köckerling, M. *Chem. Commun.* **2001**, 1380.
(277) Coldren, C. D.; Hellinga, H. W.; Caradonna, J. P. *Proc. Natl. Acad. Sci. U.S.A.* **1997**, *94*, 6635.
(278) Rabinowitz, J. *Methods Enzymol.* **1972**, *24*, 431.
(279) Sow, T.-C.; Pedersen, M. V.; Christensen, H. E. M.; Ooi, B.-L. *Biochem. Biophys. Res. Commun.* **1996**, *223*, 360.
(280) Smith, E. T.; Tomich, J. M.; Iwamoto, T.; Richards, J. H.; Mao, Y.; Feinberg, B. A. *Biochemistry* **1991**, *30*, 11669.
(281) Feinberg, B. A.; Lo, X.; Iwamoto, T.; Tomich, J. M. *Protein Eng.* **1997**, *10*, 69.
(282) Holm, R. H. *Pure Appl. Chem.* **1995**, *67*, 217.
(283) Kennedy, M. C.; Stout, C. D. *Adv. Inorg. Chem.* **1992**, *38*, 323.
(284) Beinert, H.; Kennedy, M. C.; Stout, C. D. *Chem. Rev.* **1996**, *96*, 2335.
(285) Lloyd, S. J.; Lauble, H.; Prasad, G. S.; Stout, C. D. *Protein Sci.* **1999**, *8*, 2655.
(286) Robbins, A. H.; Stout, C. D. *Proc. Natl. Acad. Sci. U.S.A.* **1989**, *86*, 3639.
(287) Coucouvanis, D.; Kanatzidis, M. G.; Simhom, E. D.; Baenziger, N. C. *J. Am. Chem. Soc.* **1982**, *104*, 1874.
(288) Saak, W.; Pohl, S. *Z. Naturforsch.* **1988**, *43b*, 813.
(289) Pohl, S.; Bierbach, U. *Z. Naturforsch.* **1991**, *46b*, 68.
(290) Pohl, S.; Bierbach, U. *Z. Naturforsch.* **1992**, *47b*, 1266.
(291) Harmjanz, M.; Junghans, C.; Opitz, U.-A.; Bahlmann, B.; Pohl, S. *Z. Naturforsch.* **1996**, *51b*, 1040.
(292) Tyson, M. A.; Demadis, K. D.; Coucouvanis, D. *Inorg. Chem.* **1995**, *34*, 4519.
(293) Walsdorff, C.; Saak, W.; Pohl, S. *J. Chem. Soc., Dalton Trans.* **1997**, 1857.
(294) van Strijdonck, G. P. F.; van Haare, J. A. E. H.; van der Linden, J. G. M.; Steggerda, J. J.; Nolte, R. J. M. *Inorg. Chem.* **1994**, *33*, 999.
(295) van Strijdonck, G. P. F.; van Haare, J. A. E. H.; Hönen, P. J. M.; van den Schoor, R. C. G. M.; Feiters, M. C.; van der Linden, J. G. M.; Steggerda, J. J.; Nolte, R. J. M. *J. Chem. Soc., Dalton Trans.* **1997**, 449.
(296) Evans, D. J.; Garcia, G.; Leigh, G. J.; Newton, M. S.; Santana, M. D. *J. Chem. Soc., Dalton Trans.* **1992**, 3229.
(297) Whitener, M. A.; Peng, G.; Holm, R. H. *Inorg. Chem.* **1991**, *30*, 2411.
(298) van Strijdonck, G. P. F.; ten Have, P. T. J. H.; Feiters, M. C.; van der Linden, J. G. M.; Steggerda, J. J.; Nolte, R. J. M. *Chem. Ber.* **1997**, *130*, 1151.
(299) Barclay, J. E.; Diaz, M. I.; Evans, D. J.; Garcia, G.; Santana, M. D.; Torralba, M. C. *Inorg. Chim. Acta* **1997**, *258*, 211.
(300) Stack, T. D. P.; Carney, M. J.; Holm, R. H. *J. Am. Chem. Soc.* **1989**, *111*, 1670.
(301) Ciurli, S.; Carrié, M.; Weigel, J. A.; Carney, M. J.; Stack, T. D. P.; Papaefthymiou, G. C.; Holm, R. H. *J. Am. Chem. Soc.* **1990**, *112*, 2654.
(302) Weigel, J. A.; Holm, R. H. *J. Am. Chem. Soc.* **1991**, *113*, 4184.
(303) Liu, H. Y.; Scharbert, B.; Holm, R. H. *J. Am. Chem. Soc.* **1991**, *113*, 9529.
(304) Zhou, C.; Holm, R. H. *Inorg. Chem.* **1997**, *36*, 4066.
(305) Mansy, S. S.; Xiong, Y.; Hemann, C.; Hille, R.; Sundaralingam, M.; Cowan, J. A. *Biochemistry* **2002**, *41*, 1195.
(306) Messick, T. E.; Chmiel, N. H.; Golinelli, M.-P.; Langer, M. R.; Joshua-Tor, L.; David, S. S. *Biochemistry* **2002**, *41*, 3931.

(307) Volbeda, A.; Charon, M.-C.; Piras, C.; Hatchikian, E. C.; Frey, M.; Fontecilla-Camps, J. C. *Nature* **2002**, *373*, 580.
(308) Goh, C.; Weigel, J. A.; Holm, R. H. *Inorg. Chem.* **1994**, *33*, 4869.
(309) Yoo, S. J.; Hu, Z.; Goh, C.; Bominaar, E. L.; Holm, R. H.; Münck, E. *J. Am. Chem. Soc.* **1997**, *119*, 8732.
(310) Smith, B. E. *Adv. Inorg. Chem.* **1999**, *47*, 160.
(311) Peters, J. W.; Stowell, M. H. B.; Soltis, S. M.; Finnegan, M. G.; Johnson, M. K.; Rees, D. C. *Biochemistry* **1997**, *36*, 1181.
(312) Mayer, S. M.; Lawson, D. M.; Gormal, C. A.; Roe, S. M.; Smith, B. E. *J. Mol. Biol.* **1999**, *292*, 871.
(313) Osterloh, F.; Sanakis, Y.; Staples, R. J.; Münck, E.; Holm, R. H. *Angew. Chem., Int. Ed.* **1999**, *38*, 2066.
(314) Zhang, Y.; Zuo, J.-L.; Zhou, H.-C.; Holm, R. H. *J. Am. Chem. Soc.* **2002**, *124*, 14292.
(315) Crane, B. R.; Siegel, L. M.; Getzoff, E. D. *Science* **1995**, *270*, 59.
(316) Crane, B. R.; Siegel, L. M.; Getzoff, E. D. *Biochemistry* **1997**, *36*, 12120.
(317) Doukov, T. I.; Iverson, T. M.; Seravalli, J.; Ragsdale, S. W.; Drennan, C. L. *Science* **2002**, *298*, 567.
(318) Holm, R. H. *Pure Appl. Chem.* **1998**, *70*, 931.
(319) Challen, P. R.; Koo, S. M.; Dunham, W. R.; Coucouvanis, D. *J. Am. Chem. Soc.* **1990**, *112*, 2455.
(320) Huang, J.; Mukerjee, S.; Segal, B. M.; Akashi, H.; Zhou, J.; Holm, R. H. *J. Am. Chem. Soc.* **1997**, *119*, 8662.
(321) Stolzenberg, A. M.; Stershic, M. T. *Inorg. Chem.* **1985**, *24*, 3095.
(322) Beinert, H.; Sands, R. H. *Biochem. Biophys. Res. Commun.* **1960**, *3*, 41.
(323) Sands, R. H.; Beinert, H. *Biochem. Biophys. Res. Commun.* **1960**, *3*, 47.
(324) *Inorganic Electronic Structure and Spectroscopy*; Solomon, E. I., Lever, A. B. P., Eds.; Wiley-Interscience: New York, 1999; Vols. I and II.
(325) *Physical Methods in Bioinorganic Chemistry*; Que, L., Jr., Ed.; University Science Books: Sausalito, CA, 2000.
(326) Gütlich, P.; Ensling, J. In *Inorganic Electronic Structure and Spectroscopy*; Solomon, E. I., Lever, A. B. P., Eds.; Wiley-Interscience: New York, 1999; Vol. I, Chapter 3.
(327) Münck, E. In *Physical Methods in Inorganic and Bioinorganic Chemistry*; Que, L., Jr., Ed.; University Science Books: Sausalito, CA, 2000; Chapter 6.
(328) Cen, W.; Lee, S. C.; Li, J.; MacDonnell, F. M.; Holm, R. H. *J. Am. Chem. Soc.* **1993**, *115*, 9515.
(329) Hauser, C.; Bill, E.; Holm, R. H. *Inorg. Chem.* **2002**, *41*, 1615.
(330) Fomitchev, D. V.; McLauchlan, C. C.; Holm, R. H. *Inorg. Chem.* **2002**, *41*, 958.
(331) Kanatzidis, M. G.; Coucouvanis, D.; Simopoulos, A.; Kostikas, A.; Papaefthymiou, V. *J. Am. Chem. Soc.* **1985**, *107*, 4925.
(332) Han, J.; Coucouvanis, D. *Inorg. Chem.* **2002**, *41*, 2738.
(333) Emptage, M. H.; Kent, T. A.; Kennedy, M. C.; Beinert, H.; Münck, E. *Proc. Natl. Acad. Sci. U.S.A.* **1983**, *80*, 4674.
(334) Kent, T. A.; Emptage, M. H.; Merkle, H.; Kennedy, M. C.; Beinert, H.; Münck, E. *J. Biol. Chem.* **1985**, *260*, 6871.
(335) Werst, M. M.; Kennedy, M. C.; Houseman, A. L. P.; Beinert, H.; Hoffman, B. M. *Biochemistry* **1990**, *29*, 10533.
(336) Kent, T. A.; Dreyer, J.-L.; Kennedy, M. C.; Huynh, B. H.; Emptage, M. H.; Beinert, H.; Münck, E. *Proc. Natl. Acad. Sci. U.S.A.* **1982**, *79*, 1096.
(337) Duin, E. C.; Lafferty, M. E.; Crouse, B. R.; Allen, R. M.; Sanyal, I.; Flint, D. H.; Johnson, M. K. *Biochemistry* **1997**, *36*, 11811.
(338) Choudens, S. O.; Sanakis, Y.; Hewitson, K. S.; Roach, P.; Baldwin, J. E.; Münck, E.; Fontecave, M. *Biochemistry* **2000**, *39*, 4165.
(339) Ugulava, N. B.; Gibney, B. R.; Jarrett, J. T. *Biochemistry* **2000**, *39*, 5206.
(340) Ollagnier, S.; Meier, C.; Mulliez, E.; Gaillard, J.; Schuenemann, V.; Trautwein, A. X.; Mattioli, T.; Lutz, M.; Fontecave, M. *J. Am. Chem. Soc.* **1999**, *121*, 6344.
(341) Mulliez, E.; Ollagnier-de Choudens, S.; Meier, C.; Cremonini, M.; Luchinat, C.; Trautwein, A. X.; Fontecave, M. *J. Biol. Inorg. Chem.* **1999**, *4*, 614.
(342) Broderick, J. B.; Duderstadt, R. E.; Fernandez, D. C.; Wojtuszewski, K.; Henshaw, T. F.; Johnson, M. K. *J. Am. Chem. Soc.* **1997**, *119*, 7396.
(343) Külzer, R.; Pils, T.; Kappl, R.; Hüttermann, J.; Knappe, J. *J. Biol. Chem.* **1998**, *273*, 4897.
(344) Khoroshilova, N.; Popescu, C.; Münck, E.; Beinert, H.; Kiley, P. J. *Proc. Natl. Acad. Sci. U.S.A.* **1997**, *94*, 6087.
(345) Popescu, C. V.; Bates, D. M.; Beinert, H.; Münck, E.; Kiley, P. J. *Proc. Natl. Acad. Sci. U.S.A.* **1998**, *95*, 13431.
(346) Cheek, J.; Broderick, J. B. *J. Biol. Inorg. Chem.* **2001**, *6*, 209.
(347) Armstrong, F. A.; Williams, R. J. P. *FEBS Lett.* **2002**, *451*, 91.
(348) Einsle, O.; Tezcan, F. A.; Andrade, S.; Schmid, B.; Yoshida, M.; Howard, J. B.; Rees, D. C. *Science* **2002**, *297*, 1696.
(349) Peters, J. W.; Lanzilotta, W. N.; Lemon, B. J.; Seefeldt, L. C. *Science* **1998**, *282*, 1853.
(350) Nicolet, Y.; de Lacey, A. L.; Vernède, X.; Fernandez, V. M.; Hatchikian, E. C.; Fontecilla-Camps, J. C. *J. Am. Chem. Soc.* **2001**, *123*, 1596.
(351) Fontecilla-Camps, J. C.; Ragsdale, S. W. *Adv. Inorg. Chem.* **1999**, *47*, 283.
(352) Dobbek, H.; Svetlitchnyi, V.; Gremer, L.; Huber, R.; Meyer, O. *Science* **2001**, *293*, 1281.
(353) Drennan, C. L.; Heo, J.; Sintchak, M. D.; Schreiter, E.; Ludden, P. W. *Proc. Natl. Acad. Sci. U.S.A.* **2001**, *98*, 11973.
(354) Verma, A. K.; Lee, S. C. *J. Am. Chem. Soc.* **1999**, *121*, 10838.
(355) Verma, A. K.; Nazif, T. N.; Achim, C.; Lee, S. C. *J. Am. Chem. Soc.* **2001**, *122*, 11013.
(356) Duncan, J. S.; Nazif, T. N.; Verma, A. K.; Lee, S. C. *Inorg. Chem.* **2003**, *42*, 1211.

CR020615+